CHAPTER 3

Synthesis and characterization of Binuclear Ru (II) arene complexes

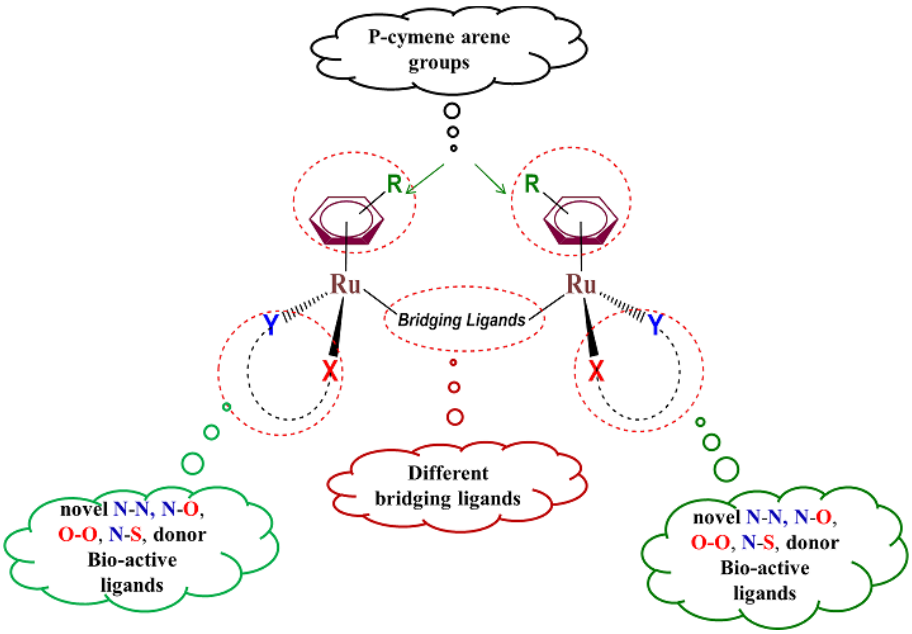

Half-sandwich 'piano-stool' type binuclear ruthenium (II) arene compounds of the general structural formula *[(η^6-p-cym)(L)Ru(μ-BL)Ru(L)(η^6-p-cym)]nCl* (*p-cym* = *p*-cymene $MeC_6H_4Pr^i$; *L* = N O, S N and O O donor ligands discussed in chapter-2 have been synthesized and characterized by means of ESI mass spectrometry, NMR, FTIR and UV-Vis spectroscopy. These organometallic complexes were found to be pseudo-octahedral in geometry with three coordination sites taken up by the arene ligand (resonating structure) forming very stable arene-Ru bond that stabilizes ruthenium in its +2 state.

TABLE OF CONTENTS

3.1 Homobinuclear Ruthenium (II)-arene complexes:

Ruthenium (II)-arene compounds are able to coordinate various types of ligands and therefore can modulate properties such as solubility, lipophilicity and pharmacokinetics. One of the first endeavour included coordination of metal arene moieties with bioactive ligands and a typical example of that approach is seen with $[Ru(\eta^6\text{-}C_6H_6)Cl_2(\text{metronidazole})]$ [1]. A viable approach for designing ruthenium complexes is the inclusion of biologically-active ligands that primarily aim at minimizing toxicity toward normal cells and provide ways to improve antiproliferative activity of metal-based drugs [2]. These ligands exhibit different coordination modes, facilitate compatibility of the complexes with the biological environment, and enhance cellular uptake. The diverse bio-relevant ligands incorporated as useful components of ruthenium complexes ranges from amino acids, peptides, proteins, carbohydrates, purine bases and oligonucleotides to steroids and other bioactive entities endowed with specific properties [3]. This methodology is confirmed by extensive studies on Ru complexes that provide unique rationale for design and production of potent ruthenium anticancer drugs with distinct transport pathways and mechanisms of action [4, 5].

Binuclear metal complexes have emerged as a unique class of biologically active compounds with promising anticancer activity. Binuclear analogues may exhibit a different spectrum of biological activity compared to mononuclear derivatives, retaining the efficacy of the mononuclear compounds to bind DNA/proteins while acting through long-range interactions rather than short range interactions typical of mononuclear species. The formation of binuclear analogues has been a successful approach toward the development of platinum metallodrugs having unique binding modes and interactions with DNA [6]. This route has led to compounds with increased potency compared to established mononuclear platinum compounds which retain high activity in cell lines resistant to cisplatin [7, 8]. In contrast, binuclear organometallic ruthenium (II) arene compounds are underexplored [9]. In the most comprehensive of these studies a series of binuclear ruthenium compounds linked via maltol-derived ligands were investigated [10-12]. It was observed that the cytotoxicity of these compounds could be modulated by changes in the chain length of the alkyl group of the linker ligand, and cytotoxicity correlated with the lipophilicity of the resulting complexes [10]. It was interesting to note that these complexes not only crosslink two DNA duplexes but also formed DNA–protein crosslinks, a novel mode of action for such complexes [12]. Binuclear Ru(II) polypyridyl complexes with the tris(benzimidazol-2-ylmethyl)amine ligand and related heteronuclear Ru(II)-Co(III) complexes were reported with antitumor activities

against a panel of cell lines [13]. Binuclear Ru(II)(η^6 - arene) compounds were prepared with the aim of developing ruthenium compounds with improved anticancer activity, lower toxicity than Pt compounds and new DNA binding modes [14]. The linkage of two Ru metal centres resulted in compounds with significantly improved anticancer activity as compared to the mononuclear species and IC_{50} values in the low μM range as observed for established platinum drugs. The biological mode of action of the binuclear Ru complexes were investigated which showed formation of DNA–protein, DNA interstrand and interduplex crosslinks, which is rare for tumor inhibiting metal complexes, and potentially a novel mode of action compared to established anticancer drugs [15]. Sadler and co-workers reported binuclear analogues of their ethylene-1,2-diamine compounds based on N,N'-bis(2-aminoethyl)-hexane-1,6-diamine linkers [16-18]. In vitro anticancer activity assays revealed similar or lower activity than the mononuclear analogues for the A2780 ovarian cancer cell line [16, 17]. The proposed modes of action are thought to involve binding to DNA and greater unwinding of plasmid DNA due to intercalation as compared to the mononuclear analogue. Moreover, interference with in vitro DNA-directed RNA synthesis and the formation of interstrand cross-links were also observed [18].

Based on the ability of ruthenium (II)-arene species to coordinate to different classes of ligands, which make them suitable for fine-tuning chemical and pharmaceutical properties and the promising biological activies of binuclear metal complexes, we have focused on the synthesis of homobinuclear ruthenium (II)–arene complexes. Multinuclearity in metal-conjugates is expected to the increase of the cytotoxicity of a drug by increasing the number of metal centres. The ligands employed are those with proven significant therapeutic properties as detailed in chapter 2 of the thesis. This chapter presents the synthesis and characterization of half-sandwich 'piano-stool' type binuclear ruthenium (II) arene complexes of the general structural formula $[Ru_2(\mu\text{-}im/\mu\text{-}azpy)(\eta^6\text{-}p\text{-}cym)_2(L)_2]Cl_n$ (*p-cym* = *p*-cymene $MeC_6H_4Pr^i$; *L* = N, S, O donor ligands, im = imidazole, azpy = 4,4'azopyridine).

3.2 General synthesis of $[Ru_2(\mu\text{-}im / \mu\text{-}azpy)(\eta^6\text{-}p\text{-}cym)_2(L)_2]Cl_n$ complexes:

3.2.1 Materials and instrumentation:

All the chemicals and solvents used for the synthesis and characterization of the precursor mononuclear and binuclear complexes were of analytical grade and used as purchased. $RuCl_3.3H_2O$ was purchased from Hi-media, Mumbai, India. α-terpinene was purchased from

Sigma-Aldrich. Elemental and spectral analysis was recorded on the same instrument models as mentioned previously.

ORCA program package (version 4.0.1.2) was used for geometry optimization. DFT calculations were performed by using the b-p functional [19] and def2-SVP [20] (def2-ecp for "Ru") [21] basis set by employing Turbomole 6.4 suite of programs [22]. The resolution of Identity (ri) [23] and multipole accelerated resolution of Identity (marij) [24] approximations with dispersion correction (disp3) [25] have been used for all the calculations. Solvent corrections were incorporated in all calculations using the COSMO model, [26] with Methanol ($\varepsilon = 32.7$) as the solvent. Mercury 4.0.0 [27] software was used for visualization.

3.2.2 General synthetic scheme:

$[Ru(\eta^6\text{-}p\text{-cymene})Cl_2]_2$ was prepared according to the procedure sited in literature [28, 29]. To a solution of $[Ru(\eta^6\text{-p-cymene})Cl_2]_2$ (in 2.5 ml CH_2Cl_2), the synthesized ligand **L** (2.5 ml methanol) was added on stirring in 1:2 ratio. The reaction mixture was stirred overnight (20-24 h) and then left for slow evaporation at room temperature. The mononuclear complex $[Ru(\eta^6\text{-p-cym})(L)Cl]$ obtained was filtered, washed with pet ether and CH_2Cl_2 and dried in air. All the precursor mononuclear complexes synthesized were characterized using various spectral techniques and their composition confirmed. Synthesis of the binuclear complex was achieved by addition of a solution of the bridging ligand imidazole (im) / 4, 4'azopyridine (azpy) to a solution of the mononuclear complex $[Ru(\eta^6\text{-p-cym})(L)Cl]$, in 1:2 mole ratio using MDC:MeOH (1:2) as a solvent. In the synthesis of binuclear complexes with imidazole as bridging ligand, 1.0 M NaOH was added to raise the pH upto ~11 in order to deprotonate the –NH present in the imidazole ring [30]. The reaction mixture was stirred for 24 h under N_2 atmosphere. The reddish brown solid obtained was then filtered, washed with pet ether and CH_2Cl_2 and dried in oven at 40°C for 1 h. The complexes were recrystallized from dichloromethane and ether which resulted in reddish brown crystalline product. All the complexes are soluble in DMSO, MeOH, CH_2Cl_2 and partially soluble in water. *Fig. 3.1* shows the general synthetic route for preparation of the complexes.

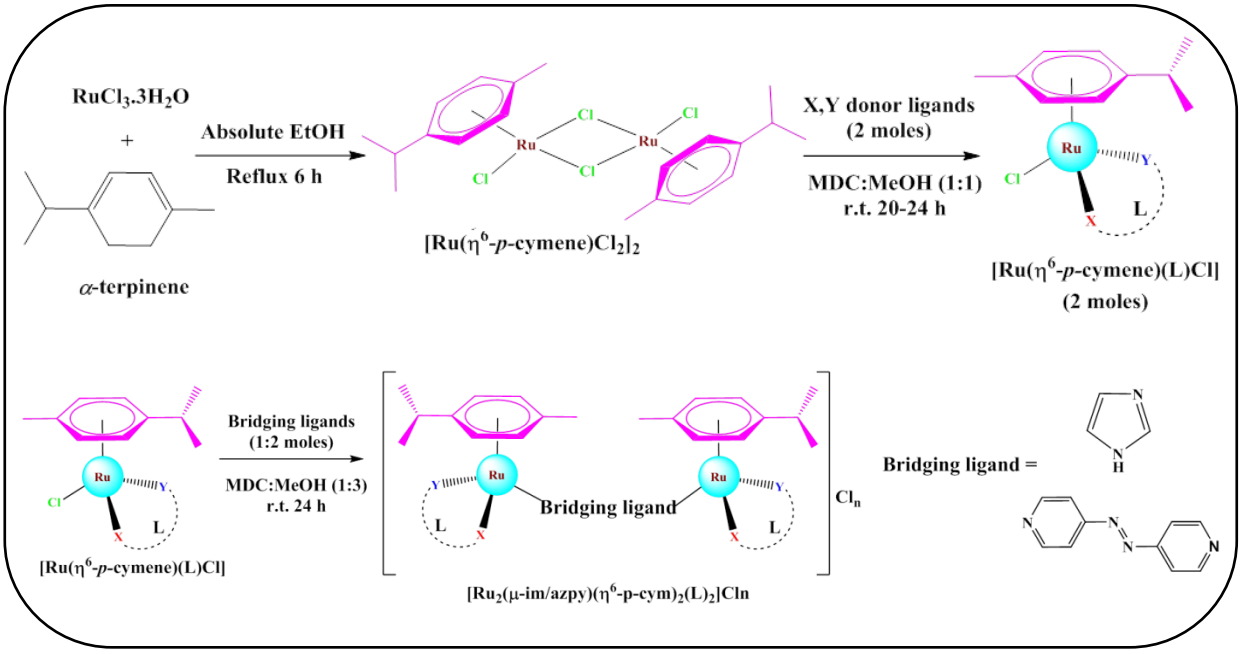

Fig. 3.1: *General synthetic scheme of* ***[Ru$_2$(μ-im/azpy)(η^6-p-cym)$_2$(L)$_2$]Cl$_n$*** *complexes*

Table 3.1: List of the different ligand series used in the synthesis of [(Ru$_2$(μ- im/μ-azpy)(η^6-*p*-cym)$_2$(L)$_2$]Cl$_n$ complexes along with their coordinating sites to the Ru(II) centre.

Donor Ligand L	Ligand code	Complex Code	X =	Y =
Diphenylpyrazol thiosemicarbazones	**L1-L4**	**C1-C8**	N	S
Diphenylpyrazol α-Amino Acids	**L5-L8**	**C9-C16**	N	O
Ferrocenyl thiosemicarbazones	**L9-L12**	**C17-C24**	N	S
Ferrocenyl amino acid mannich bases	**L13-L16**	**C25-C32**	N	O
Fluoroquinolones	**L17-L20**	**C33-C40**	O	O

The composition and structures of all the complexes have been confirmed by ESI Mass spectrometry, NMR, FTIR, UV-Vis spectroscopy and elemental analysis. Further geometry optimization of the complexes was done by performing DFT calculation. The analytical data are consistent with the proposed compositions and their molecular formulae.

3.3 [$Ru_2(\eta^6$-p-cym)$_2$(Diphenyl pyrazole thiosemicarbazone)$_2$(μ-im / azpy))]Cl_{1-2} complexes: (C1-C8)

3.3.1 Synthesis and characterization:

[Ru_2(μ-im) (η^6-p-cym)$_2$(L1)$_2$]Cl ***(C1):***

μ-imidazole – bis 1-((1, 3-diphenyl-1H-pyrazol-4-yl)methylene)thiosemicarbazone - bis 1-isopropyl-4-methyl benzene diruthenium(II) chloride

Yield: 62.9%; Molecular Weight 1214.9 g/mole; Molecular Formula $C_{57}H_{60}ClN_{12}Ru_2S_2$; Anal.: Found: C, 55.99; H, 4.78; N, 13.77. Calc.: C, 56.36; H, 4.98; N, 13.84. ESI-MS *m/z*: Obs (Calc): 1179.27 (1179.5) (M^+) ; δ_H(400 MHz, DMSO-d^6) 7.38, (tri, 1H, Ar-H); 7.55, (m,5H, Ar-H); 7.69, (d, 2H, *J* = 6.8 Hz, Ar-H); 7.77, (s, 1H, Ar-H); 7.83, (d, 2H, *J*= 7.6 Hz, Ar-H); 8.22, (s, 2H, NH_2); 8.69, (s, 1H, HC=N); 5.82-5.77; (m, 4H, *p*-cymAr-H); 2.84-2.50, (q, 1H, *p*-cym-*iso*-prop-CH); 1.97, (s, 3H, *p*-cym Ar-CH_3); 1.05, (d, 6H, *p*-cym-*iso*-prop-$(CH_3)_2$); 7.93 (d, 2H, imidazole CH=CH); FTIR (KBr/ cm^{-1}): $\nu_{(Ar)C-H}$ 2959, $\nu_{(NH2)}$ 3050, $\nu_{(C=N)}$1588, $\nu_{(C-S)sym}$ 770; $\Lambda_M(\Omega^{-1}.m^2.M^{-1})$ 75.

[Ru_2(μ-im) (η^6-p-cym)$_2$(L2)$_2$]Cl **(C2)**:

μ-imidazole–bis 1-((1, 3-diphenyl-1H-pyrazol-4-yl)methylene)-4-methyl-3-thiosemicarbazone - bis 1-isopropyl-4-methyl benzene diruthenium(II) chloride

Yield: 77.5%; Molecular Weight 1243.0 g/mole; Molecular Formula $C_{59}H_{64}ClN_{12}Ru_2S_2$; Anal. Found: C, 56.61; H, 4.89; N, 13.17. Calc.: C, 57.01; H, 5.19; N, 13.52. ESI-MS *m/z*: Obs (Calc): 1207.7 (1207.5) (M^+); δH(400 MHz, DMSO-d^6) 7.50, (tri, 1H, Ar-H); 7.59, (m,5H, Ar-H); 7.68, (d, 2H, *J* = 6.8 Hz, Ar-H); 7.79, (s, 1H, Ar-H); 7.80, (d, 2H, *J*= 7.6 Hz, Ar-H); 7.92, (s, 1H, NH-CH_3); 8.22, (s, 1H, HC=N); 5.82-5.73, (m, 4H, *p*-cymAr-H); 2.95-2.49, (q, 1H, *p*-cym-*iso*-prop-CH); 1.98, (s, 3H, *p*-cym Ar-CH_3); 1.02, (d, 6H, *p*-cym-*iso*-prop-$(CH_3)_2$); 7.92, (d, 2H, imidazole CH=CH); FTIR (KBr/ cm^{-1}): $\nu_{(Ar)C-H}$ 2962, $\nu_{(NH-CH3)}$ 3124, $\nu_{(C=N)}$1597, $\nu_{(C-S)sym}$ 748; $\Lambda_M(\Omega^{-1}.m^2.M^{-1})$ 72.

[Ru_2(μ-im) (η^6-p-cym)$_2$(L3)$_2$]Cl **(C3)**:

μ-imidazole –bis-1-((1,3-diphenyl-1H-pyrazol-4-yl)methylene)-4-phenyl-3-thiosemicarbazone - bis 1-isopropyl-4-methyl benzene diruthenium(II) chloride

Yield: 48.4%; Molecular Weight 1367.1g/mole; Molecular Formula $C_{69}H_{68}ClN_{12}Ru_2S_2$; Anal. Found: C, 60.12; H, 4.89; N, 11.98. Calc.: C, 60.62; H, 5.01; N, 12.29. ESI-MS *m/z*: Obs (Calc): 1330.3 (1331.1) (M^+-1); δH(400 MHz, DMSO-d^6) 7.38, (tri, 1H, Ar-H); 7.53,

(m,5H, Ar-H); 7.64, (d, 2H, *J* = 6.8 Hz, Ar-H); 7.79, (s, 1H, Ar-H); 7.82, (d, 2H, *J*= 7.6 Hz, Ar-H); 8.10, (s, 1H, NH-C_6H_5); 8.34, (s, 1H, HC=N); 5.81-5.50, (m, 4H, *p*-cymAr-H); 2.50-2.24, (q, 1H, *p*-cym-*iso*-prop-CH); 2.15, (s, 3H, *p*-cym Ar-CH_3); 1.15, (d, 6H, *p*-cym-*iso*-prop-$(CH_3)_2$); 7.82, (d, 2H, imidazole CH=CH); FTIR (KBr/ cm^{-1}): $\nu_{(Ar)C-H}$ 2970, $\nu_{(NH-C6H5)}$ 3163, $\nu_{(C=N)}$1589, $\nu_{(C-S)sym}$ 756; $\Lambda_M(\Omega^{-1}.m^2.M^{-1})$ 76.

[Ru_2(μ-im) (η^6-p-cym)$_2$(L4)$_2$]Cl **(C4)**:

μ-imidazole–bis1-((1,3-diphenyl-1H-pyrazol-4-yl)methylene)-4-(naphthalen-1-yl)-3-thiosemicarbazone - bis 1-isopropyl-4-methyl benzene diruthenium(II) chloride

Yield: 58.7%; Molecular Weight 1467.3 g/mole; Molecular Formula $C_{77}H_{72}ClN_{12}Ru_2S_2$; Anal. Found: C, 62.98; H, 3.79; N, 11.86. Calc.: C, 63.03; H, 4.95; N, 11.46. ESI-MS *m/z*: Obs (Calc): 1433.2. (1431.4) (M^++1); δH(400 MHz, DMSO-d^6) 7.37, (tri, 1H, Ar-H); 7.55, (m,5H, Ar-H); 7.63, (d, 2H, *J* = 6.8 Hz, Ar-H); 7.65, (s, 1H, Ar-H); 7.81, (d, 2H, *J*= 7.6 Hz, Ar-H); 7.75, (s, 1H, NH-$C_{10}H_7$); 8.32, (s, 1H, HC=N); 6.68-5.92, (m, 4H, *p*-cymAr-H), 3.93-3.35, (q, 1H, *p*-cym-*iso*-prop-CH); 2.49, (s, 3H, *p*-cym Ar-CH_3); 1.93, (d, 6H, *p*-cym-*iso*-prop-$(CH_3)_2$); 7.75, (d, 2H, imidazole CH=CH); FTIR (KBr/cm^{-1}): $\nu_{(Ar)C-H}$ 2959, $\nu_{(NH-C10H7)}$ 3138, $\nu_{(C=N)}$ 1595, $\nu_{(C-S)sym}$ 775; $\Lambda_M(\Omega^{-1}.m^2.M^{-1})$ 70.

*[Ru_2(μ-azpy) (η^6-p-cym)$_2$(**L1**)$_2$]Cl_2* **(C5)**:

μ-4,4'azopyridine – bis 1-((1, 3-diphenyl-1H-pyrazol-4-yl)methylene)thiosemicarbazone - bis 1-isopropyl-4-methyl benzene diruthenium(II) dichloride

Yield: 61.7%; Molecular Weight 1366.6 g/mole; Molecular Formula $C_{64}H_{64}Cl_2N_{14}Ru_2S_2$; Anal.: C, 58.99; H, 4.73; N, 15.07. Calc.: C, 59.33; H, 4.98; N, 15.14. ESI-MS *m/z*: Obs (Calc): 644.8 (645.7) (M^{2+}-1) ; δ_H (400 MHz, DMSO-d^6) 7.06, (tri, 1H, Ar-H); 7.10, (m,5H, Ar-H); 7.12, (d, 2H, *J* = 6.8 Hz, Ar-H); 7.81, (s, 1H, Ar-H); 7.84, (d, 2H, *J*= 7.6 Hz, Ar-H); 8.18, (s, 2H, NH_2); 8.21, (s, 1H, HC=N); 6.84-6.79, (m, 4H, *p*-cymAr-H); 3.16-2.24, (q, 1H, *p*-cym-*iso*-prop-CH); 1.75, (s, 3H, *p*-cym Ar-CH_3); 1.15, (d, 6H, *p*-cym-*iso*-prop-$(CH_3)_2$); FTIR (KBr/cm^{-1}): $\nu_{(Ar)C-H}$ 2961, $\nu_{(NH2)}$ 3159, $\nu_{(C=N)}$1589, $\nu_{(C-S)sym}$ 761, $\nu_{N=N}$ 1408; $\Lambda_M(\Omega^{-1}.m^2.M^{-1})$ 134.

*[Ru_2(μ-azpy) (η^6-p-cym)$_2$(**L2**)$_2$]Cl_2* **(C6)**:

μ-4,4'azopyridine–bis1-((1,3-diphenyl-1H-pyrazol-4-yl)methylene)-4-methyl-3-thiosemicarbazone - bis 1-isopropyl-4-methyl benzene diruthenium(II) dichloride

Yield: 78.8 %; Molecular Weight 1394.6 g/mole; Molecular Formula $C_{66}H_{68}Cl_2N_{14}Ru_2S_2$; Anal.: C, 59.52; H, 4.87; N, 14.56. Calc.: C, 59.89; H, 5.18; N, 14.82, ESI-MS *m/z*:Obs (Calc): 660.3 (661.2) (M^{2+}-1) ; δ_H (400 MHz, DMSO-d^6) 7.33, (tri, 1H, Ar-H); 7.36, (m,5H, Ar-H); 7.77, (d, 2H, *J* = 6.8 Hz, Ar-H); 7.79, (s, 1H, Ar-H); 7.81, (d, 2H, *J*= 7.6 Hz, Ar-H); 8.44, (s, 1H, NH-CH_3); 8.46, (s, 1H, HC=N); 5.82-5.77, (m, 4H, *p*-cymAr-H); 3.35-2.86, (q, 1H, *p*-cym-*iso*-prop-CH); 1.97, (s, 3H, *p*-cym Ar-CH_3); 1.17, (d, 6H, *p*-cym-*iso*-prop-$(CH_3)_2$); FTIR (KBr/cm^{-1}): $\nu_{(Ar)C-H}$ 2960, $\nu_{(NH-CH3)}$ 3162, $\nu_{(C=N)}$1588, $\nu_{(C-S)sym}$ 764, $\nu_{N=N}$ 1402; $\Lambda_M(\Omega^{-1}.m^2.M^{-1})$ 135.

$[Ru_2(\mu\text{-azpy})\ (\eta^6\text{-p-cym})_2(\boldsymbol{L3})_2]Cl_2$ **(C7)**:

μ-4,4'azopyridine–bis1-((1,3-diphenyl-1H-pyrazol-4-yl)methylene)-4-phenyl-3-thiosemicarbazone - bis 1-isopropyl-4-methyl benzene diruthenium(II) dichloride

Yield: 89.7%; Molecular Weight 1518.8 g/mole; Molecular Formula $C_{76}H_{72}Cl_2N_{14}Ru_2S_2$; Anal.: C, 62.73; H, 4.67; N, 13.16. Calc.: C, 63.05; H, 5.01; N, 13.54, ESI-MS *m/z*: Obs (Calc): 724.2 (723.9) (M^{2+}) ; δ_H(400 MHz, DMSO-d^6) 7.36, (tri, 1H, Ar-H); 7.63, (m,5H, Ar-H); 7.72, (d, 2H, *J* = 6.8 Hz, Ar-H); 7.42, (s, 1H, Ar-H); 7.64, (d, 2H, *J*= 7.6 Hz, Ar-H); 8.24, (s, 1H, NH-C_6H_5); 8.45, (s, 1H, HC=N); 5.49-5.44, (m, 4H, *p*-cymAr-H); 2.24-2.17, (q, 1H, *p*-cym-*iso*-prop-CH); 1.91, (s, 3H, *p*-cym Ar-CH_3); 1.03, (d, 6H, *p*-cym-*iso*-prop-$(CH_3)_2$); FTIR (KBr/cm^{-1}): $\nu_{(Ar)C-H}$ 2960, $\nu_{(NH-C6H5)}$ 3045, $\nu_{(C=N)}$1590, $\nu_{(C=S)sym}$ 753, $\nu_{N=N}$ 1404; $\Lambda_M(\Omega^{-1}.m^2.M^{-1})$ 133.

$[Ru_2(\mu\text{-azpy})\ (\eta^6\text{-p-cym})_2(\boldsymbol{L4})_2]Cl_2$ **(C8)**:

μ-4,4'azopyridine – bis 1-((1,3-diphenyl-1H-pyrazol-4-yl)methylene)-4-(naphthalen-1-yl)-3-thiosemicarbazone - bis 1-isopropyl-4-methyl benzene diruthenium(II) dichloride

Yield: 89.3%; Molecular Weight 1618.9 g/mole; Molecular Formula $C_{84}H_{76}\ Cl_2N_{14}Ru_2S_2$; Anal.: C, 64.79; H, 4.55; N, 12.42. Calc.: C, 65.18; H, 4.95; N, 12.67. ESI-MS *m/z*: Obs (Calc): 772.2 (773.2) (M^{2+}-1) ; δ_H (400 MHz, DMSO-d^6) 7.38, (tri, 1H, Ar-H); 7.44, (m,5H, Ar-H); 7.70, (d, 2H, *J* = 6.8 Hz, Ar-H); 7.78, (s, 1H, Ar-H); 7.99, (d, 2H, *J*= 7.6 Hz, Ar-H); 8.23, (s, 1H, NH-$C_{10}H_7$); 8.57, (s, 1H, HC=N); 7.01-6.99, (m, 4H, *p*-cymAr-H); 2.51-2.49, (q, 1H, *p*-cym-*iso*-prop-CH); 1.97, (s, 3H, *p*-cym Ar-CH_3); 1.02, (d, 6H, *p*-cym-*iso*-prop-$(CH_3)_2$); FTIR (KBr/cm^{-1}): $\nu_{(Ar)C-H}$ 2959, $\nu_{(NH-C10H7)}$ 3161, $\nu_{(C=N)}$1593, $\nu_{(C=S)sym}$ 775, $\nu_{N=N}$ 1431; $\Lambda_M(\Omega^{-1}.m^2.M^{-1})$ 131.

3.3.2 Results and discussion:

The electronic absorption spectra of the complexes **C1-8** (*Fig. 3.2*) show two major bands in the wavelength range 200-700 nm. The intense absorption bands at 223–227 nm assigned to intra-ligand $\pi \rightarrow \pi^*$ transition of the aromatic moiety of free pyrazolyl thiosemicarbazone ligands (section 2.2.4), slighted shifted to longer wavelength region at 226–230 nm in the complexes due to coordination with Ru(II) metal centre. A second sharp but medium intensity peak is found in the range of 358-380 nm owing to the intraligand N, S centred $n \rightarrow \pi^*$ transitions shifted to slightly higher wavelength than those found in the free ligands in the range 313-365 nm on complexation with the metal. This shift in the wavelength indicates coordination of the pyrazolyl ligand to the metal centre via N, S donor atoms. For the complexes **C5-8** one additional broad peak was observed at 264-280 nm, due to the intraligand $n \rightarrow \pi^*$ transitions of the bridging ligand 4, 4'azopyridine in the complexes [31]. The λ_{max} values of all the transitions have been tabulated in Table 3.2.

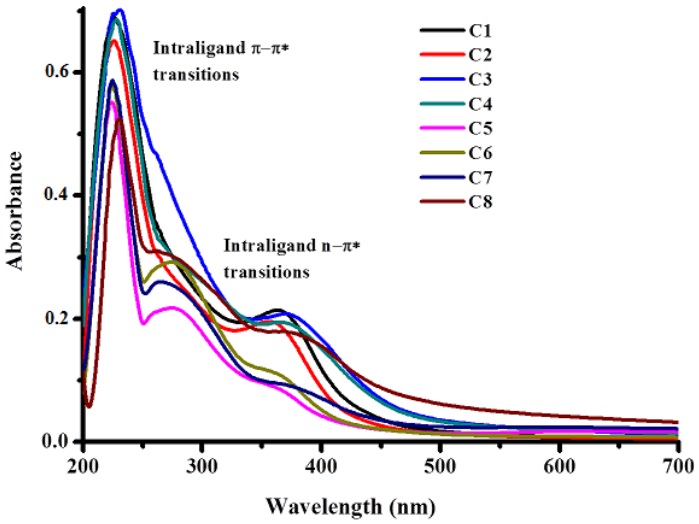

Fig. 3.2: *UV-Vis spectra of complexes*

Table 3.2: UV-Vis. peak assignments of complexes

Code	C1	C2	C3	C4	C5	C6	C7	C8
Intra-ligand transitions(nm) π-π*	226	225	229	226	224	225	225	230
Intra-ligand transitions(nm) n-π*	364	358	373	372	360	363	380	370
Intra-ligand transitions(nm) n-π*(azpy)	-	-	-	-	277	278	264	280

The ESI-Mass spectra (*Figs. 3.3* and *3.4*) show *m/z* peaks corresponding to the molecular ions which give evidence of the formation of binuclear complexes with the bridging ligand. Due to the large size of the complexes various fragments may be formed during ionization. Fragmentation of the complexes by removal of the bridging and /or the terminal ligand(s) can occur. Fragmentation of the ligand backbone while the ligand is still bound to the metal ion often occurs. The formation of the peaks given in Table 3.3 with their assigned m/z values may be rationalized in the following way. Loss of a hydrogen atom H from the organic ligand framework tends to yield a (M-1) peak whereas the (M+1) peak is due to protonated molecular ion $(M+H)^+$. The molecular ion peak values for the complexes indicate that one *p*-cymene and one Schiff base ligand is coordinated to each of the two Ru(II) ions with imidazole or 4,4'azopyridine acting as monodentate bridging ligand for each of the metal centres. Thus each of the Ru(II) ions is six coordinated with a distorted octahedral geometry. The complexes **C1-4** and **C5-8** have molar conductance (10^{-3}M in DMSO) in the range of 72-75 (Ω^{-1} m^2 M^{-1}) and 131-135 (Ω^{-1} m^2 M^{-1}) respectively at 38 ˚C suggesting 1:1 and 1:2 electrolytic behaviour. [32]

Table 3.3: m/z values of complexes

Code	**C1**	**C2**	**C3**	**C4**	**C5**	**C6**	**C7**	**C8**
Calculated Mass (g/mol)	1179.5	1207.5	1331.1	1432.4	645.7	661.2	723.9	773.2
Observed Mass (g/mol)	1179.27 (M^+)	1207.7 (M^+)	1330.3 (M^+-1)	1433.2. (M^++1)	644.8 (M^{2+}-1)	660.3 (M^{2+}-1)	724.2 (M^{2+})	772.2 (M^{2+}-1)

In the IR spectra of the complexes **C1-8**, the free ligand $\nu_{(C=S)}$ asymmetric and symmetric absorption in the region 1290-1260 and 807-824 cm^{-1} is shifted to a single $\nu_{(C-S)}$ absorption at 748-775 cm^{-1}. This shift may be due to enolization of –NH-C=S and subsequent co-ordination via deprotonated sulphur [33]. The ligands showed a strong band in the range 1597–1599 cm^{-1}, characteristic of the azomethine group $\nu_{(C=N)}$. Coordination through the azomethine nitrogen atom is expected to decrease the electron density and thus lower the $\nu_{(C=N)}$ absorption frequency in the region 1597–1588 cm^{-1}[34].The presence of weak to medium bands in the fingerprint regions 2959-2970 cm^{-1} owing to aromatic ν_{C-H} stretch and strong bands around 1457-1638 cm^{-1} due to the aromatic $\nu_{C=C}$ in plane vibrations is indicative of presence of *p*-cymene in all the complexes. The $\nu_{N=N}$ stretching of the 4,4'- azopyridine

ligand is observed at 1402-1431 cm^{-1} in the spectra of the complexes **C5-8** [35]. The overall changes in the IR spectra suggest that the pyrozlyl thiosemicarbazones act as monoanionic bidentate ligands and interact with the metal centre via the azomethine N and deprotonated sulphur.

The ^{1}H NMR spectra of C**1-8** (*Figs. 3.5* and *3.6*) show distinct peaks corresponding to *p*-cymene. The presence of a *p*-cymene ligand can be confirmed by the presence of 6 proton doublet at δ= 1.93-1.02 ppm owing to two methyl protons of *iso*-propyl group [$CH(CH_3)_2$], 3 proton singlet at δ= 2.49-1.91 ppm due to the Ar-methyl group *para* to the *iso*-propyl group, 1 proton quartet at δ= 3.95-2.24 ppm attributed to –CH of the *iso*-propyl group and two 2 proton doublets at δ= 7.01-5.44 ppm assigned to the 4 Ar-protons of *p*-cymene [36]. The imine proton observed in the range δ = 8.36-10.17 ppm in free ligands (section 2.2.4) is shifted upfield at δ = 8.22–8.69 ppm in the complexes indicating coordination via HC=N. All the aromatic protons present in pyrozole ring were observed in excepted region. The N-H proton of free imidazole observed at δ = 11-13 ppm as a sharp singlet [30] was absent in the NMR spectra of C**1-4** suggesting co-ordination of the deprotonated imidazole N with the metal centre. Apart from this, CH=CH proton of imidazole at δ = 7.75 – 7.93 ppm was observed in spectra of **C1-4** indicating the presence of imidazole ring. In case of **C5-8**, a slight upfield shift of the doublet peak due to four proton in pyridine ring of 4, 4'-azopyridine was observed at δ = 7.28 – 8.48 ppm compared with ^{1}H NMR of pure 4, 4'- azopyridine at δ = 7.75 – 8.89 ppm, indicating its co-ordination to the metal centre(s) [37].

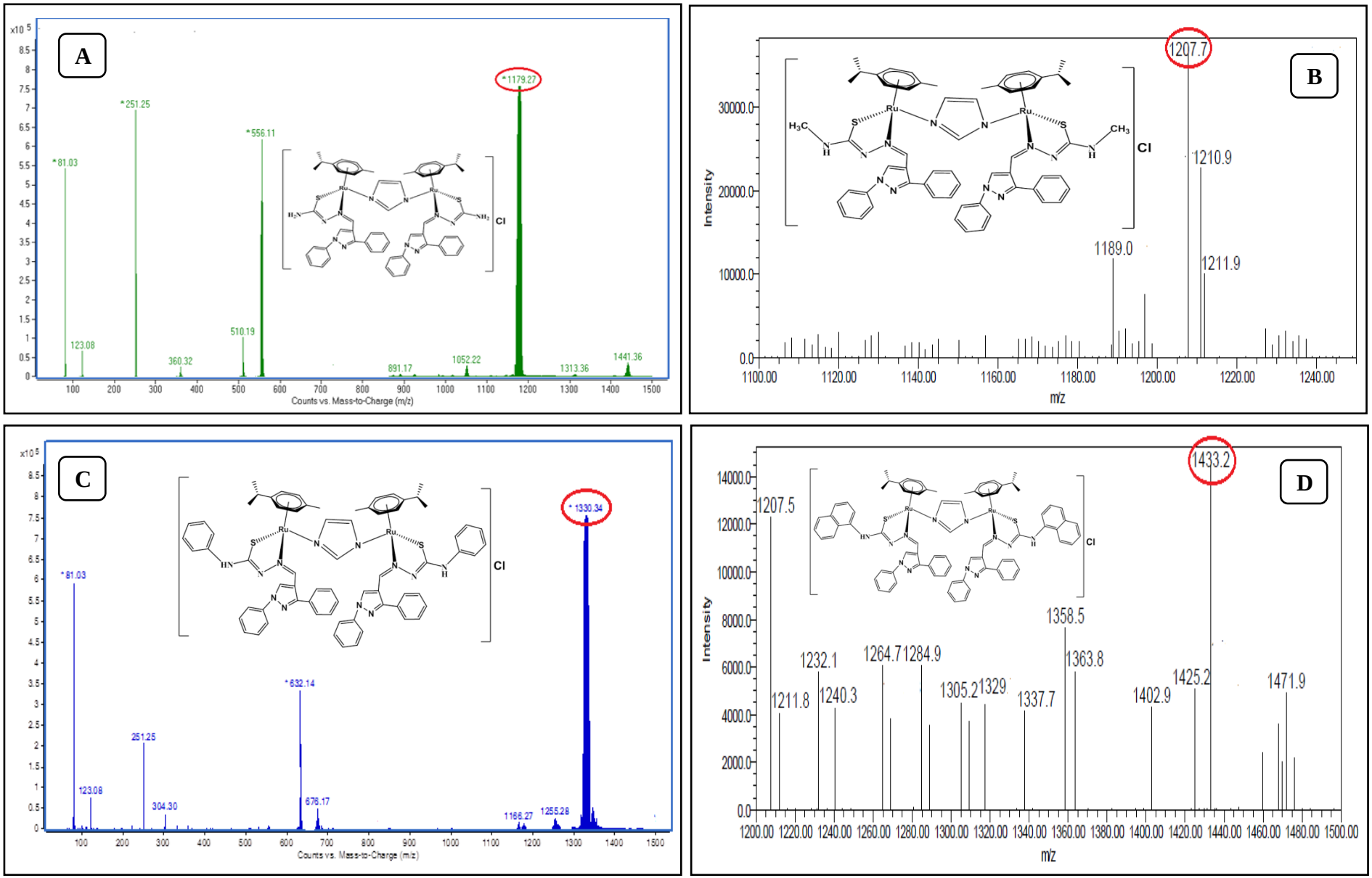

Fig. 3.3: *ESI-MS spectra of complexes (A)* ***C1*** *(B)* ***C2*** *(C)* ***C3*** *(D)* ***C4*** *indicating their molecular ion peak.*

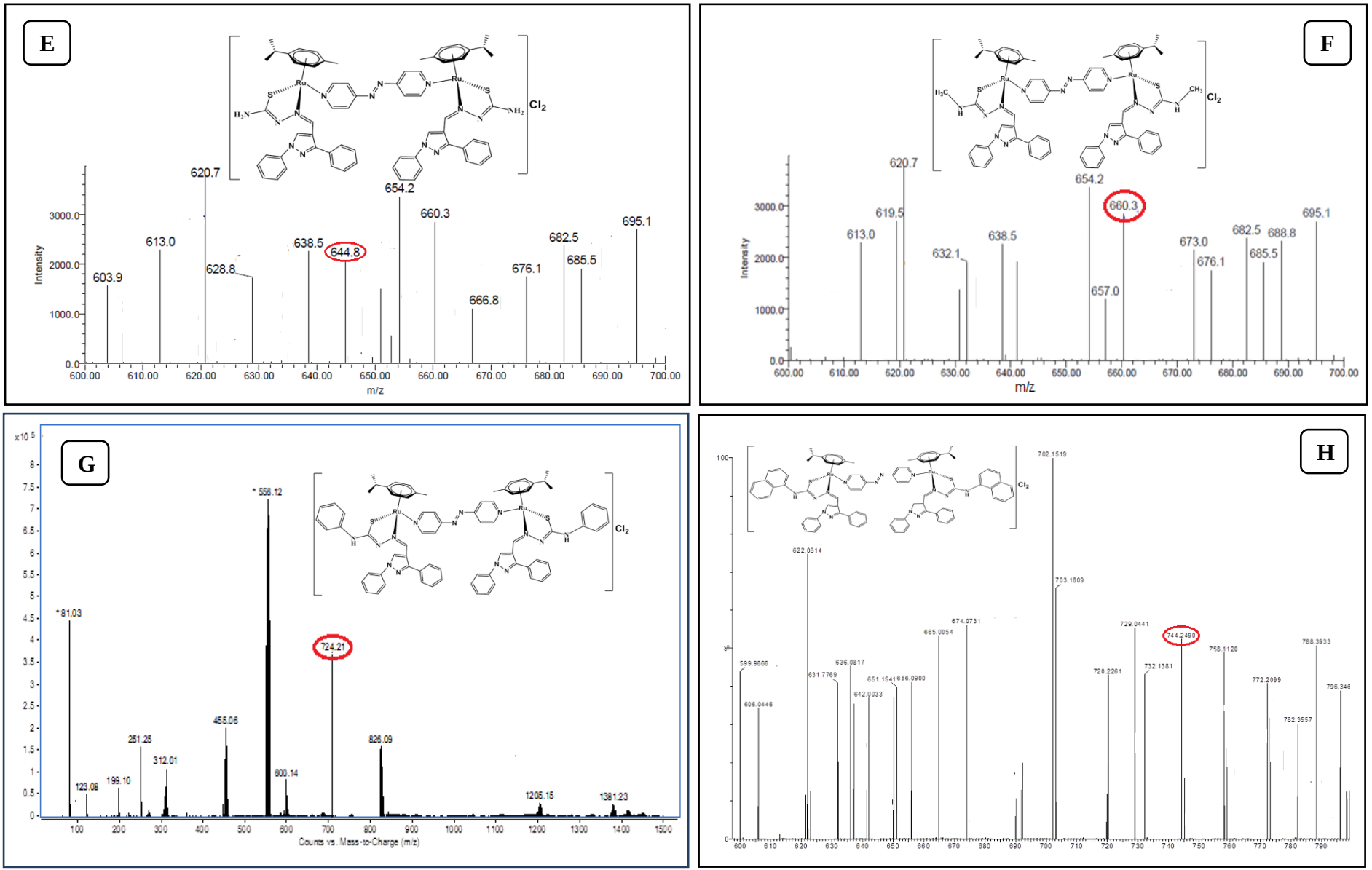

Fig. 3.4: *ESI-MS spectra of complexes (E)* ***C5*** *(F)* ***C6*** *(G)* ***C7*** *(H)* ***C8*** *indicating their molecular ion peak*

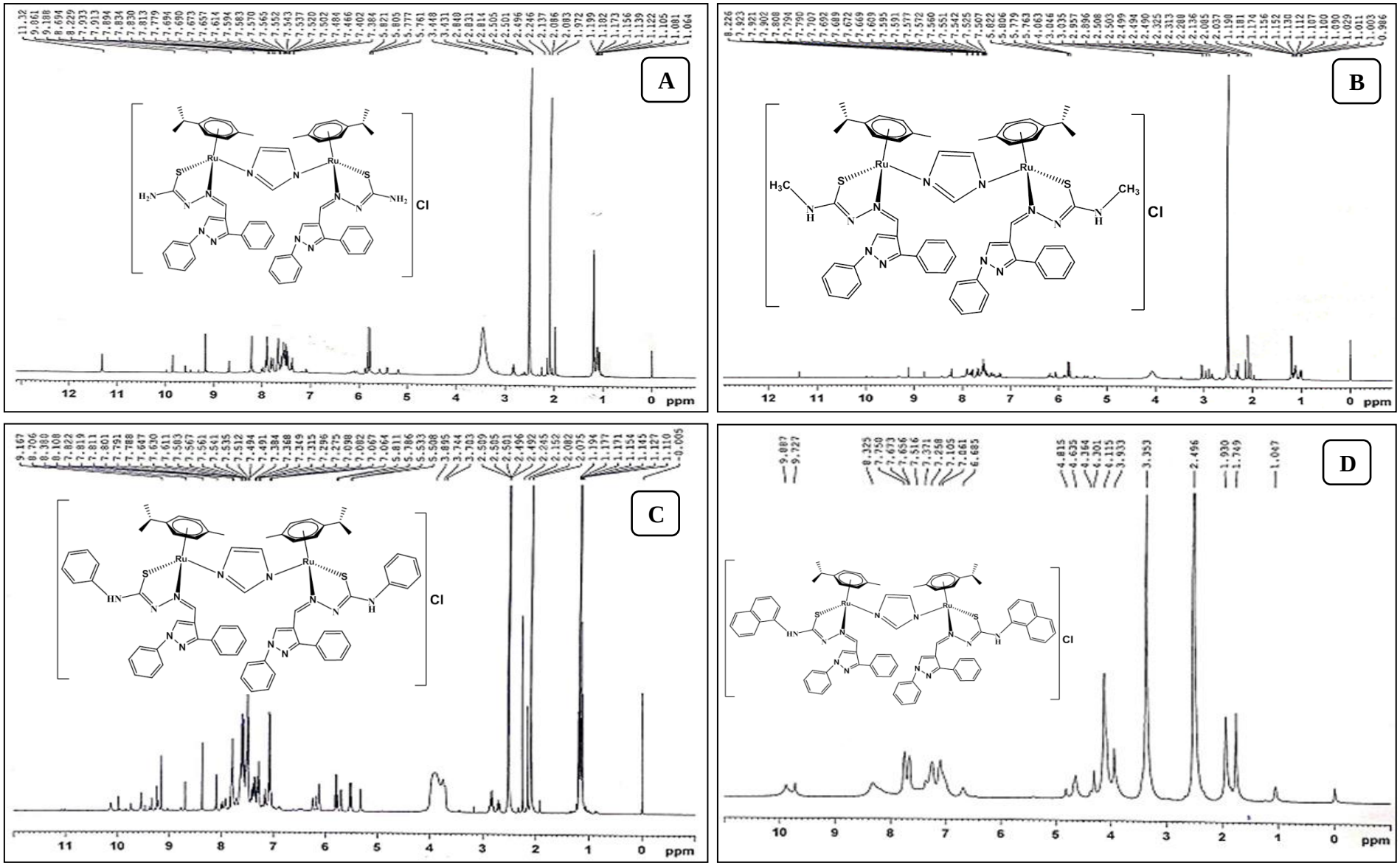

Fig. 3.5: *^{1}H NMR spectra of complexes (A)* ***C1*** *(B)* ***C2*** *(C)* ***C3*** *(D)* ***C4***

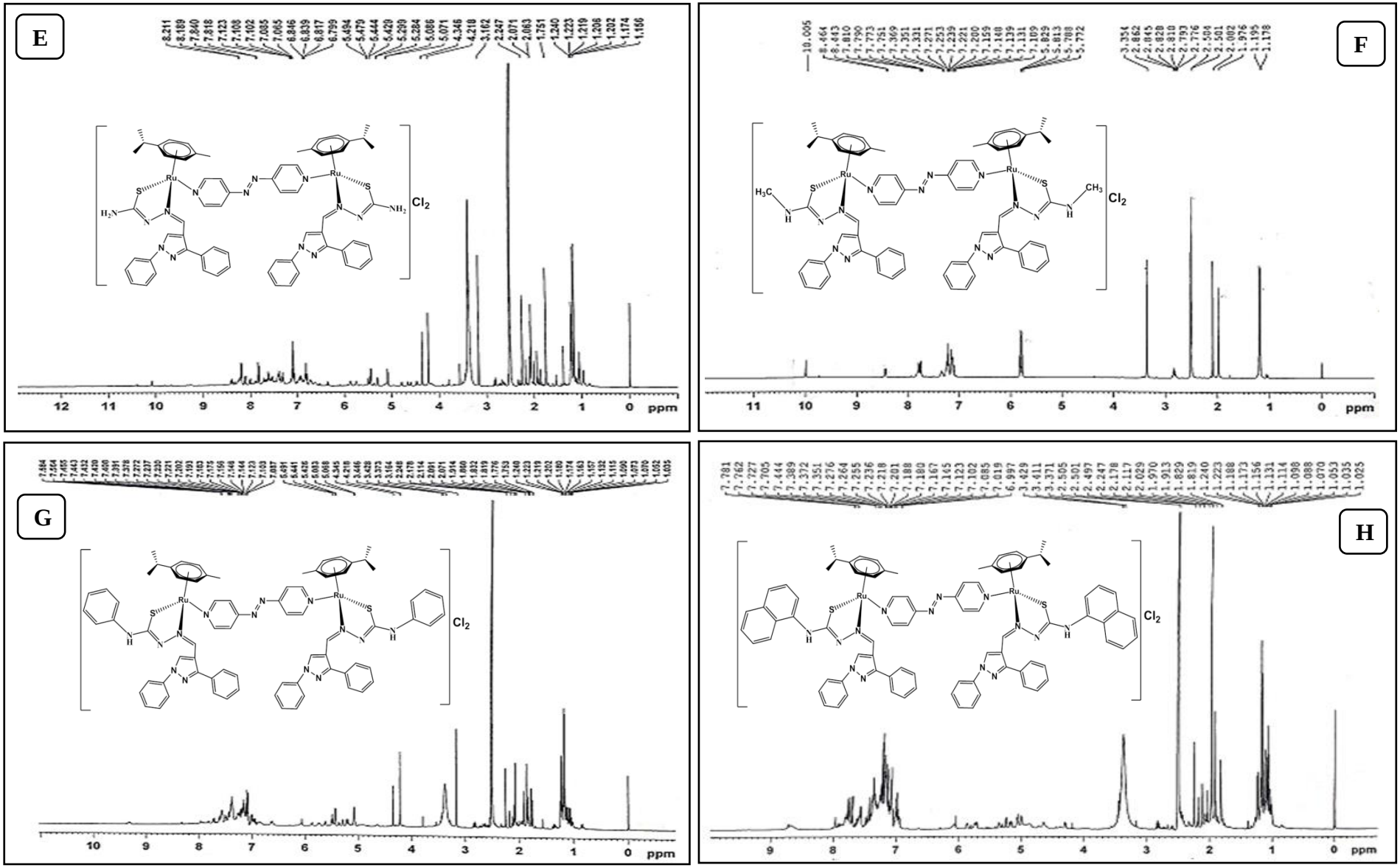

Fig. 3.6: *^{1}H NMR spectra of complexes (E)* ***C5*** *(F)* ***C6*** *(G)* ***C7*** *(H)* ***C8***

3.3.3 *Geometry optimization of [$Ru_2(\eta^6$-p-cym)$_2$(Diphenyl pyrazole thiosemicarbazone)$_2$(μ-im / azpy))]Cl_{1-2} complexes: (C1-C8)*

All calculations were performed using the approximations with dispersion correction (disp3) program. Full geometry optimizations of compounds were carried out using the DFT method at b-p functional and def2-SVP (def2-ecp for "Ru") basis set by employing Turbomole 6.4 suite of programs as mention above in section 3.2.1. This functional has been shown to give more accurate results for organometallic complexes. The DFT calculations for geometry optimization provide a great insight into the molecular structure. Optimized structures of the complexes **C1** and **C5** are shown in *Fig. 3.7*. Piano-stool type geometry is seen around each metal centre of the binuclear complexes with the Ru (II) ions π-bonded to the arene ring. The average Ru-Ru distance in the binuclear complexes with imidazole as bridging ligands is 6.14 A^0 whereas in binuclear complexes with 4, 4'azopyridine as bridging ligands is the average distance is 13.26 A^0 due to the presence of longer 4, 4'azopyridine ligand. The bond angle values reveal a pseudo octahedral coordination of the ruthenium centres. The metal–ligand bond lengths and bond angles tabulated in Table 3.4 are in well agreement with the values in the literature [38, 39].

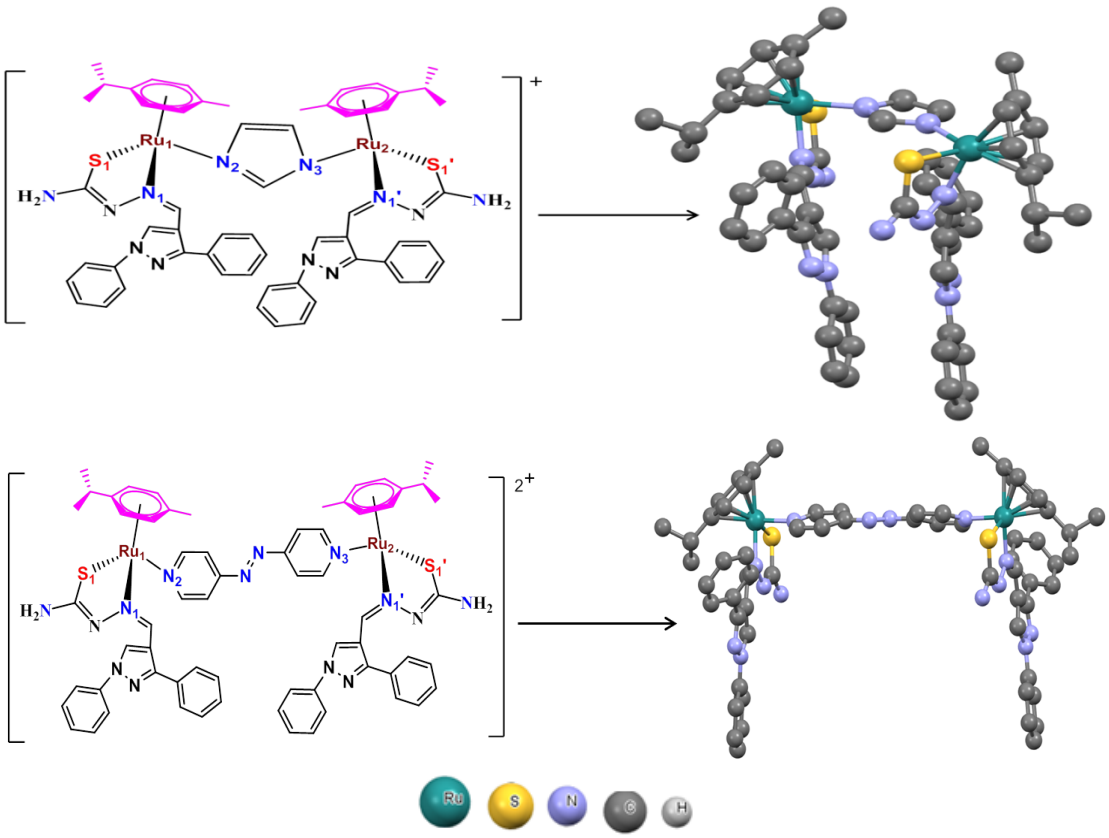

Fig. 3.7: *Optimized structures of the complexes* ***C1*** *and* ***C5***

Table 3.4: Metal ligand bond lengths and bond angles of complexes under study obtained from geometry optimization

Bond Length (in Å)	**L1**		**L2**		**L3**		**L4**	
	C1	**C5**	**C2**	**C6**	**C3**	**C7**	**C4**	**C8**
Ru1…….Ru2	6.15	13.29	6.17	13.26	6.13	13.26	6.11	13.26
Ru1-N1	2.09	2.10	2.09	2.09	2.09	2.09	2.09	2.09
Ru1-S1	2.36	2.36	2.37	2.36	2.36	2.36	2.36	2.37
Ru1-N2	2.09	2.10	2.09	2.10	2.09	2.10	2.08	2.09
Ru2-N1’	2.09	2.10	2.08	2.09	2.08	2.09	2.08	2.09
Ru2-S1’	2.39	2.36	2.42	2.36	2.40	2.36	2.40	2.37
Ru2-N3	2.09	2.10	2.10	2.10	2.10	2.10	2.10	2.09
Bond Angle (in degree)								
S1-Ru1-N1	80.9	81.1	80.7	81.2	81.0	81.1	81.1	81.0
S1-Ru1-N2	89.3	90.1	90.2	89.2	88.2	89.0	88.4	88.7
N1-Ru1-N2	81.2	84.6	84.2	84.3	83.0	84.6	83.4	84.4
S1’-Ru2-N1’	79.0	81.0	78.2	81.1	78.8	81.2	78.8	81.0
S1’-Ru2-N3	93.5	90.1	93.8	89.2	93.3	89.2	93.4	88.5
N1’-Ru2-N3	83.4	84.6	83.4	84.3	83.2	84.7	82.7	84.3

3.4 [Ru_2(μ-im /μ-azpy)(η^6-p-cym)$_2$(Diphenylpyrazole α-aminoacid)$_2$]Cl_{1-2} complexes: (C9-C16)

3.4.1 Synthesis and characterization:

*[Ru_2(μ-im) (η^6-p-cym)$_2$(**L5**)$_2$]Cl* **(C9)**:

μ-imidazole – bis ((1,3-diphenyl-1H-pyrazol-4-yl)methyl)tyrosine - bis 1-isopropyl-4-methyl benzene diruthenium(II) chloride

Yield: 73.3%; Molecular Weight 1400.4 g/mole; Molecular Formula $C_{73}H_{77}ClN_8O_6Ru_2$; Anal.: Found: C, 62.84; H, 5.30; N, 7.48. Calc.: C, 63.17; H, 5.58; N, 7.86. ESI-MS *m/z*: Obs (Calc): 1363.7 (1364.6) (M^+-1); δ_H (400 MHz, DMSO-d^6) 9.36, (s, 1H, -OH of tyrosine),7.02-7.93, (m, 4H, Ar-H of tyrosine);7.37, (tri, 1H, Ar-H); 7.54, (m,5H, Ar-H); 7.66, (d, 2H, *J* = 6.8 Hz, Ar-H); 7.78, (s, 1H, Ar-H); 7.82, (d, 2H, *J*= 7.6 Hz, Ar-H); 6.69-6.70, (m, 4H, *p*-cymAr-H); 2.07-2.35, (q, 1H, *p*-cym-*iso*-prop-CH); 1.98, (s, 3H, *p*-cym Ar-CH_3), 1.06, (d, 6H, *p*-cym-*iso*-prop-$(CH_3)_2$); 7.91, (d, 2H, imidazole CH=CH); FTIR (KBr/ cm^{-1}): $\nu_{(O-H)}$ 3431, $\nu_{(Ar)C-H}$ 2961, $\nu_{(N-H)}$ 3061, ν_{COO}assym1599, ν_{COO}sym1389, $\Delta\nu_{COO}$ 210; $\Lambda_M(\Omega^{-1}.m^2.M^{-1})$ 76.

*[Ru_2(μ-im) (η^6-p-cym)$_2$(**L6**)$_2$]Cl* **(C10)**:

μ-imidazole – bis ((1,3-diphenyl-1H-pyrazol-4-yl)methyl)phenylalanine - bis 1-isopropyl-4-methyl benzene diruthenium(II) chloride

Yield: 77.5%; Molecular Weight 1386.1 g/mole; Molecular Formula $C_{73}H_{77}ClN_8O_4Ru_2$; Anal. Found: C, 64.31; H, 5.50; N, 7.68. Calc.: C, 64.62; H, 5.71; N, 8.04. ESI-MS *m/z*: Obs (Calc): 1330.3 (1332.6) (M^+-2); δH(400 MHz, DMSO-d^6) 7.76-7.90, (m, 5H, Ar-H of phenylalanine); 7.52, (tri, 1H, Ar-H); 7.58, (m,5H, Ar-H); 7.71, (d, 2H, *J* = 6.8 Hz, Ar-H); 7.76, (s, 1H, Ar-H); 7.81, (d, 2H, *J*= 7.6 Hz, Ar-H); 5.77-5.83, (m, 4H, *p*-cymAr-H); 2.49-2.85, (q, 1H, *p*-cym-*iso*-prop-CH); 1.19, (s, 3H, *p*-cym Ar-CH_3); 1.06, (d, 6H, *p*-cym-*iso*-prop-$(CH_3)_2$); 8.95, (d, 2H, imidazole CH=CH); FTIR (KBr/ cm^{-1}): $\nu_{(Ar)C-H}$ 2969, $\nu_{(N-H)}$ 3058, ν_{COO}assym1598, ν_{COO}sym1359, $\Delta\nu_{COO}$ 239; $\Lambda_M(\Omega^{-1}.m^2.M^{-1})$ 75.

[Ru_2(μ-im) (η^6-p-cym)$_2$(L7)$_2$]Cl **(C11):**

μ-imidazole – bis ((1,3-diphenyl-1H-pyrazol-4-yl)methyl)leucine - bis 1-isopropyl-4-methyl benzene diruthenium(II) chloride

Yield: 69.7%; Molecular Weight 1300.0 g/mole; Molecular Formula $C_{67}H_{81}ClN_8O_4Ru_2$; Anal. Found: C, 62.26; H, 5.91; N, 8.08. Calc.: C, 62.50; H, 6.31; N, 8.45. ESI-MS *m/z*: Obs (Calc): 1263.9 (1264.6) (M^+-1); δH(400 MHz, DMSO-d^6) 1.59, (d, 6H, leucine-iso-prop-$(CH_3)_2$); 7.39, (tri, 1H, Ar-H); 7.54, (m,5H, Ar-H); 7.60, (d, 2H, *J* = 6.8 Hz, Ar-H); 7.89, (s, 1H, Ar-H); 7.85, (d, 2H, *J*= 7.6 Hz, Ar-H); 5.77-5.82, (m, 4H, *p*-cymAr-H); 2.49-2.78, (q, 1H, *p*-cym-*iso*-prop-CH); 2.07, (s, 3H, *p*-cym Ar-CH_3); 1.59, (d, 6H, *p*-cym-*iso*-prop-$(CH_3)_2$); 8.80, (d, 2H, imidazole CH=CH); FTIR (KBr/ cm^{-1}): $\nu_{(Ar)C-H}$ 2966, $\nu_{(N-H)}$ 3061, $\nu_{COOasym}$1599, ν_{COOsym}1361, $\Delta\nu_{COO}$ 238; $\Lambda_M(\Omega^{-1}.m^2.M^{-1})$ 72.

$[Ru_2(\mu\text{-}im)\ (\eta^6\text{-}p\text{-}cym)_2(\mathbf{L8})_2]Cl$ **(C12)**:

μ-imidazole – bis ((1,3-diphenyl-1H-pyrazol-4-yl)methyl)tryptophan - bis 1-isopropyl-4-methyl benzene diruthenium(II) chloride

Yield: 76.8%; Molecular Weight 1446.1 g/mole; Molecular Formula $C_{77}H_{79}ClN_{10}O_4Ru_2$; Anal. Found: C, 64.10; H, 5.27; N, 9.12. Calc.: C, 64.45; H, 5.55; N, 9.51. ESI-MS *m/z*: Obs (Calc): 1407.8 (1409.7) (M^+-2); δH(400 MHz, DMSO-d^6) 11.08, (s, 1H, indolinic N-H of tryptophan); 7.38, (tri, 1H, Ar-H); 7.57, (m,5H, Ar-H); 7.66, (d, 2H, *J* = 6.8 Hz, Ar-H); 7.68, (s, 1H, Ar-H); 7.83, (d, 2H, *J*= 7.6 Hz, Ar-H); 5.83-6.99 (m, 4H, *p*-cymAr-H), 3.34-3.39, (q, 1H, *p*-cym-*iso*-prop-CH), 2.51, (s, 3H, *p*-cym Ar-CH_3); 2.08, (d, 6H, *p*-cym-*iso*-prop-$(CH_3)_2$); 8.67, (d, 2H, imidazole CH=CH); FTIR (KBr/cm^{-1}): $\nu_{(Ar)C-H}$ 2960, $\nu_{(N-H)}$ 3054, $\nu_{COOassym}$1598, ν_{COOsym}1392, $\Delta\nu_{COO}$ 206; $\Lambda_M(\Omega^{-1}.m^2.M^{-1})$ 71.

$[Ru_2(\mu\text{-}azpy)\ (\eta^6\text{-}p\text{-}cym)_2(\mathbf{L5})_2]Cl_2$ ***(C13)****:*

μ-4,4'azopyridine – bis ((1,3-diphenyl-1H-pyrazol-4-yl)methyl)tyrosine - bis 1-isopropyl-4-methyl benzene diruthenium(II) dichloride

Yield: 83.7%; Molecular Weight 1552.6 g/mole; Molecular Formula $C_{80}H_{82}Cl_2N_{10}O_6Ru_2$; Anal.: C, 62.24; H, 5.09; N, 8.61. Calc.: C, 62.39; H, 5.36; N, 8.87. ESI-MS *m/z*: Obs (Calc): 739.7 (740.9) (M^{2+}-1); δ_H (400 MHz, DMSO-d^6) 9.96, (s, 1H, -OH of tyrosine); 7.21-7.33, (m, 4H, Ar-H of tyrosine); 7.02, (tri, 1H, Ar-H); 7.37, (m,5H, Ar-H); 7.18, (d, 2H, *J* = 6.7 Hz, Ar-H); 8.41, (s, 1H, Ar-H); 8.39, (d, 2H, *J*= 7.6 Hz, Ar-H); 6.16 – 6.99, (m, 4H, *p*-cymAr-H); 2.77-2.86, (q, 1H, *p*-cym-*iso*-prop-CH); 2.08, (s, 3H, *p*-cym Ar-CH_3); 1.19, (d, 6H, *p*-cym-*iso*-prop-$(CH_3)_2$); FTIR (KBr/cm^{-1}): $\nu_{(O-H)}$ 3426, $\nu_{(Ar)C-H}$ 2961, $\nu_{(N-H)}$ 3058, $\nu_{COOassym}$ 1596, ν_{COOsym} 1363, $\Delta\nu_{COO}$ 233, $\nu_{N=N}$ 1410; $\Lambda_M(\Omega^{-1}.m^2.M^{-1})$ 167.

$[Ru_2(\mu\text{-}azpy)\ (\eta^6\text{-}p\text{-}cym)_2(\mathbf{L6})_2]Cl_2$ **(C14)**:

μ-4,4'azopyridine–bis((1,3-diphenyl-1H-pyrazol-4-yl)methyl)phenylalanine - bis 1-isopropyl-4-methyl benzene diruthenium(II) dichloride

Yield: 68.9 %; Molecular Weight 1520.6 g/mole; Molecular Formula $C_{80}H_{82}Cl_2N_{10}O_4Ru_2$; Anal.: C, 63.31; H, 5.19; N, 8.72. Calc.: C, 63.68; H, 5.47; N,9.06, ESI-MS *m/z*: Obs (Calc): 723.9 (724.9) (M^{2+}-1) ; δ_H (400 MHz, DMSO-d^6) 7.20-7.44, (m, 5H, Ar-H of phenylalanine); 7.27, (tri, 1H, Ar-H); 7.37, (m,5H, Ar-H); 7.39, (d, 2H, *J* = 5.8 Hz, Ar-H); 7.45, (s, 1H, Ar-H); 7.58, (d, 2H, *J*= 7.6 Hz, Ar-H); 5.06-5.49, (m, 4H, *p*-cymAr-H); 2.24-3.14, (q, 1H, *p*-cym-*iso*-prop-CH); 1.91, (s, 3H, *p*-cym Ar-CH_3); 1.02, (d, 6H, *p*-cym-*iso*-prop-$(CH_3)_2$); FTIR (KBr/cm^{-1}): $\nu_{(Ar)C-H}$ 2960, $\nu_{(N-H)}$ 3057, $\nu_{COOassym}$ 1598, ν_{COOsym} 1357, $\Delta\nu_{COO}$ 241, $\nu_{N=N}$ 1408; Λ_M($\Omega^{-1}.m^2.M^{-1}$) 162.

$[Ru_2(\mu\text{-azpy})\ (\eta^6\text{-p-cym})_2(\boldsymbol{L7})_2]Cl_2$ **(C15)**:

μ-4,4'azopyridine–bis((1,3-diphenyl-1H-pyrazol-4-yl)methyl)leucine-bis1-isopropyl-4-methyl benzene diruthenium(II) dichloride

Yield: 82.7%; Molecular Weight 1452.6 g/mole; Molecular Formula $C_{74}H_{86}Cl_2N_{10}O_4Ru_2$; Anal.: C, 61.45; H, 5.82; N, 9.53. Calc.: C, 61.73; H, 6.0; N, 9.47, ESI-MS *m/z*: Obs (Calc): 690.6 (690.9) (M^{2+}); δ_H(400 MHz, DMSO-d^6) 8.89, (tri, 1H, Ar-H); 8.86, (m,5H, Ar-H); 7.96, (d, 2H, *J* = 6.8 Hz, Ar-H); 7.92, (s, 1H, Ar-H); 7.82, (d, 2H, *J*= 7.6 Hz, Ar-H); 5.77-5.82, (m, 4H, *p*-cymAr-H); 2.80-2.85, (q, 1H, *p*-cym-*iso*-prop-CH); 2.07, (s, 3H, *p*-cym Ar-CH_3); 1.17, (d, 6H, *p*-cym-*iso*-prop-$(CH_3)_2$); 1.32, (d, 6H,leucine-iso-prop-$(CH_3)_2$); FTIR (KBr/cm^{-1}): $\nu_{(Ar)C-H}$ 2957, $\nu_{(N-H)}$ 3058, ν_{COO}assym 1605, ν_{COO}sym 1388, $\Delta\nu_{COO}$ 217, $\nu_{N=N}$ 1450, Λ_M ($\Omega^{-1}.m^2.M^{-1}$) 168.

$[Ru_2(\mu\text{-azpy})\ (\eta^6\text{-p-cym})_2(\boldsymbol{L8})_2]Cl_2$ **(C16)**:

μ-4,4'azopyridine–bis((1,3-diphenyl-1H-pyrazol-4-yl)methyl)tryptophan - bis 1-isopropyl-4-methyl benzene diruthenium(II) dichloride

Yield: 79.4%; Molecular Weight 1589.7 g/mole; Molecular Formula $C_{84}H_{84}Cl_2N_{12}O_4Ru_2$; Anal.: C, 63.23; H, 5.02; N, 10.09. Calc.: C, 63.58; H, 5.34; N, 10.35. ESI-MS *m/z*: Obs (Calc): 764.2 (763.9) (M^{2+}+1); δ_H (400 MHz, DMSO-d^6) 9.88 (s, 1H, indolinic N-H of tryptophan), 7.37, (tri, 1H, Ar-H); 7.51, (m,5H, Ar-H); 7.65, (d, 2H, *J* = 5.2 Hz, Ar-H); 7.67, (s, 1H, Ar-H); 7.75, (d, 2H, *J*= 8.6 Hz, Ar-H); 6.68-7.01, (m, 4H, *p*-cymAr-H); 1.93-2.49, (q, 1H, *p*-cym-*iso*-prop-CH); 1.74, (s, 3H, *p*-cym Ar-CH_3); 1.04, (d, 6H, *p*-cym-*iso*-prop-

$(CH_3)_2$); FTIR (KBr/cm^{-1}): $\nu_{(Ar)C-H}$ 2961, $\nu_{(N-H)}$ 3055, $\nu_{COOassym}$ 1600, ν_{COO}sym 1353, $\Delta\nu_{COO}$ 247, $\nu_{N=N}$ 1452; $\Lambda_M(\Omega^{-1}.m^2.M^{-1})$ 163.

3.4.2 Results and discussion:

The electronic absorption spectra of the complexes C**9-16** (*Fig. 3.8*) show two major bands in the wavelength range 200-600 nm. The free ligands display intense absorption bands at 221–223 nm assigned to the intra-ligand π→π* transition of the aromatic rings of *p*-cymene as well the pyrazolyl ligands which were shifted to longer wavelength region at 227–230 nm in the complexes due to coordination. A second sharp but medium intensity peak found in the range of 270-272 nm owing to the intraligand N, O centred *n*→π* transitions have shifted to slightly higher wavelength range of 273-278 nm. This shift in the wavelength indicates coordination of the ligand to the metal centre via N, O donor atoms. The λ_{max} values of all the transitions have been tabulated in Table 3.5. The octahedral environment around the ruthenium atom was conformed from the electronic spectra of all the complexes [40].

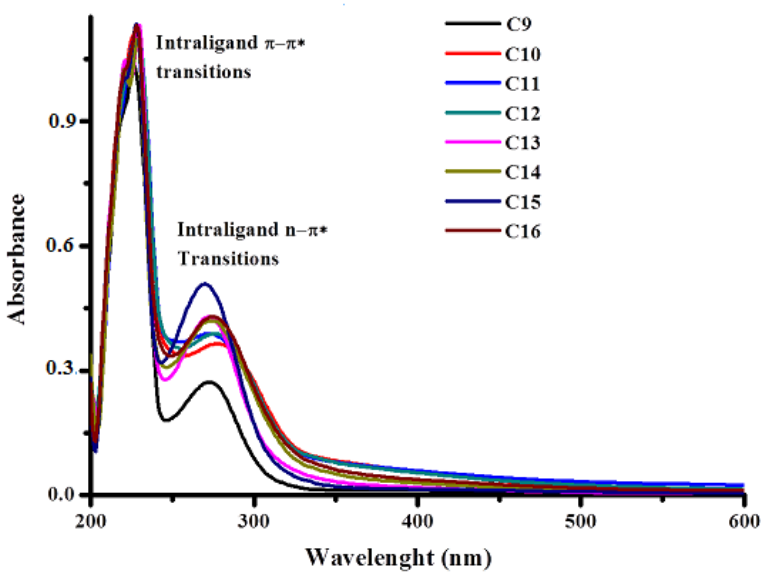

Fig. 3.8 *UV-Vis spectra of complexes*

Table 3.5: UV-Vis. peak assignments of complexes

Code	C9	C10	C11	C12	C13	C14	C15	C16
Intra-ligand transitions(nm) π-π*	229	229	227	228	227	228	228	228
Intra-ligand transitions(nm) n-π*	273	278	276	276	275	269	270	274

The m/z values obtained in the ESI-Mass spectra (*Fig 3.9* and *3.10*) of **C9-16** indicate that a tri coordinated *p*-cymene, a bi coordinated amino acid conjugated diphenylpyrazol ligand and a mono coordinated imidazole / 4, 4'-azopyridine are bound to each of the metal centres, thereby resulting in the formation of binuclear complex ions with +1 / +2 charges. The complexes are stable in methanol as evidenced from their ESI-MS spectra showing essentially the molecular ion peak. The molecular ion peaks have been provided in Table 3.6. The complexes **C9-12** have molar conductance (10^{-3}M in DMSO) in the range of 71-76 (Ω^{-1} m^2 M^{-1}) and **C13-16** have molar conductance 162-168 (Ω^{-1} m^2 M^{-1}) at 38 ˚C suggesting 1:1 and 1:2 electrolytic behaviour respectively [32].

Table 3.6: m/z values of complexes

Code	**C9**	**C10**	**C11**	**C12**	**C13**	**C14**	**C15**	**C16**
Calculated Mass (g/mol)	1364.6	1332.6	1264.6	1409.7	740.9	724.9	690.9	763.9
Observed Mass (g/mol)	1363.7 (M^+-1)	1330.3 (M^+-2)	1263.9 (M^+-1)	1407.8 (M^+-2)	739.7 (M^{2+}-1)	723.9 (M^{2+}-1)	690.6 (M^{2+})	764.2 (M^{2+}+1)

The IR spectra of the complexes **C9-16** displayed characteristic strong stretching bands at 1596-1605 cm^{-1}due to asymmetric and weaker bands at 1353-1392 cm^{-1} due to $\nu_{C=O}$ stretch of the conjugated amino acids respectively which were found as strong bands in the fingerprint region at 1595-1616 cm^{-1} in the spectra of free ligands. A monodentate coordination mode of the carboxylate group of the ligands to the metal ion is indicated by the separation frequency ($\Delta\nu = \nu_{asym(COO)}-\nu_{sym(COO)}$) values which fall in the range 206 – 247 cm^{-1} [41, 42]. The broad O-H stretching bands of free carboxylic acid group found in the ligands were not observed in the IR spectra of the complexes indicating complexation via the carboxylate oxygen. Furthermore the N-H stretching bands were found shifted from 3058-3334 cm^{-1} in the ligands to 3027-3068 cm^{-1} in **C9-16** indicating complexation of the ligands via the nitrogen of the secondary amine. The bands owing to aromatic ν_{C-H} stretch (2957-2969 cm^{-1}) and aromatic $\nu_{C=C}$ in-plane vibrations (~1450-1629 cm^{-1}) indicative of presence of p-cymene in the complexes were also observed. The overall changes in the IR spectra suggest that the diphenylpyrazol α-Amino acids derivatives act as monoanionic bidentate ligands interacting with the metal centres via nitrogen of the secondary amine and carboxylate oxygen.

The ^{1}H NMR spectra of C**9-16** (*Figs. 3.11* and *3.12*) show distinct peaks corresponding to *p*-cymene. The aromatic protons present in the pyrazole ring are observed in the excepted region. The peaks arising due to carboxylic O-H and N-H of secondary amine in the free ligands (section 2.3.4) are no longer seen in the NMR spectra of the complexes indicating coordination of the carboxylate oxygen and secondary amine nitrogen to the ruthenium metal centres. The protons present in the bridging ligand 4, 4'- azopyridine are showing upfield shifts at δ = 7.36 – 8.31ppm which appeared at δ = 7.75 – 8.89 ppm in NMR spectra of free 4,4'- azopyridine [37], suggesting the co-ordination of the Ru metal centres with 4,4'-azopyridine in **C13-16**.

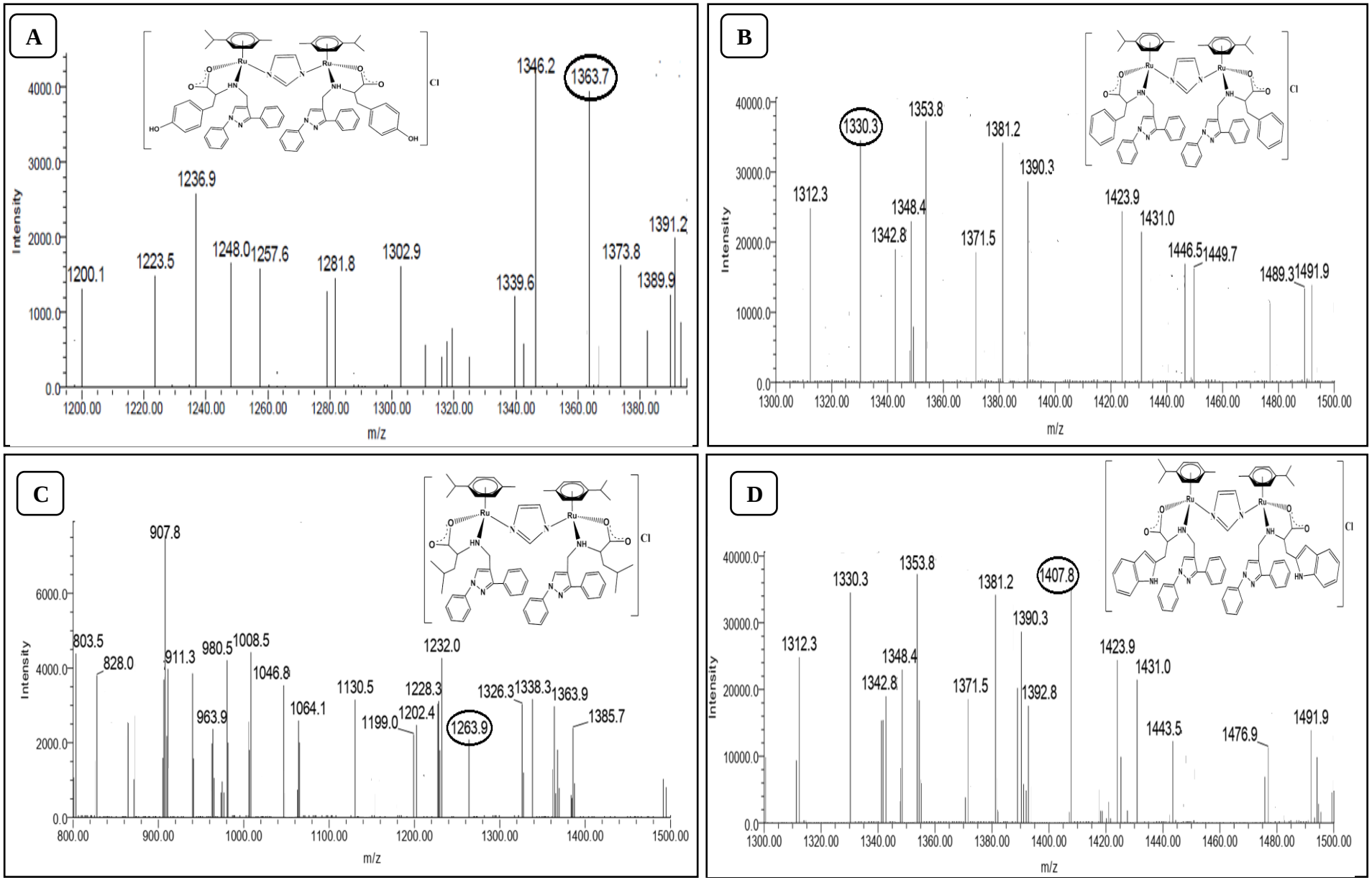

Fig. 3.9: *ESI-MS spectra of complexes (A)* ***C9*** *(B)* ***C10*** *(C)* ***C11*** *(D)* ***C12*** *indicating their molecular ion Peak*

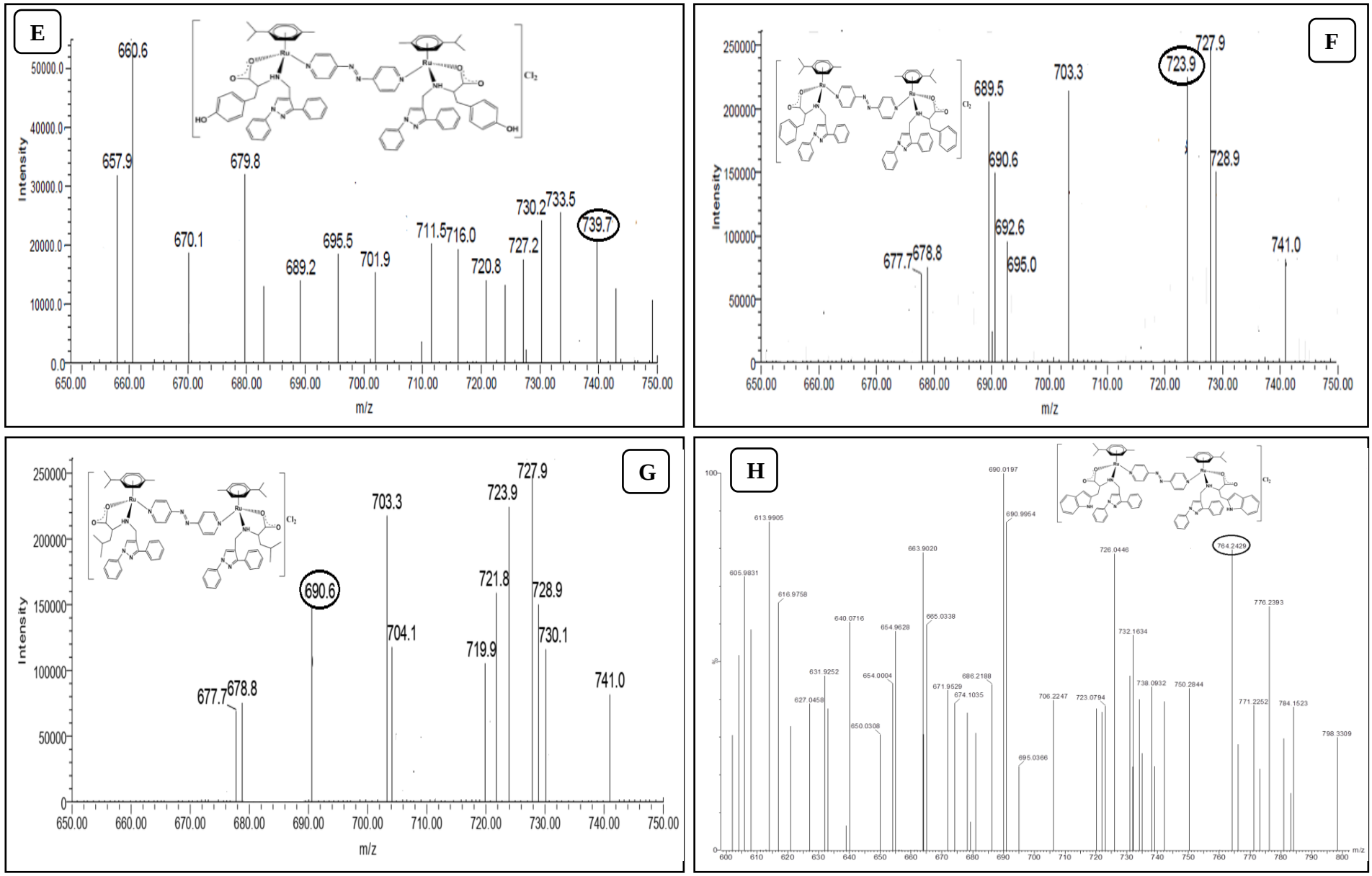

Fig. 3.10: *ESI-MS spectra of complexes (E)* ***C13*** *(F)* ***C14*** *(G)* ***C15*** *(H)* ***C16*** *indicating their molecular ion peak*

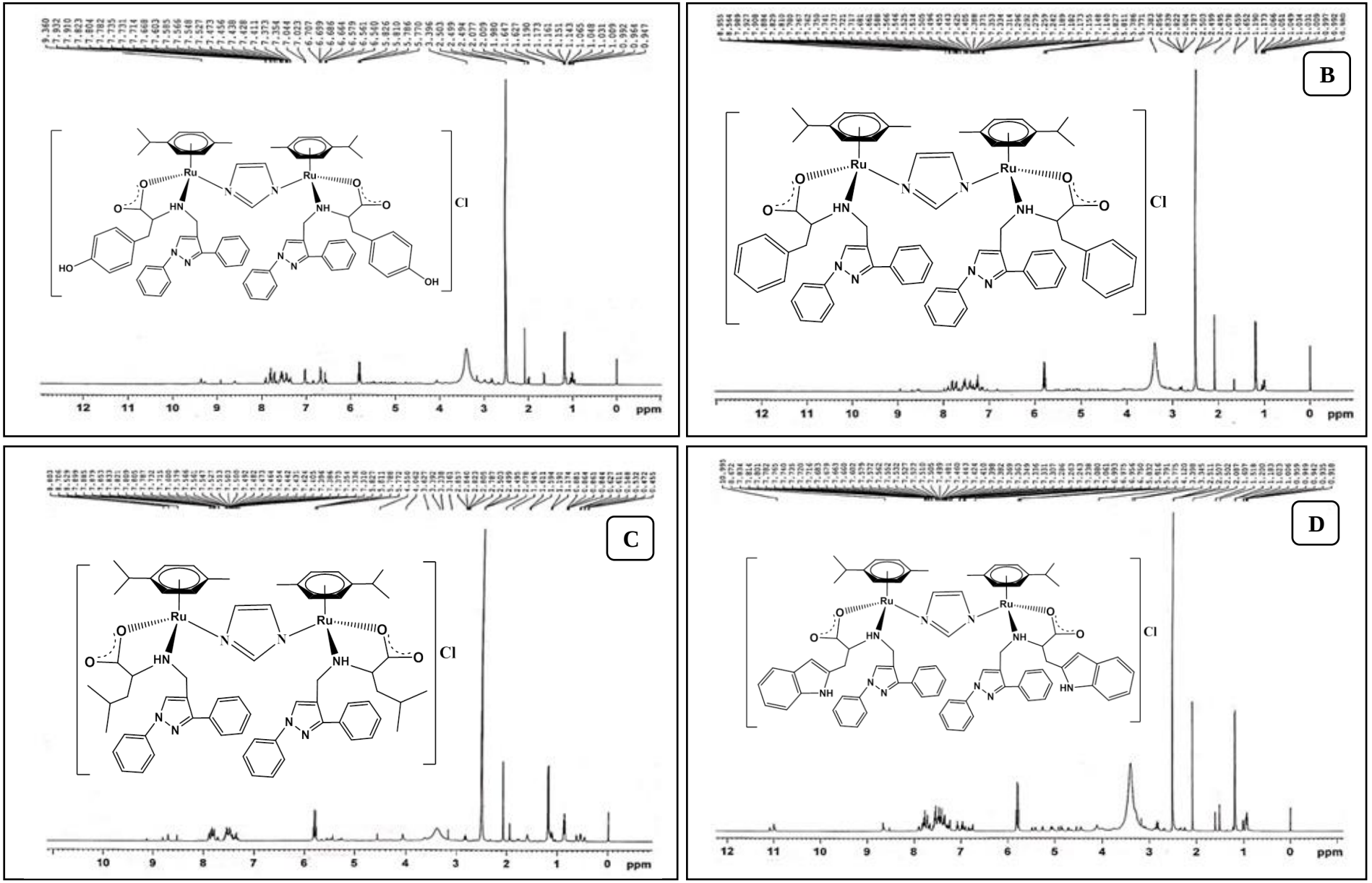

Fig. 3.11: *^{1}H NMR spectra of complexes (A)* ***C9*** *(B)* ***C10*** *(C)* ***C11*** *(D)* ***C12***

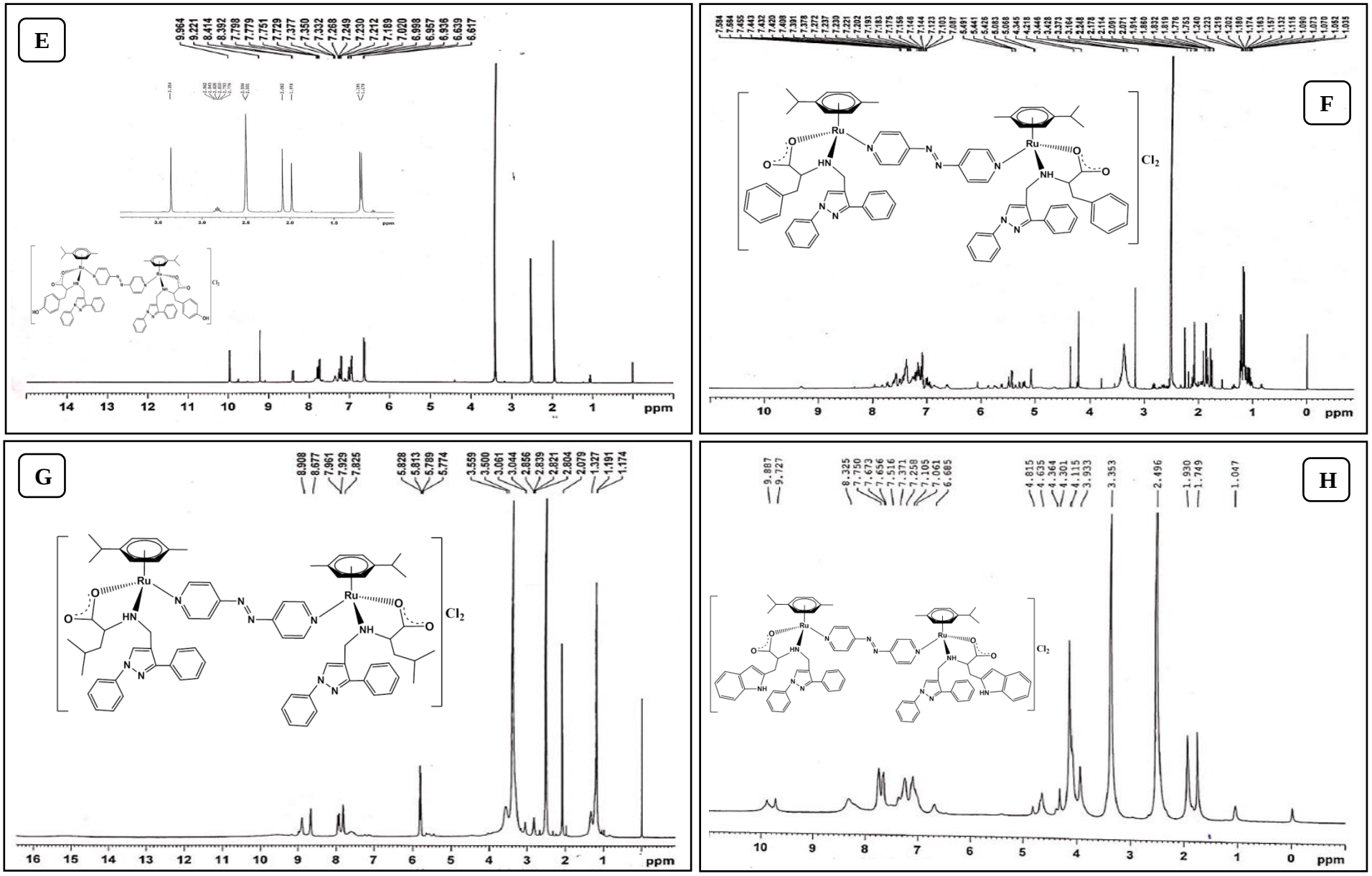

Fig. 3.12: *^{1}H NMR spectra of complexes (E)* ***C13*** *(F)* ***C14*** *(G)* ***C15*** *(H)* ***C16***

3.5 [Ru_2 (μ-im /μ-azpy)(η^6-p-cym)$_2$(Ferrocenyl thiosemicarbazones)$_2$]Cl_{1-2} complexes : (C17-C24)

3.5.1 Synthesis and characterization:

*[Ru_2(μ-im) (η^6-p-cym)$_2$(**L9**)$_2$]Cl* **(C17)**:

μ-imidazole–bis(bis(η^5-cyclopentadienyl)iron (II)-thiosemicarbazone)–bis-1-isopropyl-4-methyl benzene diruthenium(II) chloride

Yield: 52.9%; Molecular Weight 1146.5 g/mole; Molecular Formula $C_{47}H_{56}ClFe_2N_8Ru_2S_2$; Anal.: C, 48.84; H, 4.52; N, 9.37. Calc.: C, 49.24; H, 4.92; N, 9.77. ESI-MS *m/z*: Obs (Calc): 1111.2 (1112.0) (M^+-1) ; δ_H(400 MHz, DMSO-d^6) 4.32, (t, 2H, substituted cyclopentadiene); 4.68, (t, 2H, substituted cyclopentadiene); 4.42, (s, 5H, cyclopentadiene); 6.68-5.98, (m, 4H, *p*-cymAr-H); 2.49-2.34, (q, 1H, *p*-cym-*iso*-prop-CH); 1.98, (s, 3H, *p*-cym Ar-CH_3); 1.04, (d, 6H, *p*-cym-*iso*-prop-$(CH_3)_2$); 7.76, (d, 2H, imidazole CH=CH); FTIR (KBr/ cm^{-1}): $\nu_{(Ar)C-H}$ 2993, $\nu_{(NH2)}$ 3194, $\nu_{(C=N)}$1597, $\nu_{(C-S)}$ 756; Λ_M($\Omega^{-1}.m^2.M^{-1}$) 84.

*[Ru_2 (μ-im) (η^6-p-cym)$_2$(**L10**)$_2$]Cl* **(C18)**:

μ-imidazole–bis(bis(η^5-cyclopentadienyl)iron(II)-4-methyl-3-thiosemicarbazone)-bis-1-isopropyl-4-methyl benzene diruthenium(II) chloride

Yield: 67.8%; Molecular Weight 1175.1 g/mole; Molecular Formula $C_{49}H_{60}ClFe_2N_8Ru_2S_2$; Anal. Found: C, 49.76; H, 4.76; N, 9.14. Calc.: C, 50.11; H, 5.15; N, 9.54. ESI-MS *m/z*: Obs (Calc): 1141.2 (1140.1) (M^++1); δH(400 MHz, DMSO-d^6) 4.35, (t, 2H, substituted cyclopentadiene); 4.69, (t, 2H, substituted cyclopentadiene); 4.46, (s, 5H, cyclopentadiene); 5.83-5.76, (m, 4H, *p*-cymAr-H); 2.86-2.79, (q, 1H, *p*-cym-*iso*-prop-CH); 2.50, (s, 3H, *p*-cym Ar-CH_3); 1.19, (d, 6H, *p*-cym-*iso*-prop-$(CH_3)_2$); 7.83, (d, 2H, imidazole CH=CH); FTIR (KBr/ cm^{-1}): $\nu_{(Ar)C-H}$ 2959, $\nu_{(NH-CH3)}$ 3427, $\nu_{(C=N)}$1582, $\nu_{(C-S)}$748; Λ_M($\Omega^{-1}.m^2.M^{-1}$) 85.

*[Ru_2(μ-im) (η^6-p-cym)$_2$(**L11**)$_2$]Cl* **(C19)**

μ-imidazole–bis(bis(η^5-cyclopentadienyl)iron(II)-4-phenyl-3-thiosemicarbazone)-bis-1-isopropyl-4-methyl benzene diruthenium(II) chloride

Yield: 58.2%; Molecular Weight 1299.1g/mole; Molecular Formula $C_{59}H_{64}ClFe_2N_8Ru_2S_2$; Anal. Found: C, 54.28; H, 4.62; N, 8.24. Calc.: C, 54.57; H, 4.97; N, 8.63. ESI-MS *m/z*:Obs (Calc): 1263.2 (1264.5) (M^+-1); δH (400 MHz, DMSO-d^6) 4.36, (t, 2H, substituted cyclopentadiene); 4.63, (t, 2H, substituted cyclopentadiene); 4.48, (s, 5H, cyclopentadiene); 5.97-5.78, (m, 4H, *p*-cymAr-H); 2.91-2.68, (q, 1H, *p*-cym-*iso*-prop-CH); 2.19, (s, 3H, *p*-cym

Ar-CH_3); 1.16, (d, 6H, *p*-cym-*iso*-prop-$(CH_3)_2$); 7.98, (d, 2H, imidazole CH=CH); FTIR (KBr/ cm^{-1}): $\nu_{(Ar)C-H}$ 2978, $\nu_{(NH-C6H5)}$ 3039, $\nu_{(C=N)}$1597, $\nu_{(C-S)}$ 802; $\Lambda_M(\Omega^{-1}.m^2.M^{-1})$ 89.

*[Ru_2(μ-im) (η^6-p-cym)$_2$(**L12**)$_2$]Cl* **(C20)**:

μ-imidazole–bis(bis(η^5-cyclopentadienyl)iron (II)-4-(naphthalen-1-yl)-3-thiosemicarbazone)-bis 1-isopropyl-4-methyl benzene diruthenium(II) chloride

Yield: 68.7%; Molecular Weight 1399.1 g/mole; Molecular Formula $C_{67}H_{68}ClFe_2N_8Ru_2S_2$; Anal. Found: C, 57.19; H, 4.66; N, 7.86. Calc.: C, 57.53; H, 4.90; N, 8.01. ESI-MS *m/z*: Obs (Calc): 1363.8. (1364.2) (M^+-1); δH (400 MHz, DMSO-d^6) 4.34, (t, 2H, substituted cyclopentadiene); 4.59, (t, 2H, substituted cyclopentadiene); 4.21, (s, 5H, cyclopentadiene); 5.43-5.33, (m, 4H, *p*-cymAr-H); 3.37-3.16, (q, 1H, *p*-cym-*iso*-prop-CH); 2.24, (s, 3H, *p*-cym Ar-CH_3); 1.91, (d, 6H, *p*-cym-*iso*-prop-$(CH_3)_2$); 7.58, (d, 2H, imidazole CH=CH); FTIR (KBr/cm^{-1}): $\nu_{(Ar)C-H}$ 2959, $\nu_{(NH-C10H7)}$ 3411, $\nu_{(C=N)}$ 1578, $\nu_{(C-S)}$ 775; $\Lambda_M(\Omega^{-1}.m^2.M^{-1})$ 86.

*[Ru_2(μ-azpy)(η^6-p-cym)$_2$(**L9**)$_2$]Cl_2* **(C21)**:

μ-4,4'azopyridine–bis(bis(η^5-cyclopentadienyl)iron(II)-thiosemicarbazone)-bis1-isopropyl-4-methylbenzene diruthenium(II) dichloride

Yield: 71.1%; Molecular Weight 1298.1 g/mole; Molecular Formula $C_{54}H_{60}Fe_2N_{10}Cl_2Ru_2S_2$; Anal.: C, 52.21; H, 4.11; N, 11.97. Calc.: C, 52.86; H, 4.93; N, 11.41. ESI-MS *m/z*: Obs (Calc): 611.4 (612.5) (M^{2+}+1); δ_H (400 MHz, DMSO-d^6) 4.30, (t, 2H, substituted cyclopentadiene); 4.56, (t, 2H, substituted cyclopentadiene); 4.37, (s, 5H, cyclopentadiene); 4.99-4.86, (m, 4H, *p*-cymAr-H); 3.16-3.15, (q, 1H, *p*-cym-*iso*-prop-CH), 1.99, (s, 3H, *p*-cym Ar-CH_3); 1.03, (d, 6H, *p*-cym-*iso*-prop-$(CH_3)_2$); FTIR (KBr/cm^{-1}): $\nu_{(Ar)C-H}$ 2962, $\nu_{(NH2)}$ 3383, $\nu_{(C=N)}$1593, $\nu_{(C-S)}$ 772, $\nu_{N=N}$ 1415; $\Lambda_M(\Omega^{-1}.m^2.M^{-1})$ 156.

*[Ru_2(μ-azpy)(η^6-p-cym)$_2$(**L10**)$_2$]Cl_2* **(C22)**:

μ-4,4'azopyridine–bis(bis(η^5-cyclopentadienyl)iron(II)-4-methyl-3-thiosemicarbazone)-bis1-isopropyl-4-methyl benzene diruthenium(II) dichloride

Yield: 45.8 %; Molecular Weight 1326.1 g/mole; Molecular Formula $C_{56}H_{64}Fe_2N_{10}Cl_2Ru_2S_2$; Anal.: C, 53.21; H, 5.45; N, 11.07. Calc.: C, 53.59; H, 5.14; N, 11.16, ESI-MS *m/z*:Obs (Calc): 626.0 (627.1) (M^{2+}+1); δ_H (400 MHz, DMSO-d^6) 4.37, (t, 2H, substituted cyclopentadiene); 4.96, (t, 2H, substituted cyclopentadiene); 4.56, (s, 5H, cyclopentadiene); 5.35-5.18, (m, 4H, *p*-cymAr-H); 3.16-3.14, (q, 1H, *p*-cym-*iso*-prop-CH); 1.91, (s, 3H, *p*-cym

Ar-CH_3); 1.09, (d, 6H, *p*-cym-*iso*-prop-$(CH_3)_2$); FTIR (KBr/cm^{-1}): $\nu_{(Ar)C-H}$ 2959, $\nu_{(NH-CH3)}$ 3078, $\nu_{(C=N)}$1593, $\nu_{(C-S)}$736, $\nu_{N=N}$ 1405; $\Lambda_M(\Omega^{-1}.m^2.M^{-1})$ 155.

$[Ru_2(\mu\text{-azpy})(\eta^6\text{-p-cym})_2(\boldsymbol{L11})_2]Cl_2$ **(C23)**:

μ-4,4'azopyridine–bis(bis(η^5-cyclopentadienyl)iron(II)-4-phenyl-3-thiosemicarbazone)-bis1-isopropyl-4-methyl benzene diruthenium(II) dichloride

Yield: 69.7%; Molecular Weight 1450.3 g/mole; Molecular Formula $C_{66}H_{68}Fe_2N_{10}Cl_2Ru_2S_2$; Anal.: C, 57.14; H, 4.91; N, 10.56. Calc.: C, 57.47; H, 4.97; N, 10.16, ESI-MS *m/z*: Obs (Calc): 690.1 (689.6) (M^{2+}+1); δ_H (400 MHz, DMSO-d^6) 4.12, (t, 2H, substituted cyclopentadiene); 4.76, (t, 2H, substituted cyclopentadiene); 4.32, (s, 5H, cyclopentadiene); 5.83-5.77, (m, 4H, *p*-cymAr-H); 2.51-2.50, (q, 1H, *p*-cym-*iso*-prop-CH); 2.08, (s, 3H, *p*-cym Ar-CH_3); 1.51, (d, 6H, *p*-cym-*iso*-prop-$(CH_3)_2$); FTIR (KBr/cm^{-1}): $\nu_{(Ar)C-H}$ 2962, $\nu_{(NH-C6H5)}$ 3124, $\nu_{(C=N)}$1597, $\nu_{(C-S)}$748, $\nu_{N=N}$ 1435; $\Lambda_M(\Omega^{-1}.m^2.M^{-1})$ 153.

$[Ru_2(\mu\text{-azpy})(\eta^6\text{-p-cym})_2(\boldsymbol{L12})_2]Cl_2$ **(C24)**:

μ-4,4'azopyridine–bis(bis(η^5-cyclopentadienyl)iron(II)-4-(naphthalen-1-yl)-3-thiosemicarbazone)-bis-1-isopropyl-4-methyl benzene diruthenium(II) dichloride

Yield: 56.3%; Molecular Weight 1550.4 g/mole; Molecular Formula $C_{74}H_{72}Fe_2N_{10}Cl_2Ru_2S_2$; Anal.: C, 60.14; H, 4.57; N, 9.23. Calc.: C, 60.08; H, 4.91; N, 9.47. ESI-MS *m/z*:Obs (Calc): 738.1 (739.3) (M^{2+}-1) ; δ_H(400 MHz, DMSO-d^6) 4.30, (t, 2H, substituted cyclopentadiene); 4.73, (t, 2H, substituted cyclopentadiene); 4.55, (s, 5H, cyclopentadiene); 5.82-5.75, (m, 4H, *p*-cymAr-H); 2.53-2.49, (q, 1H, *p*-cym-*iso*-prop-CH); 2.05, (s, 3H, *p*-cym Ar-CH_3); 1.17, (d, 6H, *p*-cym *iso*-prop-$(CH_3)_2$); FTIR (KBr/cm^{-1}): $\nu_{(Ar)C-H}$ 2959, $\nu_{(NH-C10H7)}$ 3077, $\nu_{(C=N)}$ 1591, $\nu_{(C-S)sym}$ 778, $\nu_{N=N}$ 1401; $\Lambda_M(\Omega^{-1}.m^2.M^{-1})$ 151.

3.5.2 Results and discussion:

The electronic absorption spectra of the complexes C**17-24** (*Fig. 3.13*) show three major bands in the wavelength range 200-650 nm. The cyclopentadienyl rings of ferrocene present in ligands (section 2.4.4) display intense absorption bands at 227–228 nm assigned to intra-ligand $\pi\rightarrow\pi^*$ transition [43] which were shifted to 225–232 nm in the electronic spectra of complexes due to coordination with Ru(II) metal centre. A second sharp but medium intensity peak found in the range of 305 – 321 nm owing to the intraligand $n\rightarrow\pi^*$ transitions have shifted to 275 – 347 nm on complexation. The shoulder observed in the region 459–464 nm in the ligands may be assigned to charge transfer transition from iron to either non-

bonding or antibonding orbitals of the cyclopentadienyl ring, shifted to 463-481 nm on complexation [44] which has been shown as an expansion in the inset of *Fig. 3.13*. Moreover, the ferrocenyl ligands have low-lying π* acceptor levels which provide the electronic basis for intramolecular charge transfer and the appearance of accessible MLCT excited states. The MLCT absorption bands include contributions from multiple vibronic contributors. These bands are largely broadened into single, broad absorption bands at room temperature with evidence for vibronic structure [45]. The patterns appeared in the electronic spectra of all the complexes indicated the presence of an octahedral environment around the two ruthenium atom [40]. The λ_{max} values of all the transitions taking place in the complexes have been tabulated in Table 3.7.

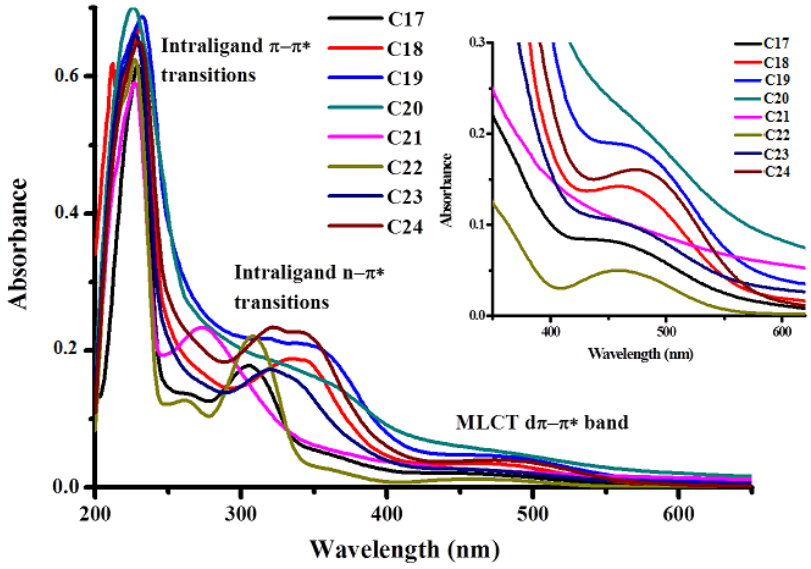

Fig. 3.13 *UV-Vis spectra of complexes*

Table 3.7: UV-Vis. peak assignments of complexes

Code	C17	C18	C19	C20	C21	C22	C23	C24
Intra-ligand transitions(nm) π-π*	230	230	232	225	227	227	226	229
Intra-ligand transitions(nm) n-π*	306	339	347	340	275	307	328	332
MLCT Fe dπ-π*	463	474	477	479	478	463	470	481

The ESI-Mass spectra show peaks corresponding to the molecular ion which gives evidence of the formation of binuclear complexes with +1 **(C17-20)** and +2 **(C21-C24)** charges. The

molecular ion peaks have been provided in table 1 and the mass spectra of all the complexes have been presented in *Figs. 3.14* and *3.15*. The complexes **C17-20** and **C21-24** (10^{-3}M in DMSO) have molar conductance in the range of 84-89 (Ω^{-1} m^2 M^{-1}) and 151-156 (Ω^{-1} m^2 M^{-1}) respectively at 38 ˚C suggesting 1:1 and 1:2 electrolytic behaviour [32].

Table 3.8: m/z values of complexes

Code	**C17**	**C18**	**C19**	**C20**	**C21**	**C22**	**C23**	**C24**
Calculated Mass (g/mol)	1112.1	1140.1	1264.5	1364.2	612.5	627.1	689.6	739.3
Observed Mass (g/mol)	1111.2 (M^+-1)	1141.2 (M^++1)	1263.2 (M^+-1)	1363.8 (M^+-1)	611.4 (M^{2+}+1)	626.0 (M^{2+}+1)	690.1 (M^{2+}+1)	738.1 (M^{2+}-1)

In the IR spectra of the complexes, the $\nu_{(C-S)}$ absorption peaks of the ferrocenyl thiosemicarbazone ligands are observed in the region 736-802 cm^{-1}. This observation may be attributed to enolization -HN-C=S → -N=C-SH and subsequent co-ordination via deprotonated sulphur. Coordination of the thiosemicarbazones to the ruthenium atom through the azomethine nitrogen atom reduce the electron density in the azomethine link and a lower $\nu_{(C=N)}$ absorption frequency compared to the free ligands, in the region 1551–1598 cm^{-1} was observed for the complexes [34]. The presence of p-cymene in the complexes is evident from characteristic bands observed in the spectra of complexes.

The ^{1}H NMR spectra of C**17-24** (*Figs. 3.16* and *3.17*), exhibit the peaks assigned to the p-cymene protons in the excepted region. The imine proton observed in the range δ=8.02 -10.09 in free ligands were shifted towards upfield region due to complex formation, indicating coordination of Ru via HC=N. The protons attributed to cyclopentadienyl ring in the free ligands in the range δ = 4.18 – 4.72 ppm show slight shift towards downfield region at δ= 4.32 – 4.96 ppm because of complexation. Due to the orientation of the ferrocenyl moiety with respect to the rest of the complex, one proton experiences through-space coupling with the imine proton resulting in a more shielded proton [46]. The N-H proton of free imidazole was not seen in the NMR spectra of C**17-20** and a slight upfield shift was observed at δ = 7.12 – 7.24 ppm in the proton of 4, 4'- azopyridine in **C21-24**, indicating co-ordination of two Ru metal centres with the bridging ligands [37].

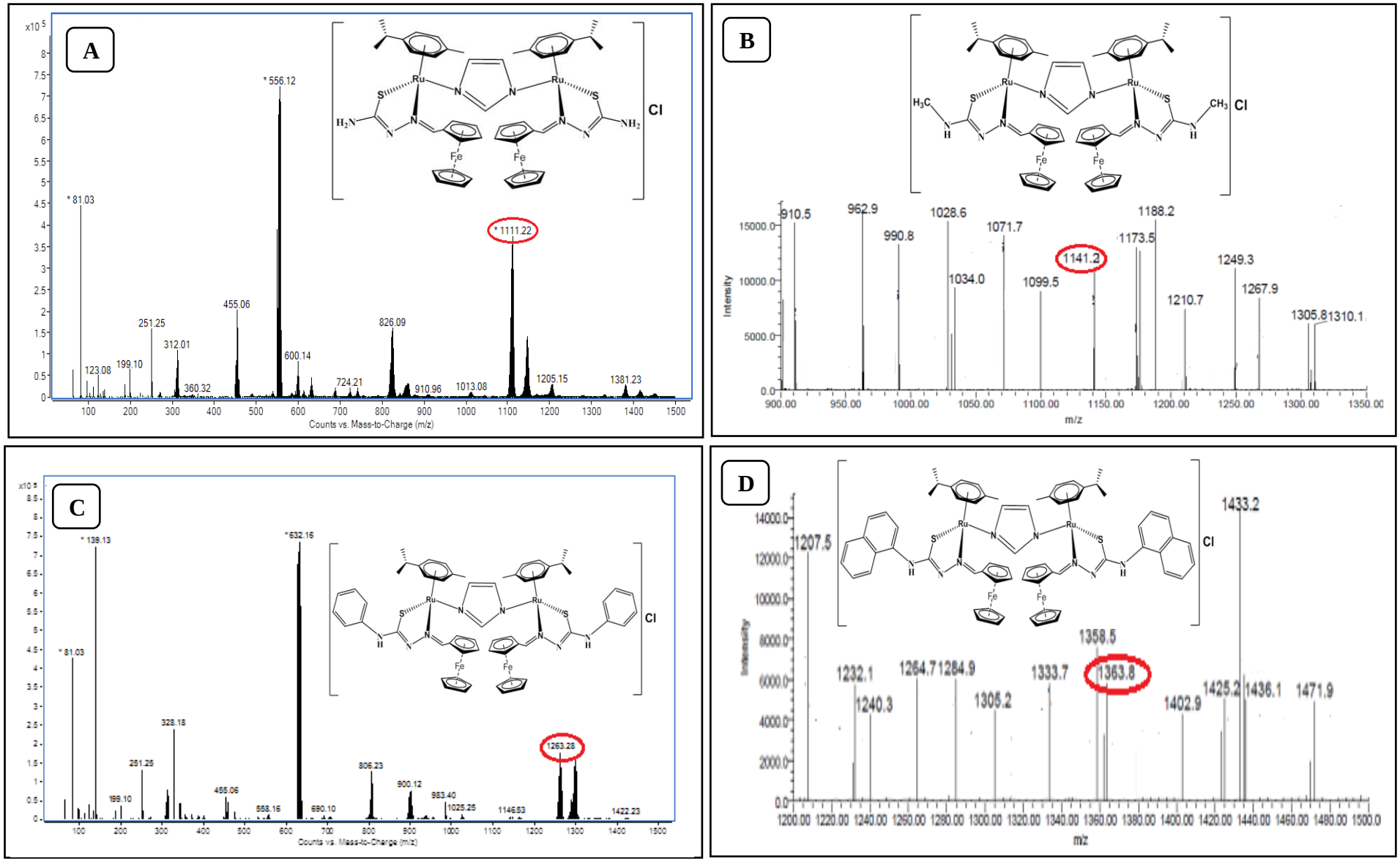

Fig. 3.14: *ESI-MS spectra of complexes (A)* ***C17*** *(B)* ***C18*** *(C)* ***C19*** *(D)* ***C20*** *indicating their molecular ion peak*

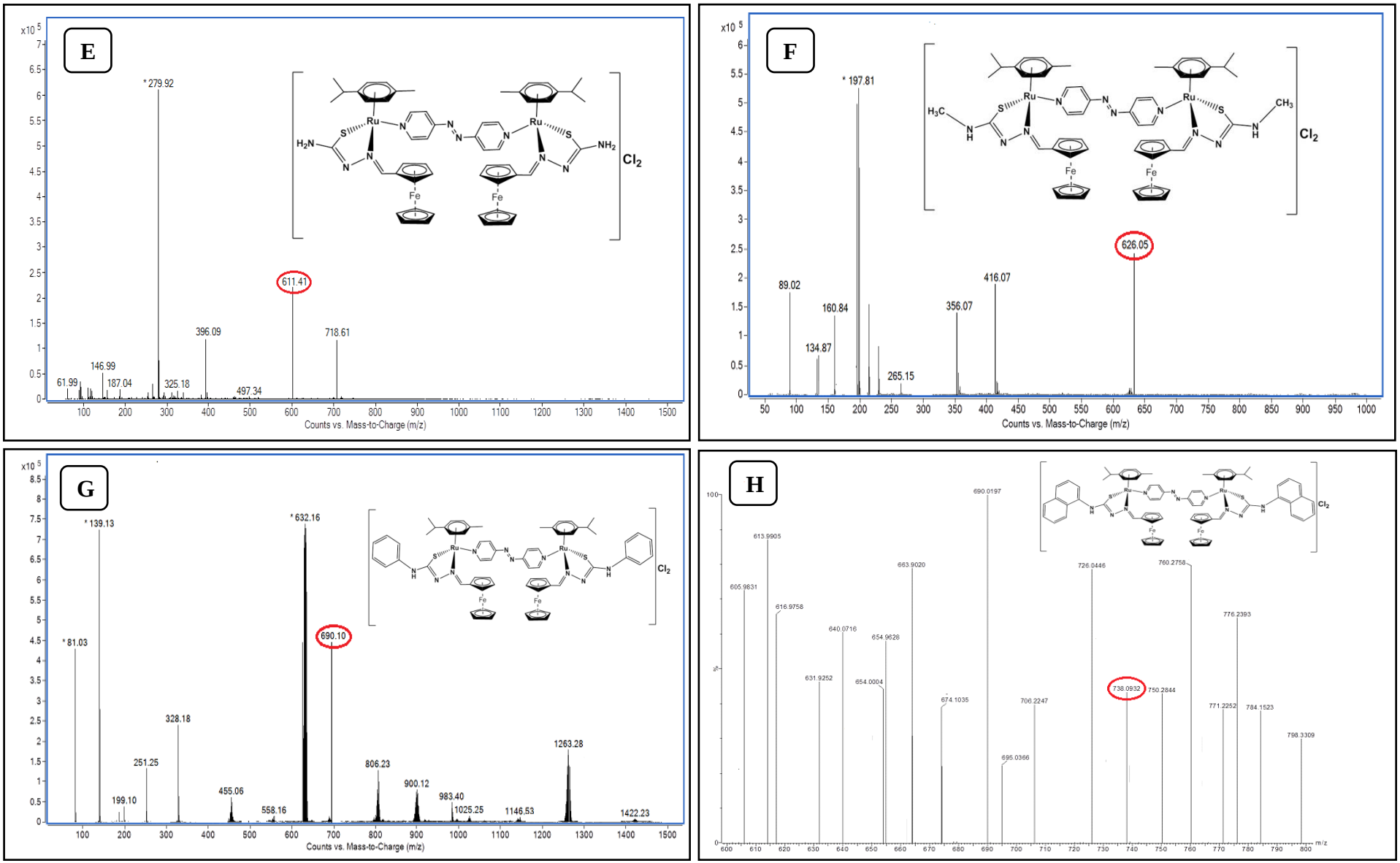

Fig. 3.15: *ESI-MS spectra of complexes (E)* ***C21*** *(F)* ***C22*** *(G)* ***C23*** *(H)* ***C24*** *indicating their molecular ion peak*

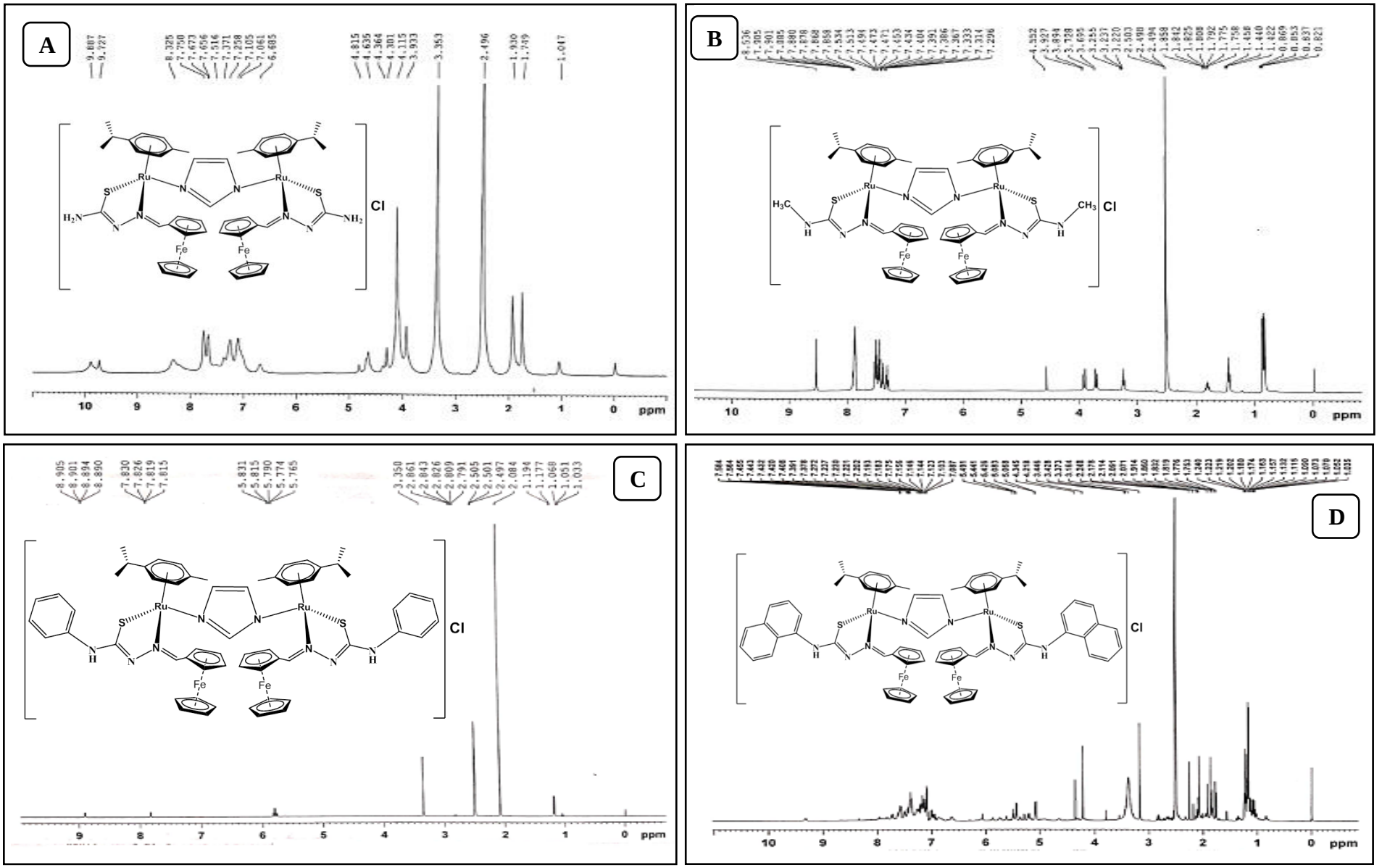

Fig. 3.16: *^{1}H NMR spectra of complexes (A)* ***C17*** *(B)* ***C18*** *(C)* ***C19*** *(D)* ***C20***

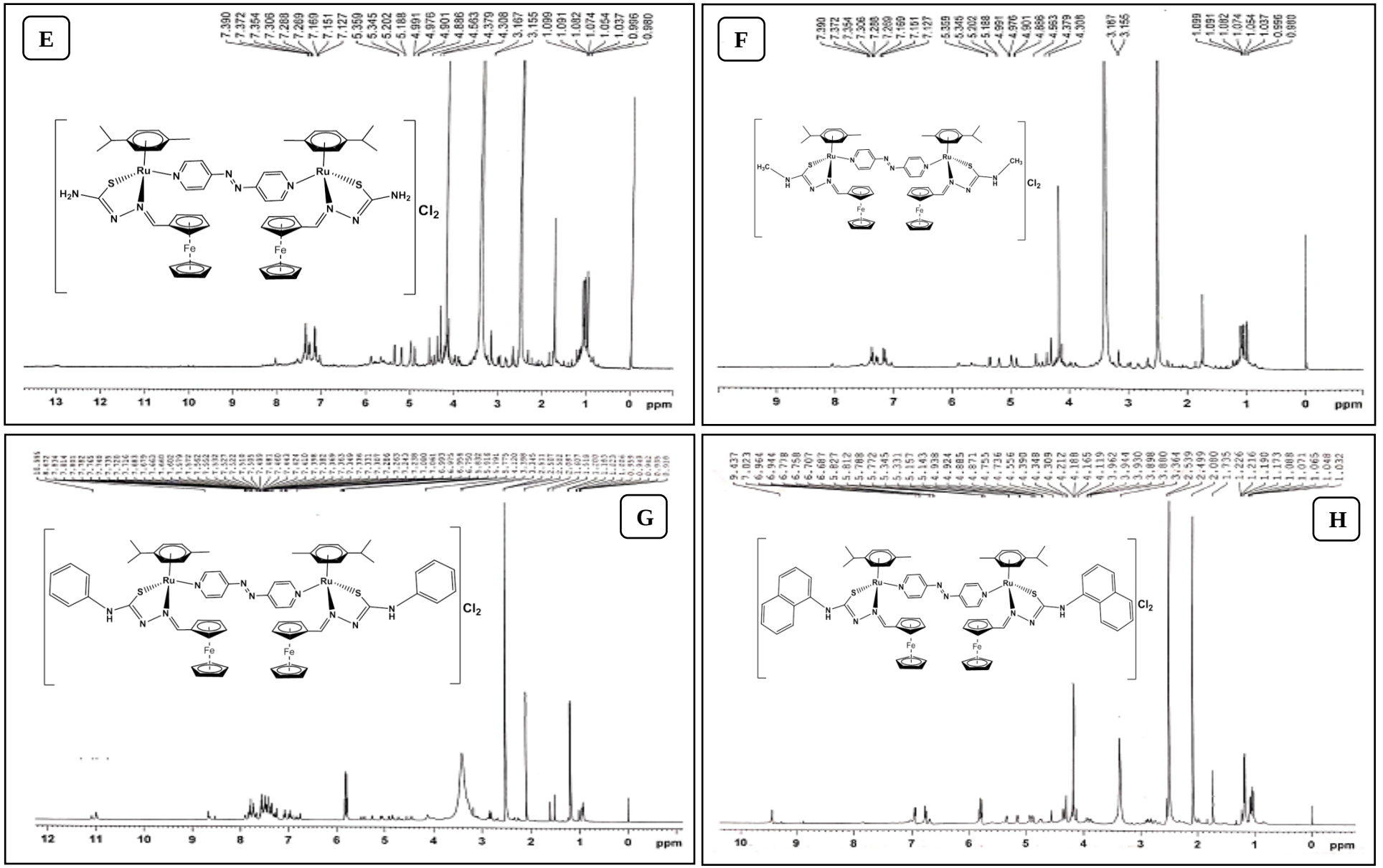

Fig. 3.17: *^{1}H NMR spectra of complexes (E)* ***C21*** *(F)* ***C22*** *(G)* ***C23*** *(H)* ***C24***

3.5.3 *Geometry optimization of [Ru_2 (μ-im /μ-azpy)(η^6-p-cym)$_2$(Ferrocenyl thiosemicarbazones)$_2$]Cl_{1-2} complexes : (C17-C24)*

All calculations were performed using the approximations with dispersion correction (disp3) program as mention above in section 3.2.1. In the absence of X-ray crystallography data, the DFT calculations for geometry optimization provide some insight into the molecular structure. Optimized structures of the representative complexes **C17** and **C21** are shown in *Fig. 3.18*. Piano-stool type geometry is observed around each metal centre of the binuclear complexes with the Ru (II) ions π-bonded to the arene ring. The average Ru-Ru distance in the binuclear complexes with imidazole as bridging ligands is 6.12 A^0 whereas in the binuclear complexes with 4, 4'azopyridine as bridging ligands the average distance is 13.22 A^0 due to the presence of a longer 4, 4'azopyridine ligand. The bond angle values reveal a pseudo octahedral coordination of the ruthenium centres. The metal–ligand bond lengths and bond angles tabulated in Table 3.9 are in well agreement with the values in the literature [38, 39].

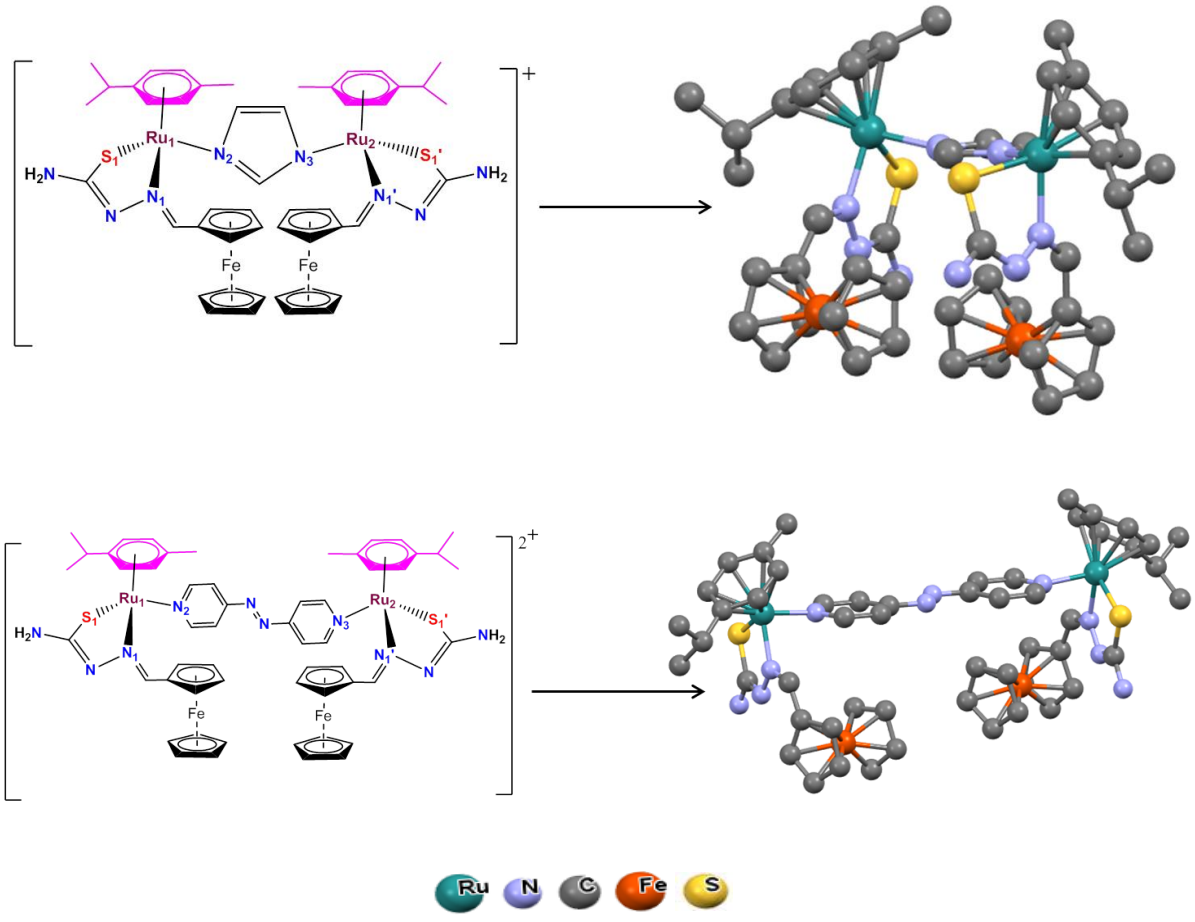

Fig. 3.18: *Optimized structures of the complexes* ***C17*** *and* ***C21***

Table 3.9: Metal ligand bond lengths and bond angles of complexes under study obtained from geometry optimization

Bond Length (in Å)	**L9**		**L10**		**L11**		**L12**	
	C17	**C21**	**C18**	**C22**	**C19**	**C23**	**C20**	**C24**
Ru1…….Ru2	6.24	13.29	6.22	12.16	6.18	13.31	6.23	13.14
Ru1-N1 (Fc)	2.10	2.10	2.11	2.11	2.10	2.09	2.10	2.10
Ru1-S1	2.37	2.36	2.37	2.36	2.36	2.36	2.37	2.36
Ru1-N2 (im/azpy)	2.10	2.11	2.10	2.11	2.10	2.11	2.12	2.11
Ru2-N1’ (Fc)	2.09	2.10	2.10	2.11	2.09	2.09	2.10	2.10
Ru2-S1’	2.38	2.36	2.37	2.36	2.37	2.36	2.36	2.36
Ru2-N3 (im/azpy)	2.10	2.11	2.10	2.11	2.10	2.11	2.11	2.11
Bond Angle (in Degree)								
S1-Ru1-N1	81.1	81.2	81.1	81.1	81.4	81.3	80.7	81.2
S1-Ru1-N2	87.5	90.6	87.3	90.7	87.6	90.9	89.6	90.8
N1-Ru1-N2	87.2	84.7	86.8	82.7	87.5	84.7	86.5	83.4
S1’-Ru2-N1’	79.9	81.2	80.8	81.1	81.2	81.3	81.1	81.2
S1’-Ru2-N3	92.7	90.6	91.0	90.7	91.1	90.9	88.2	90.8
N1’-Ru2-N3	84.1	84.7	82.4	82.9	81.9	84.7	85.7	83.3

3.6 [Ru_2 (μ-im /μ-azpy)(η^6-p-cym)$_2$(Ferrocenyl aminoacid mannich bases)$_2$]Cl_{1-2} complexes: (C25-C32)

3.6.1 Synthesis and characterization:

*[Ru_2(μ-im) (η^6-p-cym)$_2$(**L13**)$_2$]Cl* **(C25)***:*

μ-imidazole – bis(bis(η^5-cyclopentadienyl)iron (II)-Tyrosine) – bis1-isopropyl-4-methyl benzene diruthenium(II) chloride

Yield: 76.4%; Molecular Weight: 1330.32 g/mole; Molecular Formula: $C_{63}H_{73}ClFe_2N_4O_6Ru_2$; Anal.: C, 56.74; H, 5.51; N, 4.35. Calc.: C, 57.34; H, 5.85; N, 4.11. ESI-MS m/z: Obs (Calc): 1293.6 (1294.8) (M^+-1) ;δ_H (400 MHz, DMSO-d^6): 10.4, (s, 1H, -OH of tyrosine); 7.3-8.5, (m, 4H, Ar-H of tyrosine); 5.81-5.75, (m, 4H, p-cym Ar-H); 4.7, (t, 2H, substituted cyclopentadiene); 4.45, (t, 2H, substituted cyclopentadiene); 4.27, (s, 5H, cyclopentadiene); 2.7; (q, 1H, p-cym-iso-prop-CH); 2.03, (s, 3H, p-cym Ar-CH_3); 1.27, (d, 6H, p-cym- iso-prop-$(CH_3)_2$); 7.5, (d, 2H, imidazole CH=CH); FTIR (KBr/cm^{-1}):$\nu_{(O-H)}$ 3452, $\nu_{(Ar)C-H}$ 2963, ν_{COO}assym1512, ν_{COO}sym1326, $\Delta\nu_{COO}$186; Λ_M($\Omega^{-1}.m^2.M^{-1}$) 65.

*.[Ru_2(μ-im) (η^6-p-cym)$_2$(**L14**)$_2$]Cl* **(C26)***:*

μ-imidazole – bis (bis(η^5-cyclopentadienyl)iron (II)-Phenyl alanine) – bis 1 - isopropyl-4-methyl benzene diruthenium(II) chloride

Yield: 64.3%; Molecular Weight 1299.44 g/mole; Molecular Formula $C_{63}H_{73}ClFe_2N_4O_4Ru_2$; Anal.: C, 58.41; H, 5.68; N, 4.10. Calc.: C, 58.72; H, 5.99; N, 4.21. ESI-MS m/z: Obs (Calc):1262.4 (1263.9) (M^+-1) ; δ_H (400 MHz, DMSO-d^6): 7.10-7.45, (m, 5H, Ar-H of phenylalanine); 5.14-5.63, (m, 4H, p-cym Ar-H); 4.23, (t, 2H, substituted cyclopentadiene); 4.64, (t, 2H, substituted cyclopentadiene); 4.15, (s, 5H, cyclopentadiene); 2.93, (q, 1H, p-cym-iso-prop-CH); 2.12, (s, 3H, p-cymAr-CH_3); 1.25, (d, 6H, p-cym-iso-prop-$(CH_3)_2$); FTIR (KBr/cm^{-1}): $\nu_{(N-H)}$ 3056, $\nu_{(Ar)C-H}$ 2959, $\nu_{COOassym}$1626, ν_{COOsym}1367, $\Delta\nu_{COO}$ 259; Λ_M($\Omega^{-1}.m^2.M^{-1}$) 67.

*[Ru_2(μ-im) (η^6-p-cym)$_2$(**L15**)$_2$]Cl* **(C27)***:*

μ-imidazole – bis (bis(η^5-cyclopentadienyl)iron (II)-Leucine) – bis 1 - isopropyl-4-methyl benzene diruthenium(II) chloride

Yield: 67.9%; Molecular Weight 1231.42 g/mole; Molecular Formula$C_{57}H_{77}ClFe_2N_4O_4Ru_2$; Anal.: C, 54.15; H, 6.50; N, 5.35. Calc.: C, 54.54; H, 6.80; N, 5.72. ESI-MS m/z: Obs (Calc): 1196.3 (1195.9) (M^+); δ_H (400 MHz, DMSO-d^6): 5.45-5.90, (m, 4H, p-cym Ar-H); 5.46, (t,

2H,substituted cyclopentadiene); 4.15, (t, 2H, substituted cyclopentadiene); 4.25, (s, 5H, cyclopentadiene); 2.89, (q, 1H, p-cym-isoprop-CH); 2.03, (s, 3H, p-cym Ar-CH_3); 1.19, (d, 6H, p-cym-iso-prop-$(CH_3)_2$); 1.56, (d, 6H, leucine-iso-prop-$(CH_3)_2$); FTIR(KBr/cm^{-1}): $\nu_{(N-H)}$ 3087, $\nu_{(Ar)C-H}$ 2957, $\nu_{COOassym}$1603, ν_{COOsym}1326, $\Delta\nu_{COO}$ 277; $\Lambda_M(\Omega^{-1}.m^2.M^{-1})$ 61.

$[Ru_2(\mu\text{-im})\ (\eta^6\text{-p-cym})_2(\mathbf{L16})_2]Cl$ **(C28)***:*

μ-imidazole – bis (bis(η^5-cyclopentadienyl)iron (II)-Tryptophan)–bis 1-isopropyl-4-methyl benzene diruthenium(II) chloride

Yield: 62.8%; Molecular Weight: 1377.52 g/mole; Molecular Formula:$C_{67}H_{75}ClFe_2N_6O_4Ru_2$; Anal.: C, 59.29; H, 5.30; N, 5.12. Calc.: C, 58.91; H, 5.60; N, 5.51. ESI-MS m/z: Obs (Calc): 1342.02 (1342.02) (M^+); δ_H(400 MHz, DMSO-d^6): 12.6, (s, 1H, indolinic N-H of tryptophan); 5.94-5.35, (m, 4H, p-cym Ar-H); 4.72, (t, 2H, substituted cyclopentadiene); 4.59, (t, 2H, substituted cyclopentadiene); 4.78, (s, 5H,cyclopentadiene); 2.93, (q, 1H, p-cym-iso-prop-CH); 2.16, (s, 3H, p-cymAr-CH_3); 1.25, (d, 6H,p-cym-iso-prop-$(CH_3)_2$); FTIR (KBr/cm^{-1}): $\nu_{(N-H)}$ 3082, $\nu_{(Ar)C-H}$ 2961, $\nu_{COOassym}$1637, ν_{COOsym}1370, $\Delta\nu_{COO}$ 267; $\Lambda_M(\Omega^{-1}.m^2.M^{-1})$ 64.

$[Ru_2(\mu\text{-azpy})(\eta^6\text{-p-cym})_2(\mathbf{L13})_2]Cl_2$ **(C29)**:

μ-4,4'azopyridine–bis(bis(η^5-cyclopentadienyl)iron(II)-Tyrosine)-bis1-isopropyl-4-methyl benzene diruthenium (II) dichloride

Yield: 78.4%; Molecular Weight: 1484.3 g/mole; Molecular Formula: $C_{70}H_{78}N_6O_6Cl_2Fe_2Ru_2$; Anal.: C, 59.35; H, 5.17; N, 5.82. Calc: C, 59.58; H, 5.43; N, 5.96. ESI-MS m/z: Obs (Calc): 708.1 (706.6) (M^{2+}+2); (δ_H (400 MHz, DMSO-d^6): 9.06, (s, 1H, -OH of tyrosine); 7.26-7.58, (m, 4H, Ar-H of tyrosine); 5.21-5.54, (m, 4H, p-cym Ar-H); 4.68, (t, 2H, substituted cyclopentadiene); 4.25, (t, 2H, substituted cyclopentadiene); 4.43, (s, 5H, cyclopentadiene); 2.9, (q, 1H, p-cym-iso-prop-CH); 2.21, (s, 3H, p-cym Ar-CH_3); 1.69, (d, 6H, p-cym- iso-prop-$(CH_3)_2$); FTIR (KBr/cm^{-1}):$\nu_{(O-H)}$ 3452, $\nu_{(N-H)}$ 3031, $\nu_{(Ar)C-H}$ 2964, $\nu_{COOassym}$ 1599,ν_{COO}sym 1326, $\Delta\nu_{COO}$ 273, $\nu_{N=N}$ 1414; $\Lambda_M(\Omega^{-1}.m^2.M^{-1})$ 125.

$[Ru_2(\mu\text{-azpy})(\eta^6\text{-p-cym})_2(\mathbf{L14})_2]Cl_2$ **(C30)**:

μ-4,4'azopyridine–bis(bis(η^5-cyclopentadienyl)iron(II)-Phenylalanine)-bis1-isopropyl-4-methylbenzene diruthenium (II) dichloride

Yield: 67.3%; Molecular Weight 1452.3 g/mole; Molecular Formula $C_{70}H_{78}N_6O_4Cl_2Fe_2Ru_2$; Anal.: C, 60.76; H, 5.34; N, 6.57. Calc: C, 60.96; H, 5.55; N, 6.90. ESI-MS m/z: Obs (Calc):

691.8 (690.6) (M^{2+}+1); δ_H (400 MHz, DMSO-d^6): 7.24-7.68, (m, 5H, Ar-H of phenylalanine); 5.23-5.79, (m, 4H, p-cym Ar-H); 4.23, (t, 2H, substituted cyclopentadiene); 4.64, (t, 2H, substituted cyclopentadiene); 4.24, (s, 5H, cyclopentadiene); 2.87, (q, 1H, p-cym-iso-prop-CH); 2.34, (s, 3H, p-cymAr-CH_3); 1.35, (d, 6H, p-cym-iso-prop-$(CH_3)_2$); FTIR (KBr/cm^{-1}): $\nu_{(N-H)}$ 3081, $\nu_{(Ar)C-H}$ 2963, $\nu_{COOassym}$ 1626, ν_{COOsym} 1374, $\Delta\nu_{COO}$ 252, $\nu_{N=N}$ 1411; Λ_M(Ω^{-1}.m^2.M^{-1}) 131.

*[Ru_2(μ-azpy)(η^6-p-cym)$_2$(**L15**)$_2$]Cl_2* **(C31)**:

μ-4,4'azopyridine–bis-(bis(η^5-cyclopentadienyl)iron(II)-Leucine)-bis-1-isopropyl-4-methylbenzene diruthenium(II) dichloride

Yield: 69.9%; Molecular Weight 1384.2 g/mole; Molecular Formula $C_{64}H_{82}N_6O_4Cl_2Fe_2Ru_2$; Anal.: C, 58.41; H, 6.26; N, 6.30. Calc.: C, 58.63; H, 6.15; N, 6.41. ESI-MS m/z: Obs (Calc): 655.2 (656.6) (M^{2+}-1); δ_H (400 MHz, DMSO-d^6): 5.58-5.89, (m, 4H, p-cym Ar-H); 5.57, (t, 2H,substituted cyclopentadiene); 4.23, (t, 2H, substituted cyclopentadiene); 4.36, (s, 5H, cyclopentadiene); 2.76, (q, 1H, p-cym-isoprop-CH); 2.12, (s, 3H, p-cym Ar-CH_3); 1.26, (d, 6H, p-cym-iso-prop-$(CH_3)_2$); 1.78, (d, 6H,leucine-iso-prop-$(CH_3)_2$); FTIR(KBr/cm^{-1}): $\nu_{(N-H)}$ 3047, $\nu_{(Ar)C-H}$ 2957, $\nu_{COOassym}$ 1605, ν_{COOsym} 1387, $\Delta\nu_{COO}$ = 218, $\nu_{N=N}$ 1450; Λ_M(Ω^{-1}.m^2.M^{-1}) 122.

*[Ru_2(μ-azpy)(η^6-p-cym)$_2$(**L16**)$_2$]Cl_2* **(C32)**:

μ-4,4'azopyridine–bis(bis(η^5-cyclopentadienyl)iron(II)-Tryptophan)-bis1-isopropyl-4-methylbenzene diruthenium (II) dichloride

Yield: 62.8%; Molecular Weight: 1530.3 g/mole; Molecular Formula: $C_{74}H_{80}N_8O_4Cl_2Fe_2Ru_2$; Anal.: C, 60.78; H, 5.43; N, 7.45. Calc.: C, 60.99; H, 5.40; N, 7.69. ESI-MS m/z: Obs (Calc): 726.3 (728.6) (M^{2+}- 2) ; δ_H (400 MHz, DMSO-d^6): 11.6, (s, 1H, indolinic N-H of tryptophan); 5.86-5.45, (m, 4H, p-cym Ar-H); 4.78, (t, 2H, substituted cyclopentadiene); 4.34, (t, 2H, substituted cyclopentadiene); 4.84, (s, 5H,cyclopentadiene); 2.74, (q, 1H, p-cym-iso-prop-CH); 2.21, (s, 3H, p-cymAr-CH_3); 1.45, (d, 6H,p-cym-iso-prop-$(CH_3)_2$); FTIR (KBr/cm^{-1}): $\nu_{(N-H)}$ 3080, $\nu_{(Ar)C-H}$ 2960, $\nu_{COOassym}$ 1629, ν_{COOsym} 1380, $\Delta\nu_{COO}$ 249, $\nu_{N=N}$ 1457; Λ_M(Ω^{-1}.m^2.M^{-1}) 136.

3.6.2 Results and discussion:

Crystal structure of the mononuclear complex [Ru(η^6-p-cymene)(L14)Cl]

(bis(η^5-cyclopentadienyl)iron(II)-Phenylalanine)–1-isopropyl-4-methyl benzene ruthenium (II) chloride

The structure of the complex [Ru(η^6-p-cymene)(L14)Cl] which could be obtained as single crystals with appropriate size, used as a precursor for the synthesis of **C26** is shown in (*Fig. 3.19*) with the atom numbering scheme. The molecular structure of the complex adopts pseudo-octahedral "piano-stool" geometry, where the p-cymene ligand forms the seat of the piano stool and the σ and π-bonded chloride (Cl3) as well as the secondary amine nitrogen (N15) and carboxylato oxygen (O) atoms of the chelating ferrocenyl amino acid ligand resemble the legs. Selected bond angles and distances are given in table. The Ru-O and Ru-N distances are 2.069 Å and 2.145 Å respectively while the Ru-Cl bond is longer at 2.411 Å. The Ru-C (arene) distances are in the range 2.150 Å -2.228 Å (Table 3.10). All these measurements are similar to the relevant complexes in references [47, 48]. The complex crystallizes in orthorombic system with $P2_12_12_1$ space group. The N-Ru-Cl and O-Ru-Cl angles are 84.61^o (11) and 84.03^o (11) respectively. The O-Ru-N angle is reduced to 77.94^o (14) probably due to steric repulsion of the phenyl group in proximity. Selected crystallographic data have been provided in the Table 3.11.

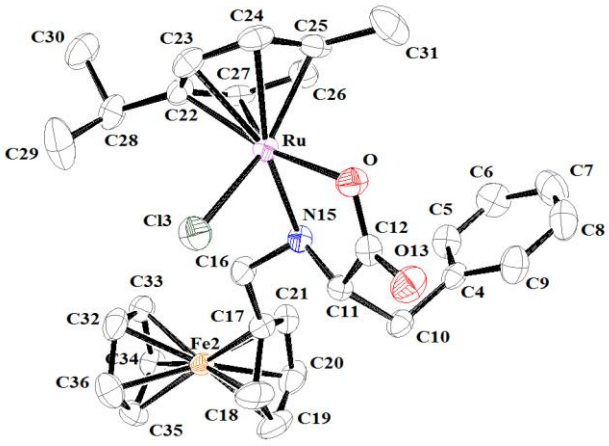

Fig. 3.19: *Molecular structure of [Ru(η^6-p-cymene)(L14)Cl] with atom numbering*

Table 3.10: Selected bond lengths (A˚) and bond angles (^{o}) for [Ru(η^6-p-cymene)(L14)Cl]

Ru-O	Ru-N15	Ru-Cl3	Ru-C22	Ru-C23	Ru-C24
2.069(4)	2.145(4)	2.411(13)	2.228(5)	2.179(5)	2.176(4)
Ru-C25	Ru-C26	Ru-C27	O-Ru-Cl3	O-Ru-N15	N15-Ru-Cl3
2.150(5)	2.168(5)	2.170(5)	84.03(11)	77.94(14)	84.61(11)

Table 3.11: Crystallographic data for [Ru(η^6-p-cymene)(L14)Cl]

Empirical formula	$C_{30}H_{34}ClFeNO_2Ru$
Molecular weight	632.95
Crystal system	Orthorhombic
Space group	$P2_12_12_1$
a (A)	6.8729(7)
b (A)	10.7444(8)
c (A)	35.938(3)
α (deg)	90
β (deg)	90
γ (deg)	90
V (Å3), Z	2653.9(4), 4
λ (Å)	0.71073
Size	0.25 x 0.17 x 0.12
T (K)	293
Dcalcd (g/cm3)	1.584
μ (mm^{-1})	1.245
GOF on F2	1.030
Final R indices I > 2σ(I)	0.0493
R indices (all data)	0.0915
Reflection collection	17441
Independent reflections	6133 (R_{int} = 0.0503 ; R_{sigma}=0.0631
Absorption coefficient	1.245
F(000)	1292
Θ range (^{o})	3.81-26.05
Index range	$-8 \leq h \leq 8$ $-14 \leq k \leq 14$ $-48 \leq h \leq 48$
Absorption correction	MULTI-SCAN
Data / Restrain / Parameters	6133/0/328

The electronic absorption spectra of the complexes C**25-32** (*Figs. 3.20* and *3.21*) were recorded in CH_3OH solution in the region 200-500 nm. The electronic spectra of free ligands displayed intense intra ligand π→π* absorption bands of the cyclopentadienyl rings at 203-206 nm [43] which red shifted to 211-229 nm in the complexes due to coordination. Absorption peaks in the region 275-299 nm corresponding to *n*→π* transitions were also

observed the spectra of complexes which has been shown in the *Fig. 3.20* and as an expansion in the inset of *Fig. 3.21* for **C29-32**. Moreover, MLCT band was observed in the complexes from the region 375 – 412 nm due to presence of ferrocenyl group, which has been shown in the as an expansion in the inset of *Figs. 3.20* and *3.21*. (Table 3.12).

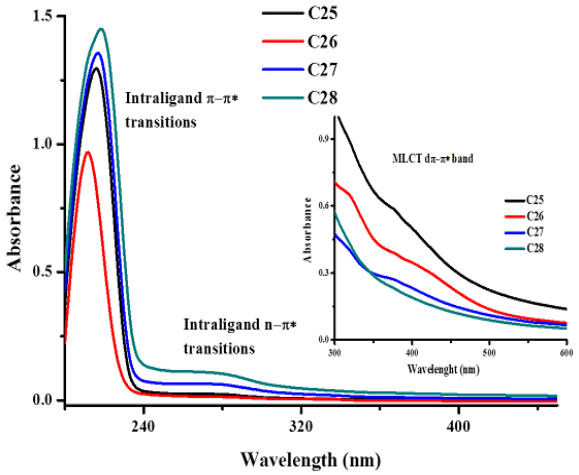

Fig. 3.20: *UV-Vis spectra of* ***C25-C28***

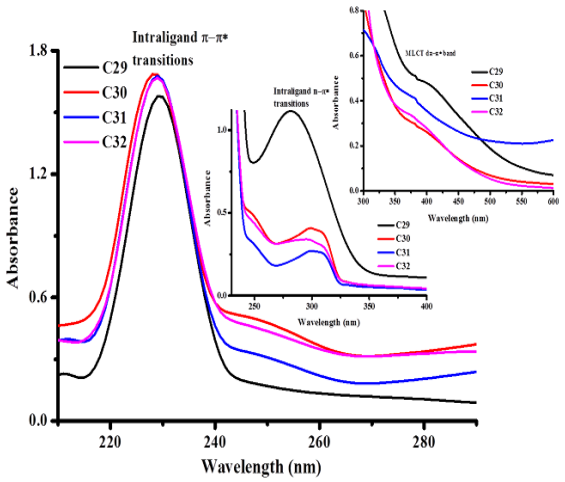

Fig. 3.21: UV-Vis spectra of **C29-C32**

Table 3.12: UV-Vis. peak assignments of complexes

Code	C25	C26	C27	C28	C29	C30	C31	C32
Intra-ligand transitions(nm) π-π*	216	211	216	218	229	228	228	228
Intra-ligand transitions(nm) n-π*	275	276	277	275	282	299	298	298
MLCT Fe dπ-π*	379	412	389	375	407	384	383	387

The ESI-Mass spectra of **C25-C32** (*Fig. 3.22* and *3.23*) show *m/z* peaks corresponding to the molecular ions. A *p*-cymene and an amino acid conjugated ferrocenyl ligands are coordinated to each of the metal centres with a deprotonated imidazole / 4, 4'-azopyridine as a bridging ligand, thereby resulting in the formation of a binuclear complex as indicated by the peak values (Table 3.13). The molar conductance values of the complexes recorded in DMSO (10^{-3}M) at 38 ˚C suggest 1:1(**C25-C28**) and 1:2 (**C29-C32**) electrolytic behaviour. The electrolytic nature of these compounds is due to the presence of chloride ions outside the coordination sphere [32].

Table 3.13: m/z values of complexes

Code	**C25**	**C26**	**C27**	**C28**	**C29**	**C30**	**C31**	**C32**
Calculated Mass (g/mol)	1294.8	1263.9	1195.9	1342.0	706.6	690.6	656.6	728.6
Observed Mass (g/mol)	1293.6 (M^+-1)	1262.4 (M^+-1)	1196.3 (M^+)	1342.02 (M^+)	708.1 (M^{2+}+2)	691.0 (M^{2+}+1)	655.2 (M^{2+}-1)	726.3 (M^{2+}- 2)

The IR spectra of the complexes **C25 – 32** displayed bands at 1530 – 1660 cm^{-1} and 1325 – 1373 cm^{-1} due to asymmetric and symmetric COO^- stretch of the conjugated amino acids respectively indicating monodentate coordination of the carboxylate group of the ligands. Furthermore the N-H stretching bands were shifted to 3050 – 3200 cm^{-1} in **C25 – 32** indicating complexation of the ligands via the nitrogen of the secondary amine [43]. The overall changes in the IR spectra suggest that the ferrocenyl-amino acid conjugates act as monoanionic bidentate ligands interacting with the metal centres via nitrogen of the secondary amine and the carboxylate oxygen.

The ^{1}H NMR spectra of **C25-32** (*Figs. 3.24* and *3.25*) show the distinct peaks corresponding to the *p*-cymene ligand. The peak arising due to carboxylic O-H observed in the free ferrocenyl ligands is no longer seen and the peak of the secondary amine (N-H) is found to be shifted due to coordination to the ruthenium metal centres [43]. Moreover the peaks owing to the aromatic protons in amino acid nucleus are observed in the region δ = 7-9 and the substituted methyl protons appeared around δ = 1-2 ppm. The ferrocenyl protons appear at 4.23 – 4.64 ppm.

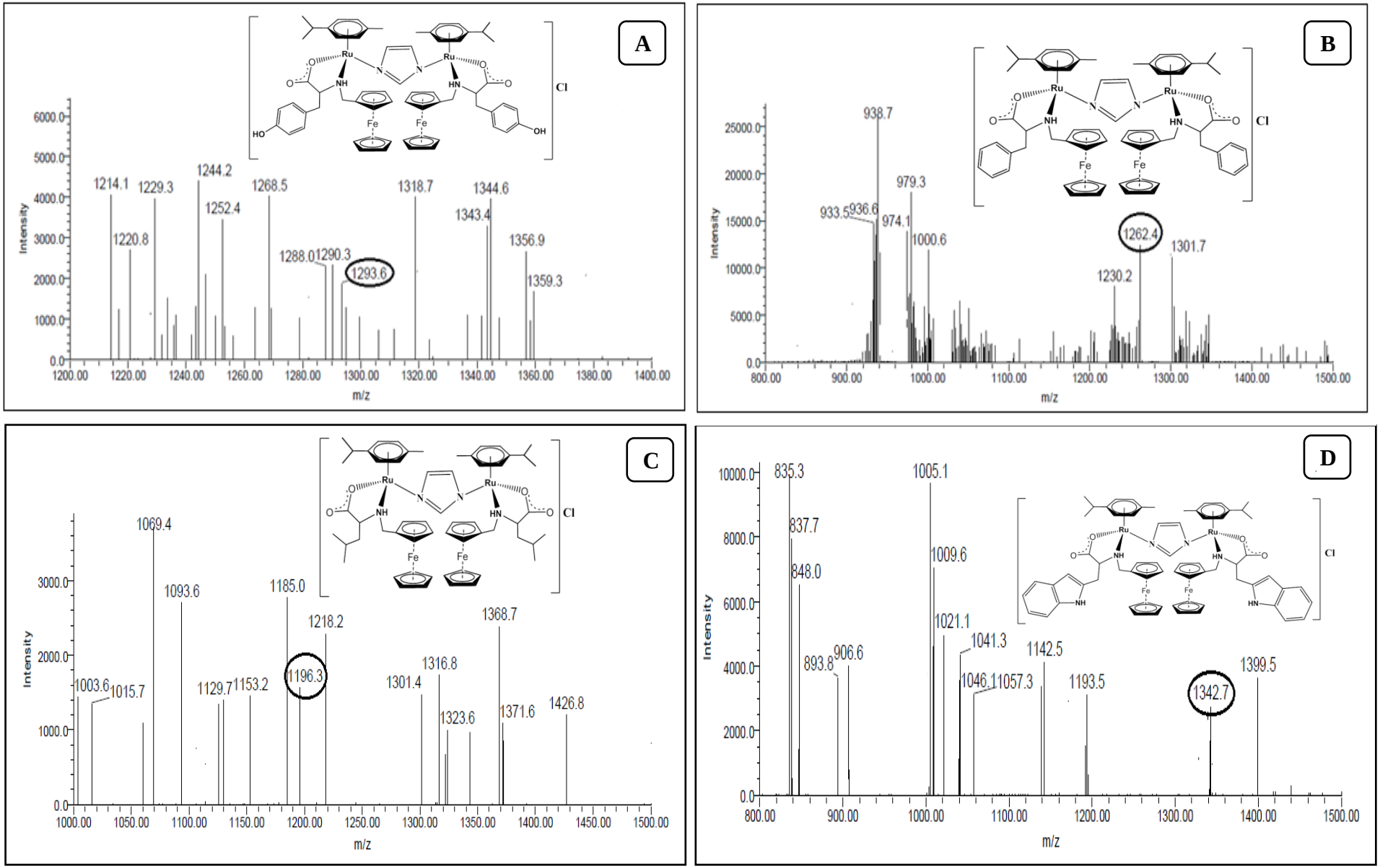

Fig. 3.22: *ESI-MS spectra of complexes (A)* ***C25*** *(B)* ***C26*** *(C)* ***C27*** *(D)* ***C28*** *indicating their molecular ion peak.*

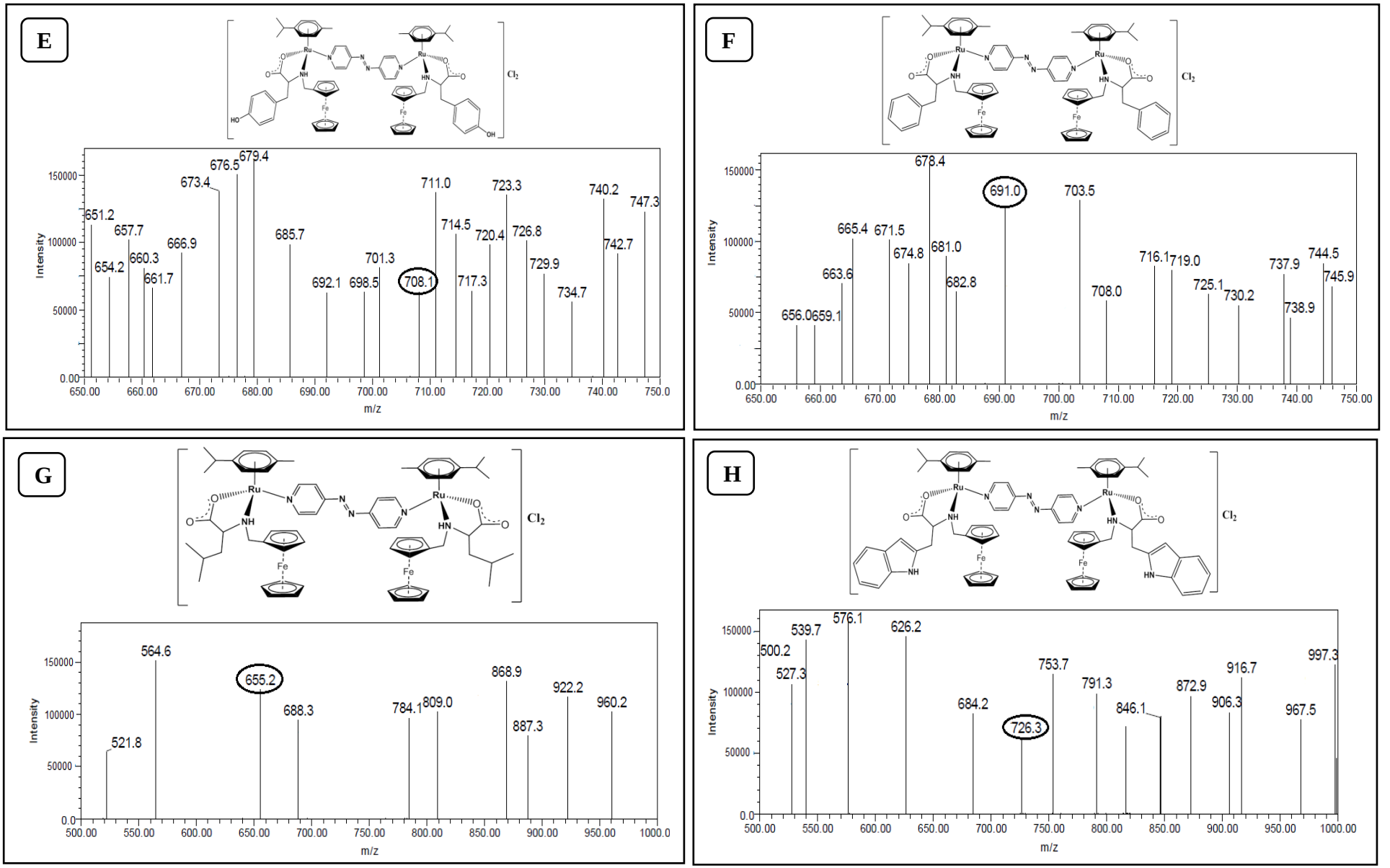

Fig. 3.23: *ESI-MS spectra of complexes (E)* ***C29*** *(F)* ***C30*** *(G)* ***C31*** *(H)* ***C32*** *indicating their molecular ion peak*

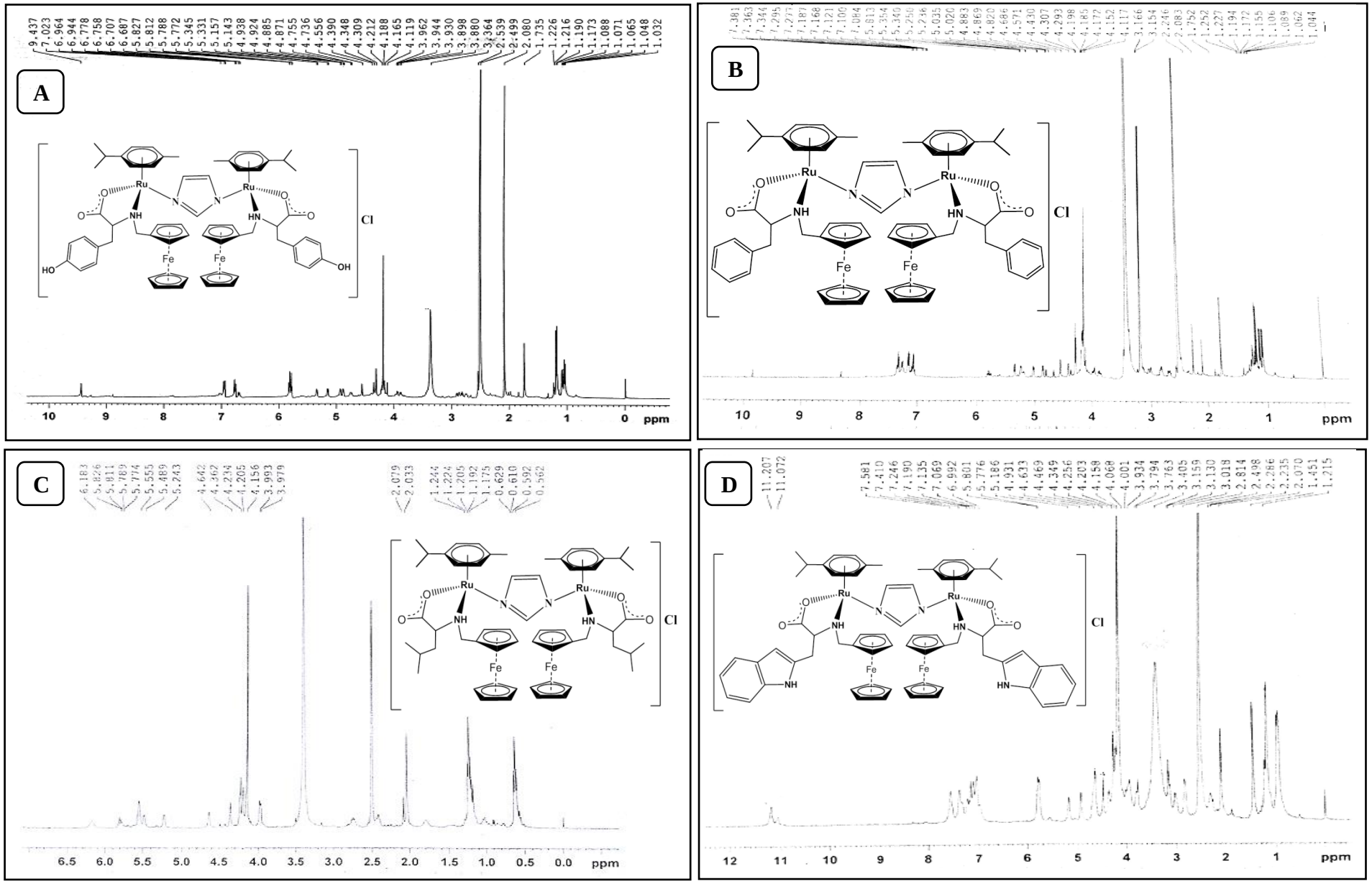

Fig. 3.24: *^{1}H NMR spectra of complexes (A)* ***C25*** *(B)* ***C26*** *(C)* ***C27*** *(D)* ***C28***

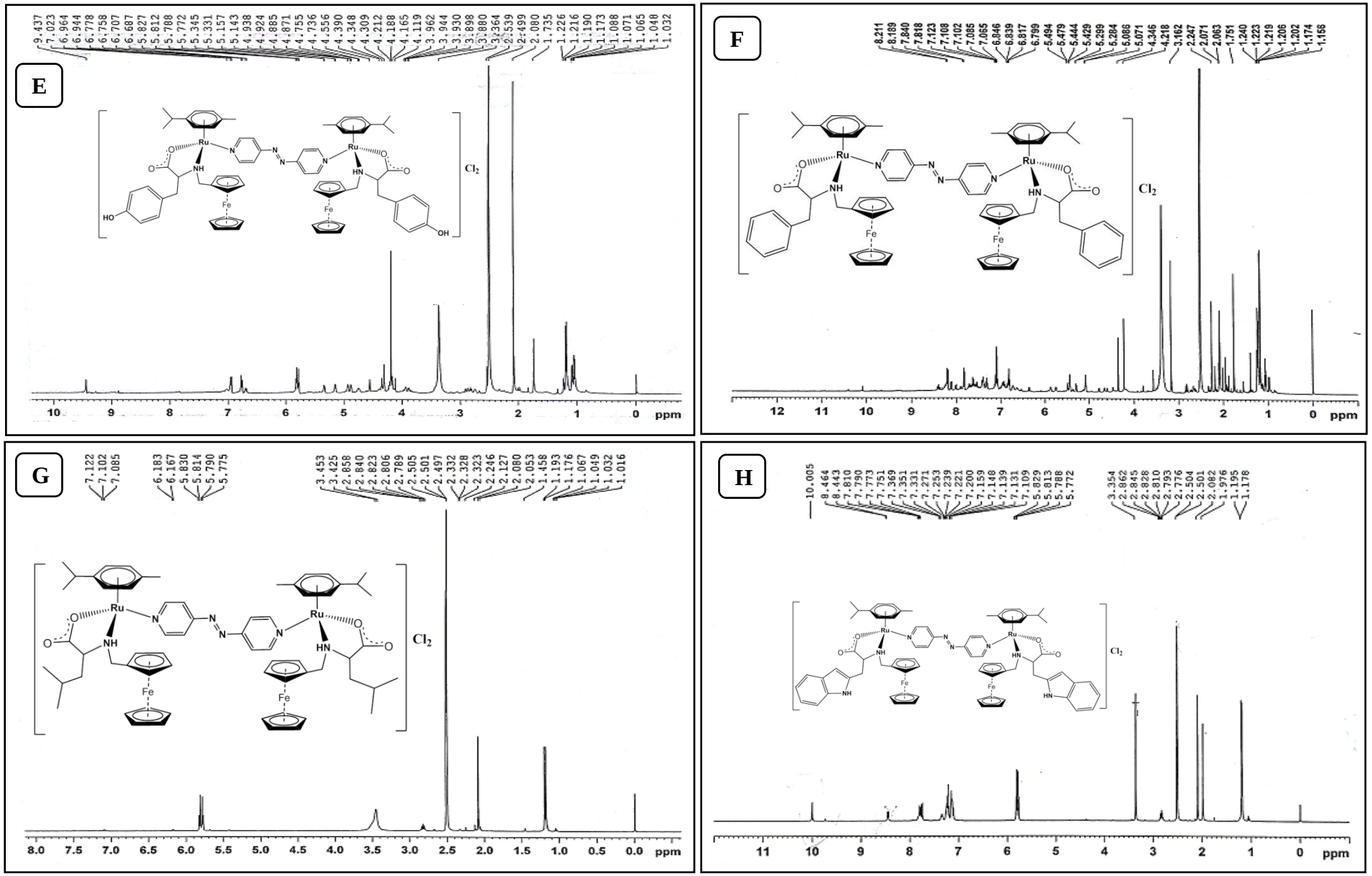

Fig. 3.25: *^{1}H NMR spectra of complexes (E)* ***C29*** *(F)* ***C30*** *(G)* ***C31*** *(H)* ***C32***

3.7 [Ru_2 (μ-im /μ-azpy)(η^6-p-cym)$_2$(Fluroquinolones)$_2$]Cl_{1-2} complexes: (C33-C40)

3.7.1 Synthesis and characterization:

*[Ru_2(μ-im)(η^6-p-cym)$_2$(**L17**)$_2$]Cl* **(C33)**:

μ-imidazole–bis-1-ethyl-6,8-difluoro-7-(3-methylpiperazin-1-yl)-4-oxoquinoline-3-carboxylate – bis-1 - isopropyl-4-methyl benzene diruthenium(II) chloride

Yield: 62.1%; Molecular Weight 1279.5 g/mole; Molecular Formula $C_{57}H_{73}ClF_4N_8O_6Ru_2$; Anal.: C, 54.14; H, 6.51; N, 8.56. Calc.: C, 54.20; H, 6.72; N, 8.25. ESI-MS *m/z*:Obs (Calc): 1244.2 (1244.6) (M^+) ; δ_H(400 MHz, DMSO-d^6) 5.92-5.87, (m, 4H, *p*-cymAr-H); 2.81-2.74, (q, 1H, *p*-cym-*iso*-prop-CH); 2.05, (s, 3H, *p*-cym Ar-CH_3); 1.34, (d, 6H, *p*-cym-*iso*-prop-$(CH_3)_2$); 7.4, (d, 2H, imidazole CH=CH); FTIR (KBr/ cm^{-1}): $\nu_{(Ar)C-H}$ 2964, $\nu_{(pyridone)C=O}$ 1619, $\nu_{COOassym}$ 1587, ν_{COOsym}1399, $\Delta\nu_{COO}$ 188; $\Lambda_M(\Omega^{-1}.m^2.M^{-1})$ 52

*[Ru_2(μ-im)(η^6-p-cym)$_2$(**L18**)$_2$]Cl* **(C34)**:

μ-imidazole–bis-7-fluoro-2-methyl-6-(4-methylpiperazin-1-yl)-10-oxo-4-oxa-1-azatricyclo [7.3.1.$0^{5,13}$] trideca-5(13),6,8,11-tetraene-11-carboxylate– bis 1 - isopropyl-4-methyl benzene

Yield: 73.8%; Molecular Weight 1295.5 g/mole; Molecular Formula $C_{59}H_{71}ClF_2N_8O_8Ru_2$; Anal. Found: C, 55.13; H, 6.37; N, 8.43. Calc.: C, 55.20; H, 6.42; N, 8.65. ESI-MS *m/z*: Obs (Calc):1263.9 (1263.3) (M^+); δH(400 MHz, DMSO-d^6) 5.9-5.8, (m, 4H, *p*-cymAr-H); 2.93-2.72, (q, 1H, *p*-cym-*iso*-prop-CH); 2.1, (s, 3H, *p*-cym Ar-CH_3); 1.29, (d, 6H, *p*-cym-*iso*-prop-$(CH_3)_2$); 7.8, (d, 2H, imidazole CH=CH); FTIR (KBr/ cm^{-1}): $\nu_{(Ar)C-H}$ 2913, $\nu_{(pyridone)C=O}$ 1622, $\nu_{COOassym}$1587, ν_{COOsym}1366, $\Delta\nu_{COO}$ 221; $\Lambda_M(\Omega^{-1}.m^2.M^{-1})$ 54.

*[Ru_2(μ-im) (η^6-p-cym)$_2$(**L19**)$_2$]Cl* **(C35)**:

μ-imidazole–bis-1-cyclopropyl-6-fluoro-4-oxo-7-piperazin-1-ylquinoline-3-carboxylate–bis-1 - isopropyl-4-methyl benzene diruthenium(II) chloride

Yield: 69.5%; Molecular Weight 1235.8 g/mole; Molecular Formula $C_{57}H_{67}ClF_2N_8O_6Ru_2$; Anal. Found: C, 55.66; H, 5.40; N, 9.85. Calc.: C, 55.86; H, 5.36; N, 9.98. ESI-MS *m/z*:Obs (Calc): 1204.6 (1204.8) (M^+); δH(400 MHz, DMSO-d6) 5.74-5.68, (m, 4H, *p*-cymAr-H); 2.93-2.87, (q, 1H, *p*-cym-*iso*-prop-CH); 2.2, (s, 3H, *p*-cym Ar-CH_3); 1.29, (d, 6H, *p*-cym-*iso*-prop-$(CH_3)_2$); 7.5, (d, 2H, imidazole CH=CH); FTIR (KBr/ cm^{-1}): ν(Ar)C-H 2963, ν(pyridone)C=O 1632, $\nu_{COOassym}$1581, ν_{COOsym}1390, $\Delta\nu_{COO}$ 191; $\Lambda_M(\Omega^{-1}.m^2.M^{-1})$ 57.

*[Ru_2(μ-im) (η^6-p-cym)$_2$(**L20**)$_2$]Cl* **(C36):**

μ-imidazole – bis – 7-[(4aS,7aS)-1,2,3,4,4a,5,7,7a-octahydropyrrolo[3,4-b]pyridin-6-yl]-1-cyclopropyl-6-fluoro-8-methoxy-4-oxoquinoline-3-carboxylate – bis 1 - isopropyl-4-methyl benzene diruthenium(II) chloride

Yield: 55.7%; Molecular Weight 1376.0 g/mole; Molecular Formula $C_{65}H_{79}ClF_2N_8O_8Ru_2$; Anal. Found: C, 57.61; H, 5.29; N, 7.63. Calc.: C, 57.86; H, 5.12; N, 7.62. ESI-MS *m/z*: Obs (Calc): 1342.8. (1343.4) (M^+ - 1); δH (400 MHz, DMSO-d^6) 5.74-5.68, (m, 4H, *p*-cymAr-H); 2.93-2.87, (q, 1H, *p*-cym-*iso*-prop-CH); 2.2, (s, 3H, *p*-cym Ar-CH_3); 1.29, (d, 6H, *p*-cym-*iso*-prop-$(CH_3)_2$); 7.5, (d, 2H, imidazole CH=CH); FTIR (KBr/ cm^{-1}): $\nu_{(Ar)C-H}$ 2967, $\nu_{(pyridone)C=O}$ 1631, $\nu_{COOassym}$1579, ν_{COOsym}1369, $\Delta\nu_{COO}$ 210; $\Lambda_M(\Omega^{-1}.m^2.M^{-1})$ 53.

*[Ru_2(μ-azpy)(η^6-p-cym)$_2$(**L17**)$_2$]Cl_2* **(C37)**:

μ-4,4'azopyridine–bis-1-ethyl-6,8-difluoro-7-(3-methylpiperazin-1-yl)-4-oxoquinoline-3-carboxylate-bis-1-isopropyl-4-methylbenzene diruthenium(II) dichloride

Yield: 78.1%; Molecular Weight 1432.4 g/mole; Molecular Formula $C_{64}H_{78}N_{10}O_6Cl_2F_4Ru_2$; Anal.: C, 57.21; H, 5.11; N, 9.97. Calc.: C, 57.13; H, 5.81; N, 10.09. ESI-MS *m/z*: Obs (Calc): 678.8 (680.7) (M^{2+}-2) ; δ_H (400 MHz, DMSO-d^6) 4.92-4.87, (m, 4H, *p*-cymAr-H); 2.21-2.54, (q, 1H, *p*-cym-*iso*-prop-CH); 2.01, (s, 3H, *p*-cym Ar-CH_3); 1.29, (d, 6H, *p*-cym-*iso*-prop-$(CH_3)_2$); FTIR (KBr/cm^{-1}): $\nu_{(Ar)C-H}$ 2920, $\nu_{(pyridone)C=O}$ 1617, $\nu_{COOassym}$ 1592, ν_{COOsym}1379, $\Delta\nu_{COO}$ 213, $\nu_{N=N}$ 1453; $\Lambda_M(\Omega^{-1}.m^2.M^{-1})$ 124.

*[Ru_2(μ-azpy)(η^6-p-cym)$_2$(**L18**)$_2$]Cl_2* **(C38):**

μ-4,4'azopyridine–bis-7-fluoro-2-methyl-6-(4-methylpiperazin-1-yl)-10-oxo-4-oxa-1-azatricyclo[7.3.1.$0^{5,13}$]trideca-5(13),6,8,11-tetraene-11-carboxylate-bis1-isopropyl-4-methylbenzene diruthenium(II) dichloride

Yield: 85.8 %; Molecular Weight 1448.5 g/mole; Molecular Formula $C_{66}H_{76}N_{10}O_8Cl_2F_2Ru_2$; Anal.: C, 58.95; H, 5.51; N, 10.56. Calc.: C, 57.55; H, 5.56; N, 10.17, ESI-MS *m/z*:Obs (Calc): 685.2 (684.1) (M^{2+}-1) ; δ_H (400 MHz, DMSO-d^6) 5.74-5.65, (m, 4H, *p*-cymAr-H); 2.98-2.82, (q, 1H, *p*-cym-*iso*-prop-CH); 1.98, (s, 3H, *p*-cym Ar-CH_3); 1.10, (d, 6H, *p*-cym-*iso*-prop-$(CH_3)_2$); FTIR (KBr/cm^{-1}): $\nu_{(Ar)C-H}$ 2958, $\nu_{(pyridone)C=O}$ 1622, $\nu_{COOassym}$ 1581, ν_{COOsym}1270, $\Delta\nu_{COO}$ 311, $\nu_{N=N}$ 1457; $\Lambda_M(\Omega^{-1}.m^2.M^{-1})$ 122.

$[Ru_2(\mu\text{-azpy})(\eta^6\text{-p-cym})_2(\mathbf{L19})_2]Cl_2$ **(C39)**:

μ-4,4'azopyridine–bis-1-cyclopropyl-6-fluoro-4-oxo-7-piperazin-1-ylquinoline-3-carboxylate-bis1-isopropyl-4-methylbenzene diruthenium(II) dichloride

Yield: 64.7%; Molecular Weight 1388.5 g/mole; Molecular Formula $C_{64}H_{72}N_{10}O_6Cl_2F_2Ru_2$; Anal.: C, 58.14; H, 5.91; N, 10.56. Calc.: C, 58.35; H, 5.51; N, 10.63, ESI-MS *m/z*:Obs (Calc): 657.0 (658.7) (M^{2+}-1) ; δ_H(400 MHz, DMSO-d^6) 6.01-5.98, (m, 4H, *p*-cymAr-H); 2.57-2.42, (q, 1H, *p*-cym-*iso*-prop-CH); 2.21, (s, 3H, *p*-cym Ar-CH_3); 1.56, (d, 6H, *p*-cym-*iso*-prop-$(CH_3)_2$); FTIR (KBr/cm^{-1}): $\nu_{(Ar)C-H}$ 2961, $\nu_{(pyridone)C=O}$ 1628, $\nu_{COOassym}$ 1597, ν_{COOsym} 1381, $\Delta\nu_{COO}$ 216, $\nu_{N=N}$ 1408; $\Lambda_M(\Omega^{-1}.m^2.M^{-1})$ 125.

$[Ru_2(\mu\text{-azpy})(\eta^6\text{-p-cym})_2(\mathbf{L20})_2]Cl_2$ **(C40)**:

μ-4,4'azopyridine–bis-7-[(4aS,7aS)-1,2,3,4,4a,5,7,7a-octahydropyrrolo[3,4-b]pyridin-6-yl]-1-cyclopropyl-6-fluoro-8-methoxy-4-oxoquinoline-3-carboxylate-bis1-isopropyl-4-methylbenzene diruthenium(II) dichloride

Yield: 76.3%; Molecular Weight 1528.6 g/mole; Molecular Formula $C_{72}H_{84}N_{10}O_8Cl_2F_2Ru_2$; Anal.: C, 59.78; H, 5.21; N, 9.56. Calc.: C, 59.25; H, 5.94; N, 9.60. ESI-MS *m/z*:Obs (Calc): 728.9 (728.8) (M^{2+}) ; δ_H (400 MHz, DMSO-d^6) 5.85-5.74, (m, 4H, *p*-cymAr-H); 2.71-2.64, (q, 1H, *p*-cym-*iso*-prop-CH); 1.92, (s, 3H, *p*-cym Ar-CH_3); 1.12, (d, 6H, *p*-cym-*iso*-prop-$(CH_3)_2$); .FTIR (KBr/cm^{-1}): $\nu_{(Ar)C-H}$ 2962, $\nu_{(pyridone)C=O}$ 1629, $\nu_{COOassym}$ 1599, ν_{COOsym} 1380, $\Delta\nu_{COO}$ 219, $\nu_{N=N}$ 1414; $\Lambda_M(\Omega^{-1}.m^2.M^{-1})$ 121.

3.7.2 Results and discussion:

The electronic absorption spectra of the complexes C**33-40** (*Fig. 3.26*) show three major bands in the wavelength range 200-500 nm. The first band appearing within 223-231 nm is attributable to the intraligand π→π* transition of the aromatic rings of the arene ligand (*p*-cymene) as well as the fluoroquinolone ligand. A second sharp but medium intensity peak is found in the range of 269-286 nm owing to the intraligand *n*→π* transitions which have blue shifted on complexation as compared to the free ligands [36]. The third broad band observed within 327-339 nm is also due to the intraligand *n*→π* transitions which remains fairly unchanged as seen in the free ligand. The λ_{max} values of all the transitions taking place in the complexes have been tabulated in Table 3.14.

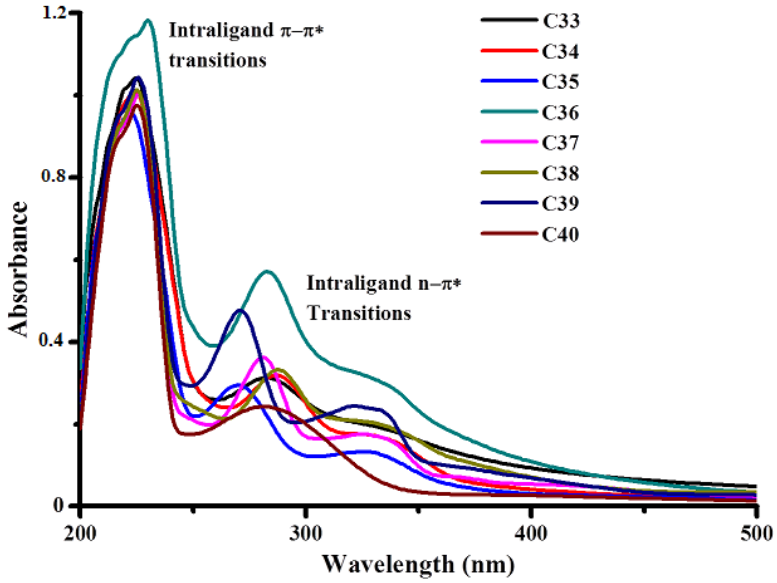

Fig. 3.26: *UV-Vis spectra of* ***C33-40***

Table 3.14: UV-Vis. peak assignments of complexes

Code	C33	C34	C35	C36	C37	C38	C39	C40
Intra-ligand transitions(nm) π-π*	224	224	223	231	225	225	226	224
Intra-ligand transitions(nm) n-π*	283,333	286, 334	269, 329	282, 332	281, 331	288, 331	270, 327	284, 339

The ESI-Mass spectra of C**33-40** given in *Figs. 3.27* and *3.28* show *m/z* peaks corresponding to the molecular ions which indicate that *p*-cymene, fluoroquinolone and imidazole or 4,4'azopyridine ligands are coordinated to the Ru centres, resulting in the formation of complex ions with +1 (**C33-C36**) or +2 (**C37-C40**) charges. The m/z values affirm the proposed stoichiometry of the complexes which are in good agreement with that obtained from microanalytical data. To confirm the charges on the complexes, molar conductance were measured in 10^{-3}M DMSO solution at 38 ˚C and the values suggest the formation of 1:1 (**C33-C36**) and 1:2 (**C37-C40**) electrolytes.

Table 3.15: m/z values of complexes

Code	**C1**	**C2**	**C3**	**C4**	**C5**	**C6**	**C7**	**C8**
Calculated Mass (g/mol)	1244.6	1263.1	1204.8	1343.7	680.7	684.7	658.1	728.8
Observed Mass (g/mol)	1244.2 (M^+)	1263.9 (M^+)	1204.6 (M^+)	1342.8 (M^+-1)	678.8 (M^{2+}-2)	685.2 (M^{2+}-1)	657.0 (M^{2+}-1)	728.9 (M^{2+})

The characterization of complexes **C33-40** can be achieved by studying the most typical vibrations that are characteristic of the coordinated fluoroquinolones. The vibration of the carboxylic stretch $\nu_{(C=O)}$ found at 1709 – 1714 cm^{-1} as a very strong band [49] in the infrared spectrum of FQ ligands has disappeared in the IR spectra of complexes. Two characteristic bands, at around 1579 – 1599 cm^{-1} and 1270 – 1399 cm^{-1} with different intensities assigned to (O–C–O) asymmetric and symmetric stretching vibrations, respectively are seen in the IR spectra of the complexes,. The bands at 1620 – 1630 cm^{-1}, assigned to $\nu_{(C=O)}$ stretching mode of ring carbonyl group are shifted slightly upon coordination which suggests the binding of FQs to the Ru ions through the ring carbonyl oxygen atom [50]. The difference $\Delta = \nu_{(COO)asym} - \nu_{(COO)sym}$ is a useful characteristic for determining the coordination mode of the ligands. The Δ values in the range 188 – 311 cm^{-1} indicate a monodentate coordination mode of the carboxylato group of the ligand [51]. The coordination of p-cymene is revealed by the presence of the characteristic bands. The overall changes of the IR spectra suggest that the ligand is coordinated to metals via the pyridone and carboxylate oxygen

The ^{1}H NMR spectra of **C33-40** (*Figs. 3.29* and *3.30*) show distinct peaks corresponding to *p*-cymene as discussed in section 3.3.2. Rest of the peaks are associated with the fluoroquinolone ligands. Coordination of the carboxylate oxygen to the ruthenium metal centre is evident from the absence of the peak corresponding to carboxylic O-H proton. The aromatic protons of the quinolone nucleus are observed at δ = 7-9 ppm while those arising due to piperazine protons are obtained in the region δ = 3-4 ppm. The methyl and substituted methyl protons appear at around δ = 1-2 ppm. Coordination of the deprotonated imidazole is evident from the absence of the peak corresponding to N-H proton at in the NMR spectra of C**33-36.** .

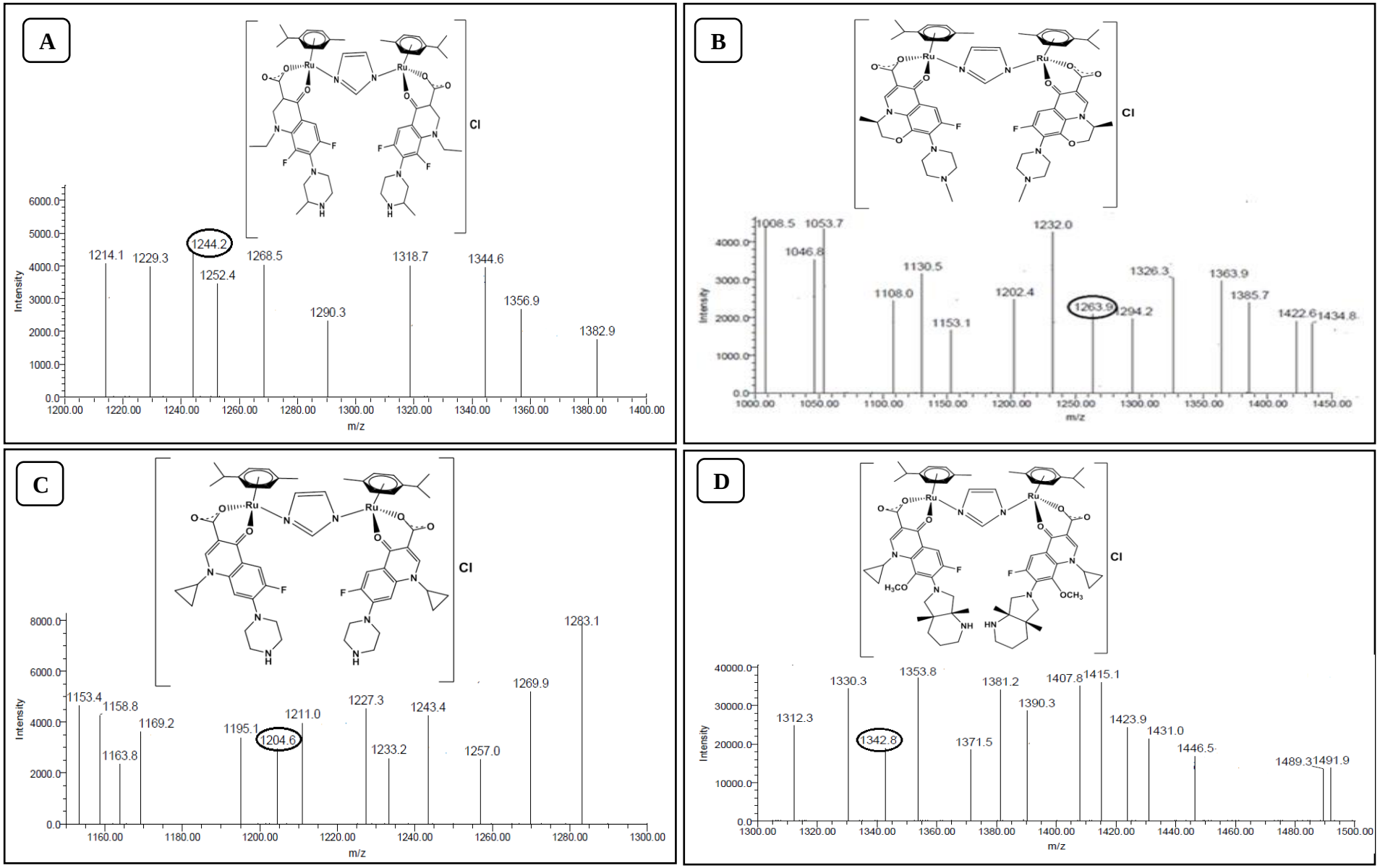

Fig. 3.27: *ESI-MS spectra of complexes (A)* ***C33*** *(B)* ***C34*** *(C)* ***C35*** *(D)* ***C36*** *indicating their molecular ion peak*

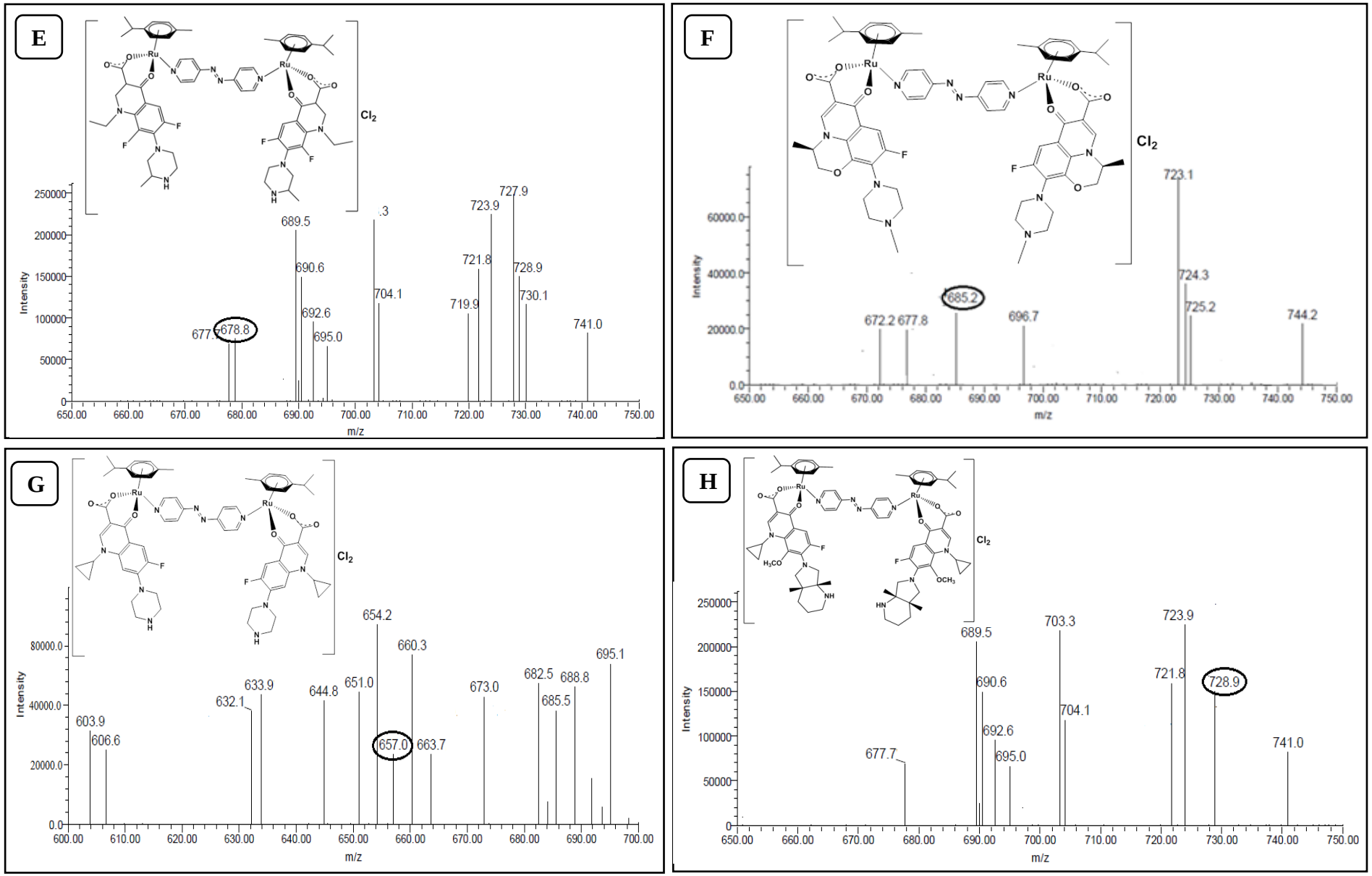

Fig. 3.28: *ESI-MS spectra of complexes (E)* ***C37*** *(F)* ***C38*** *(G)* ***C39*** *(H)* ***C40*** *indicating their molecular ion peak*

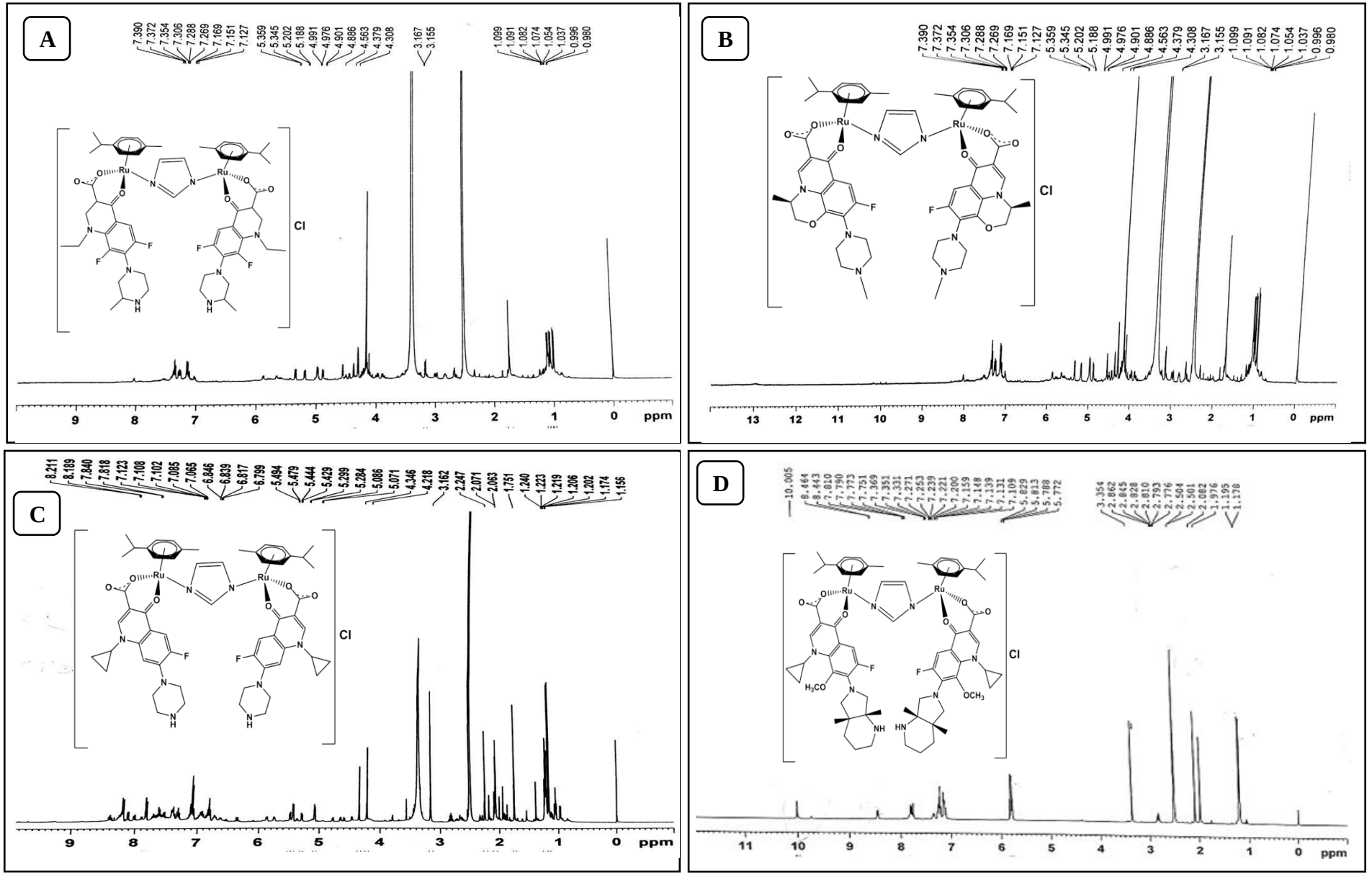

Fig. 3.29: *^{1}H NMR spectra of complexes (A)* ***C33*** *(B)* ***C34*** *(C)* ***C35*** *(D)* ***C36***

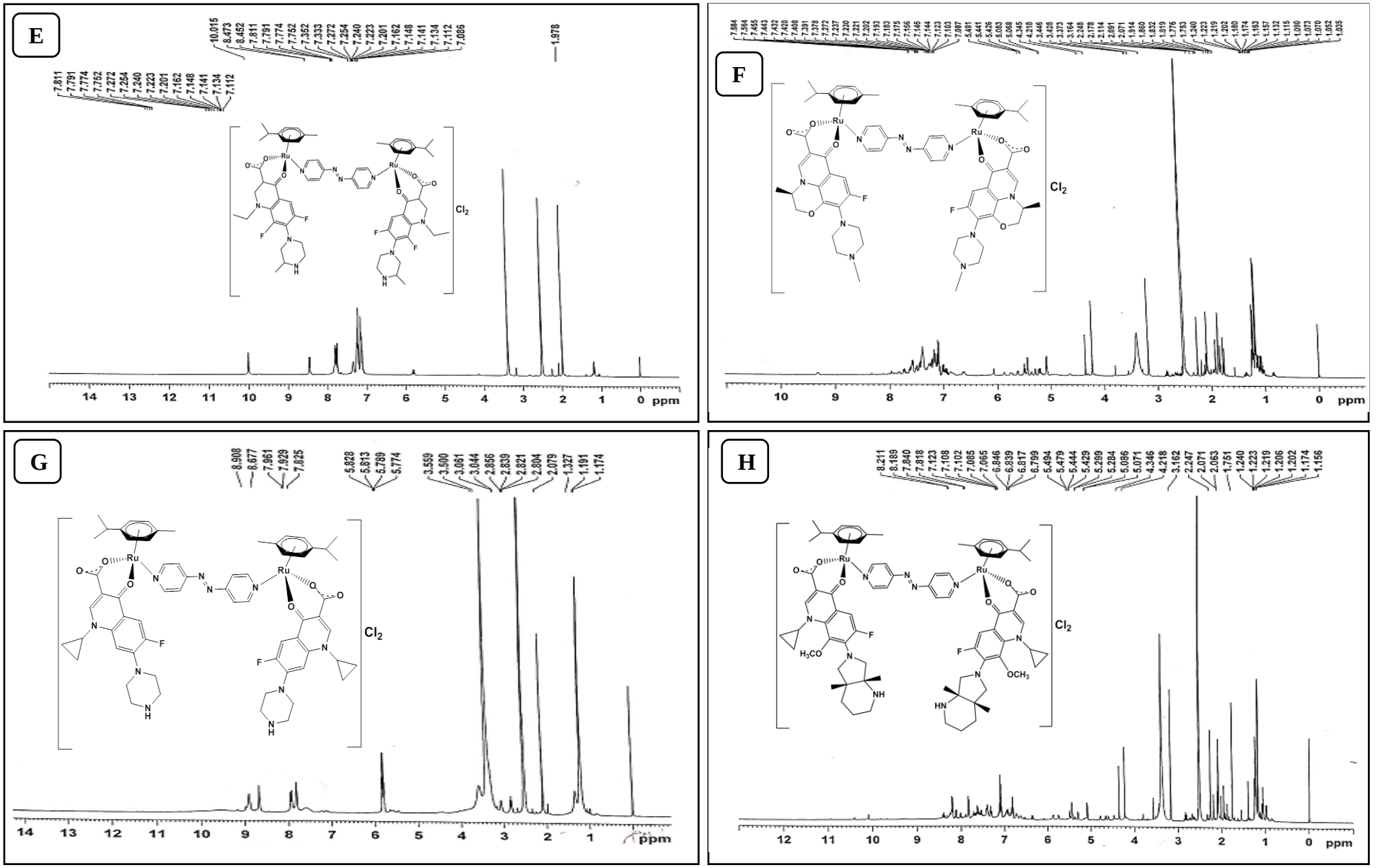

Fig. 3.30: *^{1}H NMR spectra of complexes (E)* ***C37*** *(F)* ***C38*** *(G)* ***C39*** *(H)* ***C40***

3.7.3 *Geometry optimization of [Ru_2 (μ-im /μ-azpy)(η^6-p-cym)$_2$(Fluroquinolones)$_2$]Cl_{1-2} complexes: (C33-C40)*

All calculations were performed using the approximations with dispersion correction (disp3) program. Full geometry optimizations of compounds were carried out using the DFT method as mention above in section 3.2.1. This functional has been shown to give more accurate results for organometallic complexes. The DFT calculations for geometry optimization provide a great insight into the molecular structure. Optimized structures of the complexes **C33** and **C37** are shown in *Fig. 3.31*. Piano-stool type geometry is seen around each metal centre of the binuclear complexes with the Ru (II) ions π-bonded to the arene ring. The average Ru-Ru distance in the binuclear complexes with imidazole as bridging ligands is 6.11 A^0 whereas in binuclear complexes with 4, 4'azopyridine as bridging ligands is the average distance is 13.22 A^0 due to the presence of longer 4, 4'azopyridine ligand. The bond angle values reveal a pseudo octahedral coordination of the ruthenium centres. The metal–ligand bond lengths and bond angles tabulated in Table 3.16 are in well agreement with the values in the literature [38, 39].

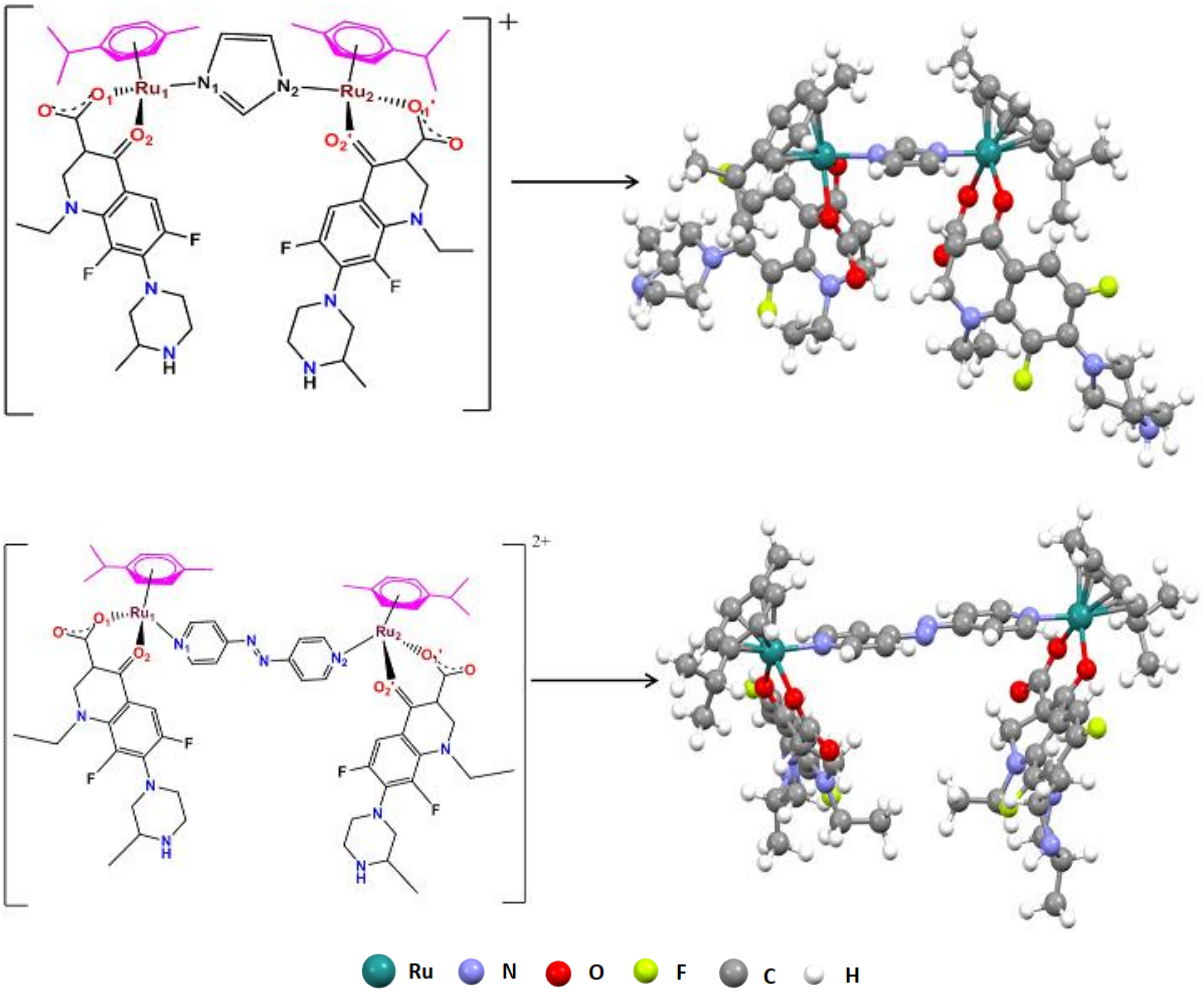

Fig. 3.31: *Optimized structures of the complexes* ***C33*** *and* ***C36*** *under study*

Table 3.16: Metal ligand bond lengths and bond angles of complexes under study obtained from geometry optimization

Bond Length (in Å)	**L17**		**L18**		**L19**		**L20**	
	C33	**C37**	**C34**	**C38**	**C35**	**C39**	**C36**	**C40**
Ru1……Ru2	6.16	6.11	6.10	6.09	13.25	13.18	13.22	13.23
Ru1-O1 (COO)	2.09	2.07	2.07	2.07	2.06	2.06	2.06	2.06
Ru1-O2 (C=O)	2.13	2.07	2.08	2.08	2.07	2.06	2.06	2.05
Ru1-N1	2.08	2.08	2.06	2.06	2.09	2.09	2.08	2.08
Ru2-O1’ (COO)	2.09	2.06	2.06	2.06	2.06	2.06	2.06	2.06
Ru2-O2’ (C=O)	2.10	2.08	2.07	2.07	2.07	2.06	2.06	2.06
Ru2-N2	2.07	2.09	2.08	2.08	2.09	2.09	2.08	2.08
Bond Angle (in Degree)								
O1-Ru1-O2	90.3	85.6	86.6	86.1	87.8	88.2	88.3	88.3
O1-Ru1-N1	81.8	85.7	83.8	83.7	84.3	85.3	85.0	84.7
O2-Ru1-N1	87.6	83.0	83.2	83.0	83.5	83.0	83.7	84.0
O1’-Ru2-O2’	86.6	86.1	87.7	87.7	87.5	88.1	87.9	88.0
O1’-Ru2-N2	86.4	84.5	85.7	85.5	84.5	85.3	85.1	84.8
O2’-Ru2-N2	88.4	84.6	80.6	80.9	83.6	83.0	83.6	84.1

3.8 Summary

The different $[Ru_2\ (\mu\text{-im}\ /\ \mu\text{-azpy})\ (\eta^6\text{-p-cym})_2\ (L)_2]Cl_n$ binuclear complex series discussed in this chapter have been synthesized and well characterized with an aim to evaluate them for their biomolecular interactions with DNA and BSA protein and *in cellulo* anticancer activities against HeLa human cervical cell line.

3.9 References

[1] Ivanović, I.; Gligorijević, N.; Aranđelović, S.; Radulović, S.; Roller, A.; Keppler, B.K.; Tešić, Z. Lj.; Grgurić-Šipka, S. *Polyhedron*, **2013**, 61, 112.

[2] Mu, C.; Walsby, C.J. *Med. Inorg. Chem*.; Storr, T., Ed; John Wiley & Sons, Chichester, UK, **2014**, Chapter 15.

[3] Dragutan, I.; Dragutan, V.; Demonceau, A. *Molecules* **2015**, 20, 17244.

[4] Collins, I.; Jones, A.M. *Molecules* **2014**, 19, 17221.

[5] Devi, C.S.; Nagababu, P.; Natarajan, S.; Deepika, N.; Venkat Reddy, P.; Veerababu, N.; Singh, S.S.;Satyanarayana, S. *Eur. J. Med. Chem.* **2014**, 72, 160.

[6] Ruhayel, R.A.; Langner, J.S.; Oke, M. -J.; Berners-Price, S.J.; Zgani, I.; Farrell, N.P. *J. Am. Chem. Soc.*, **2012**, 134, 7135.

[7] Billecke, C.; Finniss, S.; Tahash, L.; Miller, C.; Mikkelsen, T.; Farrell, N.P.; B¨ogler, O.; *Neurooncology*, **2006**, 8, 215.

[8] Gatti, L.; Perego, P.; Leone, R.; Apostoli, P.; Carenini, N.; Corna, E.; Allievi, C.; Bastrup, U.; De Munari, S.; Di Giovine, S.; Nicoli, P.; Grugni, M.; Natangelo, M.; Pardi, G.; Pezzoni, G.; Singer, J.W.; Zunino, F. *Mol. Pharmaceutics*, **2010**, 7, 207.

[9] Hartinger, C.G.; Phillips, A.D.; Nazarov, A.A. *Curr. Top. Med. Chem.*, **2011**, 11, 2688.

[10] Mendoza-Ferri, M. G.; Hartinger, C.G.; Eichinger, R.E.; Stolyarova, N.; Severin, K.; Jakupec, M.A.; Nazarov, A.A.; Keppler, B.K. *Organomet.*, **2008**, 27, 2405.

[11] Mendoza-Ferri, M.G.; Hartinger, C.G.; Mendoza, M.A.; Groessl, M.; Egger, A.E.; Eichinger, R.E.; Mangrum, J.B.; Farrell, N. P.; Maruszak, M.; Bednarski, P.J.; Klein, F.; Jakupec, M.A.; Nazarov, A.A.; Severin, K.; Keppler, B.K. *J. Med. Chem.*, **2009**, 52, 916.

[12] Novakova, O.; Nazarov, A.A.; Hartinger, C. G.; Keppler, B.K.; Brabec, V. *Biochem. Pharmacol.* , **2009**, 77, 364.

[13] Mishra, L.; Sinha, R. *Monatsh. Chem.*, **2002**, 133, 59.

[14] Hartinger, C.G.; Phillips, A.D.; Nazarov, A.A. *Cur. Topics Med. Chem.*, **2011**, 11, 2688.

[15] Nováková, O.; Nazarov, A. A.; Hartinger, C. G.; Keppler, B. K.; Brabec, V. *Biochem. Pharmacol.*, **2009**, *77*, 364.

[16] Morris, R. E.; Sadler, P. J.; Chen, H.; Jodrell, D.; The University Court, The University of Edinburgh, UK: WO, **2001**, 36.

[17] Morris, R. E.; Sadler, P. J.; Jodrell, D.; Chen, H.; University Court, The University of Edinburgh, UK: WO, **2002**, 32.

[18] Chen, H.; Parkinson, J. A.; Novakova, O.; Bella, J.; Wang, F.; Dawson, A.; Gould, R.; Parsons, S.; Brabec, V.; Sadler, P. J. *Proc. Natl. Acad. Sci. USA*, **2003**, 100, 14623.

[19] (a) Becke, A.D. *Phys. Rev.*, **1988**, A 38, 3098. (b) Perdew, J.P. *Phys. Rev.*, **1986**, B 33, 8822.

[20] Schäfer, A.; Horn, H.; Ahlrichs, R. *J. Chem. Phys.*, **1992**, 97, 2571.

[21] Hättig, C.; Schmitz, G.; Koßmann, J. *Phys. Chem. Chem. Phys.*, **2012**, 14, 6549.

[22] Ahlrichs, R.; Bar, M.; Häser, M.; Horn, H.; Kölmel, C. *Chem. Phys. Lett.*, **1989**, 162, 165.

[23] Eichkorn, K.; Treutler, O.; Öhm, H.; Haser, M.; Ahlrichs, R. *Chem. Phys. Lett.*, **1995**, 240, 283.

[24] Sierka, M.; Hogekamp, A.; Ahlrichs, R. *J. Chem. Phys.*, **2003**, 118, 9136.

[25] (*a*) Hepburn, J.; Scoles, G.; Penco, R. *Chem. Phys. Lett.*, **1975, 36,** 451. (b) Grimme, S.; Antony, J.; Ehrlich, S.; Krieg, H. *J. Chem. Phys.*, **2010, 132,** 154104.

[26] Klamt, A.; Schuurmann, G. *J. Chem. Soc. Perkin Trans.*, **1993**, 2, 799.

[27] Macrae, C.F.; Edgington, P.R.; McCabe, P.; Pidcock, E.; Shields, G.P.; Taylor, R.; Towler, M. *J. Van de Streek, J. Appl. Cryst.*, **2006**, 39, 453.

[28] Bennett, M.A.; Smith, A.K. *J. Chem. Soc. Dalton Trans*, **1974**, 233.

[29] Bennett, M.A.; Huang, T.N.; Matheson, T.W.; Smith, A.K.; Ittel, S.; Nickerson, W. *Inorg. Synth.*, **1982**, 21, 74.

[30] Patel, R.N.; Singh, N.; Shukla, K.K.; Chauhan, U.K. *Spectrochim. Acta*, **2005**, A 61, 287.

[31] Zhu, L.N.; Yi, L.; Dong, W.; Wang, W.Z.; Liu, Z.Q.; Wang, Q.M.; Liao, D.Z.; Jiang, Z.H.; Yan, S.P. *J. Coord. Chem.*, **2006**, 59, 457.

[32] Ali, I.; Wani, W.A.; Saleem, K. *Synth. React. Inorg. Met.-Org. Nano-Met. Chem.*, **2013**, 43, 1162.

[33] Mahalingam, V.; Chitrapriya, N.; Fronczek, F.R.; Natarajan, K. *Polyhedron*, **2010**, 29, 3363.

[34] Bechford, F.A.; Leblanc, G.; Thessing, J.; Shaloski, Jr. M.; Frost, B.J.; Li, L.; Seeram, N.P. *Inorg. Chem. Commun.*, **2009**, 12, 1094.

[35] Zhu, L.N.; Zhang, L.Z.; Wang, W.Z.; Liao, D.Z.; Cheng, P.; Yan, S.P.; Jiang, Z.H. *J. Coord. Chem*., **2003**, 56, 1447.

[36] Pulipaka, R.; Dash, S.R.; Khanvilkar, P.; Jana, S.S.; Devkar, R.V.; Chakraborty, D. *Trans. Met. Chem.*, **2019**, 38, 603.

[37] Liu, X.M.; Xie, L.H.; Lin, J.B.; Lin, R.B.; Zhang, J.P.; Chen, X.M. *Dalton Trans.*, **2011**, 40, 8549.

[38] Ya-Wen, T.; Yun-Fan, C.; Yong-Jie, L.; Kuan-Hung, C.; Lin, C-H.; Jui-Hsien, H. *Molecules*, **2018**, 23, 59.

[39] Adebayo, A.A.; Ajibade, P.A. *J Chem*., **2016**, 15, Article ID 3672062.

[40] (a) Muthukumar, M.; Sivakumar, S.; Viswanathamurthi, P.; Karvembu, R.; Prabhakaran, R.; Natarajan, K. *J. Coord. Chem.*, **2010**, 63, 296. (b) Muthukumar, M.; Viswanathamurthi, P.; Prabhakaran, R.; Natarajan, K. *J. Coord. Chem.*, **2010**, 63, 3833.

[41] Deacon, G.B.; Phillips, R.J. *Coord. Chem. Rev.*, **1980**, 33, 227.

[42] Gehad, G.; Mohamed, H.F.; El-Halim, A.; Maher, M.I.; El-Dessouky, W.; Mahmoud, H. *J. Mol. Struct.*, **2011**, 999, 29.

[43] Pulipaka, R.; Singh, R.; Jana, S.S.; Devkar, R.; Chakraborty, D. *J. Organomet. Chem.*, **2017**, 833, 80.

[44] Prabhakaran, R.; Anantharaman, S.; Thilagavathi, M.; Kaveri, M.V.; Kalaivani, P.; Karvembu, R.; Dharmaraj, N.; Bertagnolli, H.; Dallermer, F.; Natarajan, K. *Spectrochim. Acta Part A*, **2011**, 78, 844.

[45] Thompson, D.W.; Ito, A.; Meyer, T.J. *Pure Appl. Chem.*, **2013**, 85, 1257.

[46] Adams, M.; Li, Y.; Khot, H.; Kock, D. C.; Smith, J. P.; Land, K.;Chibale, K.; Smith, S. G. *Dalton Trans*., **2013**, 42, 4677.

[47] Schleicher, D.; Tronnier, A.; Leopold, H.; Borrmann, H.; Strassner, T. *Dalton Trans*., **2016**, 45, 3260.

[48] Hudej, R.; Kljun, J.; Kandioller, W.; Repnik, U.; Turk, B.; Hartinger, C.G.; Keppler, B.K.; Miklavčič, D.; Turel, I. *Organomet.*, **2012**, 31, 5867.

[49] Sadeek, A. S.; El-Shwiniy, W. H.; El-Attar, M. S. *Spectrochim. Acta Part A*, **2011**, 84, 99.

[50] Sultana, N.; Arayne, M.S.; Rizvi, S.B.S.; Haroon, U.; Mesaik, M. A. *Med. Chem. Re.* **2013**, 19, 617.

[51] Efthimiadou, E.K.; Psomas, G.; Sanakis, Y.; Katsaros, N.; Karaliota, A. *J Inorg. Biochem.*, **2007**, 101, 525.